Technischen Universität München
Fakultät für Medizin

The oncolytic adenovirus XVir-N-31 and CDK4/6 inhibitors: Elucidating the mechanisms driving the therapeutic synergy

Sruthi Hindupur Vasantamadhava

Vollständiger Abdruck der von der Fakultät für Medizin der Technischen Universität München zur Erlangung des akademischen Grades eines

Doctor of Philosophy (Ph.D.)

genehmigten Dissertation.

Vorsitzender: Prof. Dr. Marc Schmidt-Supprian

Betreuer: Priv.-Doz. Dr. Roman Nawroth

Prüfer der Dissertation:

1. Prof. Dr. Per Sonne Holm

2. Prof. Dr. Dieter Saur

Die Dissertation wurde am 25.04.2022 bei der Fakultät für Medizin der Technischen Universität München eingereicht und durch die Fakultät für Medizin am 26.06.2022 angenommen.

To my parents…

Abstract

Oncolytic virotherapy is one of the rapidly evolving therapeutic strategies in the domain of cancer therapeutics. One of the key factors for the successful implementation of oncolytic viruses in the clinic is their replicative ability. We have demonstrated earlier in our group that the lytic potency of the oncolytic adenovirus XVir-N-31 is enhanced upon combining with CDK4/6 inhibitors in RB-positive cell lines in bladder cancer cells. Adenoviruses have been demonstrated to rely on RB and E2F family of proteins for their successful replication. Contradictorily, CDK4/6 inhibitors reduce the levels of RB and E2F1 proteins. Thus, in this thesis, we investigated the molecular mechanisms driving this therapeutic synergy to better understand the viral biology.

Firstly, we showed that the enhanced replication of the adenoviruses upon CDK4/6 inhibition is not an effect caused by cell synchronization upon CDK4/6 inhibition. We also observe that the enhancement in cell lysis upon CDK4/6 inhibition follows a linear kinetic with the RB-protein levels. Interestingly, viral gene expression was advanced significantly upon treatment with CDK4/6 inhibitors at earlier time points of the infection. Adenoviral genome has E2F binding sites which are crucial for their replication, and these E2F proteins are dysregulated upon CDK4/6 inhibition. siRNA mediated knockdown of single E2F proteins revealed that they do not have a direct effect on viral replication and particle formation. However, sequestering of E2F proteins using a mutated adenoviral construct, ADWT/Trap showed enhanced viral replication compared to ADWT, especially at early time points. Another novel adenovirus with mutations in E2F binding sites of E2-early promoter, ADWT/E2Fm, showed reduced replication, suggesting that the complete removal of E2F proteins throughout the adenoviral lifecycle is detrimental for replication. Interestingly, we observe a far better response in replication when ADWT/E2Fm is treated with CDK4/6 inhibitors compared to ADWT. Thus, we hypothesize that the E2F proteins have a repressive role in the early phases of adenoviral life cycle but are required in the later stages of infection. This is supported by transcriptomic analysis which showed reduction of expression of E2F targets upon Palbociclib treatment as early as 8hrs post treatment. In conclusion, our findings suggest that the synergy of the oncolytic adenovirus XVir-N-31 and CDK4/6 inhibitors is mediated by the dysregulation of repressive E2F proteins.

In a second project, we evaluated the therapeutic potential of targeting the JAK-STAT signalling pathway components in bladder cancer cell lines. High STAT3 expression was

detected in 51.3% of invasive bladder cancer patient specimens by immunohistochemistry. STAT3 inhibition, but not JAK1/2 inhibition, showed reduced cell survival in bladder cancer cell lines. Both JAK1/2 inhibition and STAT3 inhibition increased the lytic potential and replication of the oncolytic adenovirus XVir-N-31. Our results provide evidence that inhibitors against JAK1/2 and STAT3 are promising combination therapy with oncolytic viruses in bladder cancer.

Abbreviations

°C	degree Celsius
µg	microgram
µl	microliter
µm	micrometer
µM	micromolar
AdV	Adenovirus
ADWT	Adenovirus Wildtype
ATF	Activating Transcription Factor
BCG	Bacillus Calmette-Guerin
BLCA	Bladder Cancer
bp	Base Pair
BSA	Bovine Serum Albumin
CaCl	Calcium Chloride
CDK	Cyclin-Dependent Kinase
CDK4/6i	CDK4/6 inhibitors
Chk1/2	Checkpoint Kinase 1/2
CI	Combination Index
CAR	Coxsackie Adenovirus Receptor
CPE	Cytopathic Effect
CTLA4	Cytotoxic T-Lymphocyte Associated Protein 4
CIS	Carcinoma Insitu
cm	Centimeter
CrAD	Conditionally Replicative Adenovirus
DAB	3,3-Diaminobenzidine
DAMP	Damage-Associated Molecular Patterns
DBP	DNA Binding Protein
dH_2O	Distilled Water
DMEM	Dulbecco's Modified Eagle's Medium
DMSO	Dimethyl Sulfoxide
DNA	Deoxyribonucleic Acid
dNTP	Deoxynucleoside Triphosphate
dpi	Days Post Infection
DTT	Dithiothreitol

ECL	Enhanced Chemiluminescent Substrate
EDTA	Ethylenediamine Tetra Acetic Acid
EMSA	Electrophoretic Mobility Shift Assay
FBS	Foetal Bovine Serum
ICD	Immunogenic Cell Death
FDA	Food And Drugs Administration
FGFR	Fibroblast Growth Factor Receptor
GAPDH	Glyceraldehyde 3-Phosphate Dehydrogenase
GM-CSF	Granulocyte-Macrophage Colony-Stimulating Factor
H_2O	Water
H_2O_2	Hydrogen Peroxide
HCl	Hydrochloric Acid
hpi	Hours Post Infection
HRP	Horseradish Peroxidase
HSV	Herpes Simplex Virus
IFU	Infectious Units
ICI	Immune Checkpoint Inhibitors
IgG	Immune Globulin G
IHC	Immunohistochemistry
kb	Kilobase
kDa	Kilo Dalton
M	Molar
mg	Milligram
MIBC	Muscle Invasive Bladder Cancer
ml	Milliliter
MLP	Major Late Promoter
mM	Millimolar
MOI	Multiplicity of Infection
mRNA	Messenger Ribonucleic Acid
NaCl	Sodium Chloride
NEAA	Non-Essential Amino Acids
ng	Nanogram
nm	Nanometer
nM	Nanomolar
NMIBC	Non-Muscle Invasive Bladder Cancer

OAdV	Oncolytic Adenovirus
OV	Oncolytic Virus
PAMP	Pathogen Associated Molecular Pattern
PBS	Phosphate Buffered Saline
PCR	Polymerase Chain Reaction
PD	PD-0332991
PD-1	Programmed Cell Death Protein 1
PD-L1	Programmed Cell Death Ligand 1
PVDF	Polyvinylidene Difluoride
qPCR	Quantitative PCR
Rb	Retinoblastoma Protein
rcf	Relative Centrifugal Force
RC	Radical Cystectomy
RGD	Arginyl-Glycyl-Aspartic Acid
rpm	Rotations Per Minute
RPMI	Roswell Park Memorial Institute Medium
RT	Room Temperature, Reverse Transcription
SD	Standard Deviation
SE	Standard Error
SDS	Sodium Dodecyl Sulphate
SRB	Sulphorhodamine B
TBP	TATA-Box Binding Protein
TCA	Trichloroacetic Acid
TE	Tris-EDTA
TEMED	Tetramethyl ethylene diamine
TAA	Tumour Associated Antigens
TME	Tumour Microenvironment
TURB	Transurethral Resection of The Bladder Tumours
V	Volt
WB	Western Blot
WT	Wild Type
YB1	Y-Box Binding Protein 1

Contents

1. Introduction

1.1.Cancer and the treatment landscape

The treatment landscape of cancer is most rapidly changing owing to the advances in basic research and understanding of the tumour biology (Tsimberidou, Fountzilas et al. 2020). Traditionally, cancer therapy included surgery, radiation, and chemotherapy for most of the last century. However, both radiation and chemotherapy have severe side effects since they also affect healthy cells while effectively killing cancer cells. Towards the end of 20th century, a new mode of therapy called targeted therapy entered the treatment regimen, driven by the progress in understanding of the molecular characteristics of tumour cells (Tsimberidou, Fountzilas et al. 2020). This included development of drugs with intrinsic specificity to target cells based on specific molecules. These drugs showed significant responses in many cancers with tolerable toxicities. Cell surface markers such as receptors or antigens, or genomic alterations in cancer cells were most commonly used to select patients eligible for such therapies, thereby opening avenues for personalised therapy for cancers (Hanahan and Weinberg 2011).

One of the hallmarks of cancers is evasion of the host's immune system, thus making themselves 'invisible' to the immune system (Hanahan and Weinberg 2011). Focus was directed in the past decade to develop immunotherapies to make tumours susceptible to the host immune system. Immunotherapies can vary widely in terms of the mechanisms of treatment, but they share the common aspect of activating the host immune system to detect, neutralize and eliminate the tumour cells (Emens, Ascierto et al. 2017). One such mode is checkpoint blockade, targeting PD-1, PD-L1, CTLA4 receptors which aid in tumour immune escape, which has shown success in a wide range of tumour entities and is better tolerated than cytotoxic therapies. Other modes of immunotherapies include adoptive cell transfer involving modification of host T-cell and reintroducing them in the system to specifically target cancer cells (Zhang and Zhang 2020). Microbial therapies have also been implemented, for example, intravesical immunotherapy using Bacillus Calmette–Guérin therapy in bladder cancer which is one of the most successful immunotherapies in use. While the exact mechanism of action of BCG therapy is still debated, it is understood that the bacteria upon reaching the cancer cells turn the immune system 'on' and attract the host immune system to attack the tumour (Han, Gu et al. 2020). More recently, oncolytic viruses have entered the domain of cancer immunotherapy. These genetically modified viruses can specifically kill the infected cancer

cells and trigger an immune response against the tumours. Combining two or more of these existing options are increasing becoming common since they have shown enhanced efficacy with tolerable side effects, further advancing the current treatment landscape (Mantwill, Klein et al. 2021).

1.2. Oncolytic virotherapy as a novel anti-cancer therapeutic strategy

Oncolytic viruses (OV) as therapeutic agents in cancer have been gaining attention in recent years. The fact that viruses could kill and eliminate tumours was known since the 19th century, where several reports observed tumour regression in patients with viral infections, but little development was seen in the field of virotherapy due to safety concerns and hurdles in genetic engineering (Mantwill, Klein et al. 2021). However, with the advent in modern genetic engineering technologies, understanding of virology and development of viral vectors, oncolytic virotherapy has made a significant progress in the past two decades. Oncolytic viruses, meaning 'cancer-killing' viruses, are wildtype or engineered viruses that can selectively replicate in tumour cells and lead to cell lysis, while leaving the surrounding normal cells unaffected (Fig-1.1). The tumour-selectivity is achieved by making changes within the viral genome making its replication mechanisms dependent on molecular changes of the cancer cells (Goradel, Mohajel et al. 2019, Chaurasiya, Fong et al. 2021, Mantwill, Klein et al. 2021) In addition to their cell lytic ability, they can evoke an immune response not only against the viral infection, but also against the tumour. The ability of OVs to attract the immune system through immunogenic cell death can potentially turn 'cold tumours', which are unlikely to trigger an immune response, into hot tumours, which trigger an immune response. In some studies, abscopal effect has also been observed in distant metastases sites upon treatment with OVs (Havunen, Santos et al. 2018, Kuryk, Moller et al. 2019). A wide range of viruses, such as adenovirus, poxviruses, herpes simplex viruses, rhabdovirus, reovirus, paramyxovirus, parvovirus, and picornavirus, have been tested for their oncolytic potential in the past two decades (Chaurasiya, Fong et al. 2021, Teijeira Crespo, Burnell et al. 2021).

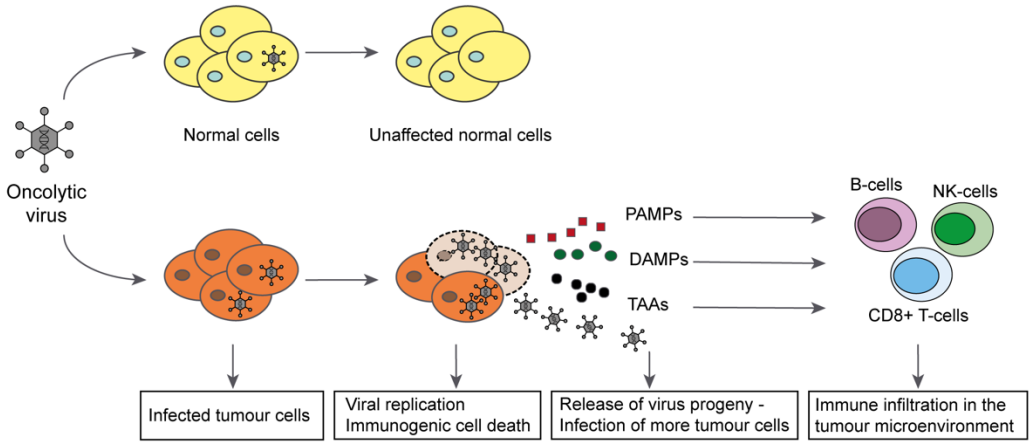

Figure 1.1. *Principle of oncolytic virotherapy.*

In normal, healthy cells, the oncolytic viruses can infect, but cannot replicate, leaving the cells unaffected. In a tumour cell, the oncolytic virus can successfully infect and replicate leading to production of more viral progeny which is then released upon cell lysis. The newly produced viral progeny infects neighbouring tumour cells furthering the infection and leads to tumour clearance. The successful viral infection causes immunogenic cell death (ICD). leading to release of virus progeny, pathogen-associated molecular patterns (PAMP), damage-associated molecular patterns (DAMPs) and Tumour-associated antigens (TAA) into the tumour microenvironment (TME) which attracts the host immune system to the tumour leading to the activation of both innate and adaptive immunity against the tumour (Adapted from Mantwill 2021 (Mantwill, Klein et al. 2021)).

Three OVs have been approved for the treatment of advanced cancers to date (Mondal, Guo et al. 2020). An RNA virus derived from the native ECHO-7 strain of a picornavirus, called Rigvir, was approved for melanoma treatment by Latvia in 2004, which recently showed 4.39–6.57-fold lower mortality in stage-II melanoma patients in a retrospective study (Alberts, Tilgase et al. 2018). In 2005, Chinese food and drug administration approved a genetically modified adenovirus, H101 in combination with cytotoxic chemotherapy, for the treatment of nasopharyngeal carcinoma. A significant breakthrough in the field of OVs happened in 2015 with the approval of Talimogene laherparepvec (T-VEC), an attenuated herpes simplex virus, type 1 (HSV-1) encoding additionally for granulocyte-macrophage colony-stimulating factor (GM-CSF) for the treatment of unresectable melanoma by the U.S. Food and Drug Administration (FDA) (Macedo, Miller et al. 2020, Mondal, Guo et al. 2020). In a multi-institutional retrospective analysis of melanoma patients treated with T-VEC performed in Germany, Austria and Switzerland, an overall response rate of 63.7% (Ressler, Karasek et al. 2021), was observed in patients who received T-VEC. These successful data from a real-life cohort are encouraging to further explore OVs for transition into clinic. Among the several

clinical trials with plethora of oncolytic viruses, oncolytic adenoviruses are the most common ones and are also the most well studied (Macedo, Miller et al. 2020).

1.3. Bladder cancer

Bladder Cancer (BLCA) is one of the most common cancers of the genitourinary tract which includes tumours typically arising from the transitional cells of the bladder wall. Worldwide, it is the 10th most diagnosed cancer, with an incidence of 573,000 and mortality of 213,000 in the year 2020 alone, according to GLOBOCAN estimates, with men being nearly five times more affected than women (Sung, Ferlay et al. 2021). Majority of the bladder cancers are of urothelial in origin that are responsible for around 95%, whereas minority encompasses squamous cell carcinomas, adenocarcinomas, and sarcomas. Geographically, its incidence is highest in Europe, making it a cancer of the developed world. Despite advances in treatment regimen, it is still the costliest cancer to treat in terms of cost per patient due to high rates of recurrence, causing significant burden on the healthcare system (Leal, Luengo-Fernandez et al. 2016, Richters, Aben et al. 2020).

Bladder cancers can be broadly categorised into two subtypes – non-muscle invasive bladder cancer (NMIBC) which represents nearly 75% of all cases, and muscle-invasive bladder cancer (MIBC) (Kamat, Hahn et al. 2016, Minoli, Kiener et al. 2020). The standard therapy for NMIBC includes transurethral resection of the bladder tumours (TURB) followed by adjuvant treatments such as single installation (SI) of Bacillus Calmette–Guérin (BCG) or intravesical chemotherapy with mitomycin C, epirubicin or doxorubicin (Babjuk, Burger et al. 2022). NMIBC shows high rate of recurrence (50-70%) and these patients require extensive lifelong surveillance with cystoscopies, and multiple therapeutic interventions, making BC the most expensive malignancy to treat(Lindskrog, Prip et al. 2021). Patients with high-grade Ta or T1 tumours show a 10-year recurrence-free survival after TURBT and BCG immunotherapy of about 80%. However, about 15% of these patients can also progress into MIBC.

The current standard of treatment for MIBC is neoadjuvant chemotherapy with methotrexate, vinblastine, doxorubicin, and cisplatin or gemcitabine and cisplatin, followed by radical cystectomy (RC) (Tran, Xiao et al. 2021, Witjes, Bruins et al. 2021). Despite RC, nearly half of the patients develop metastasis in distant sites because of disseminated micrometastases (Patel, Oh et al. 2020), and 10-15% of cases present with metastasis at the time of diagnosis. Neoadjuvant chemotherapy is related to high toxicity and causes grade-3 adverse events in

nearly 80% of cases and treatment related deaths have also been reported in 3-4% of cases (Bednova and Leyton 2020). MIBC treatment landscape changed drastically with the introduction of immune checkpoint inhibitors (ICIs) which have drastically low toxicity profile compared to chemotherapeutics (Lenis, Lec et al. 2020). As many as 5 ICIs have been approved since 2016 by the FDA targeting PD-1 or PD-L1 for the treatment of metastatic and refractory bladder cancer, which is an exemplary achievement. The biggest advantage with ICIs is that they have lower and more tolerable toxicity profile when compared to chemotherapeutics. A major disadvantage associated with these drugs is that the response rates are still relatively low, and the cost is exorbitant, and are restricted by the biomarker profile of the patients to make them eligible to receive ICIs (Tran, Xiao et al. 2021).

In addition to ICIs, targeted therapy as a treatment strategy has been explored in the recent years in the treatment of MIBC. Fibroblast growth factor receptor (FGFR) is a receptor tyrosine kinase involved in cell proliferation, survival and migration and its expression level and mutation frequency is elevated in bladder cancers (Lenis, Lec et al. 2020, Tran, Xiao et al. 2021). Erdafitinib, an FGFR kinase inhibitor was approved by the FDA in 2019 for patients with bladder cancer and an FGFR mutation, which are frequently found altered in bladder cancer patients, in nearly 20% of advanced bladder cancer patients (Lenis, Lec et al. 2020, Tran, Xiao et al. 2021). Bladder cancers are highly heterogeneous in histology and in genetic profile, which makes it difficult to have a one-for-all therapeutic approach. Despite advances in therapies in recent years, there is a necessity to develop more targeted therapy approaches and alternative therapy options to be able to achieve better response rates in patients, and to tackle multiple recurrences.

1.3.1. Oncolytic virotherapy in bladder cancer

Bladder cancer is uniquely accessible for therapeutic purposes via the urinary tract. Intravesical administration of drugs not only avoids drug sequestration, but also prevents or minimizes possible toxicity from off- target effects. Intravesical treatment can propagate their immunogenic effects to distant sites. Hence combining therapies that can generate a tolerable local response within the bladder would potentially allow tumour-specific abscopal effects (Li, Zhang et al. 2021). Since intravesical administration of BCG for bladder cancer therapy is already established, it is easy to adapt the technology for administration of oncolytic viruses. The feasible local administration would also avoid any potential immune reaction that may

happen upon systemic administration. The papillary structure of the urothelium increases the surface area for topical application and virus infection (Taguchi, Fukuhara et al. 2017).

A wide range of viruses and oncolytic strategies are currently being tested *in vitro*, *in vivo* and in clinical trials in bladder cancer. A recombinant vaccinia virus expressing influenza hemagglutinin or nucleoprotein antigens was successfully tested in a murine orthotopic bladder cancer model and was well tolerated in a phase-I clinical trial in MIBC patients, with mild dysuria as the most common side effect (Li, Zhang et al. 2021). When compared to intravesical BCG-treatment, intravesical reovirus treatment showed a response rate of 90% in rat models of bladder cancer with significantly less side effects compared to BCG treatment. An oncolytic Herpes simplex virus named Oncovex reduced tumour volumes by 95% in an orthotopic rat bladder cancer model (Li, Zhang et al. 2021).

CAVATAK is a bio- selected formulation of Coxsackie virus A21, which has demonstrated oncolytic and immunotherapeutic activity both *in vitro* and *in vivo* and was well tolerated in a phase-I clinical trial in patients with NMIBC. The Coxsackievirus A21 is being tested in an ongoing clinical trial as a monotherapy and in combination with pembrolizumab in metastatic bladder cancer patients (Li, Zhang et al. 2021).

CG0070, a conditionally replicating oncolytic adenovirus based on serotype 5 is the most studied oncolytic virus in the pipeline for bladder cancer (Ramesh, Ge et al. 2006). Its E1A region is placed under the control of E2F1 promoter, and it also encodes for GM-CSF, a pro-inflammatory cytokine, to induce anti-inflammatory response upon infection. In a phase I clinical trial in patients with NMIBC recurring after intravesical BCG, complete response rate and median duration of complete response were 48.6% and 10.4 months. The most common adverse effects were grade 1–2 bladder toxicities such as dysuria, haematuria, urinary frequency, and urgency. The six-month CR rates in patients with CIS and pure CIS were 50% and 58%, respectively with no development of muscle-invasive disease in patients with CIS. In contrast, progression occurred in approximately 9.8% to 40% of patients with intravesical BCG treatment. This could also be followed up by the interim data from phase-II study where a 6- month CR of 47% was observed, with enhanced efficacy of 55.3% in patients with CIS (Li, Zhang et al. 2021, Mantwill, Klein et al. 2021).

The oncolytic adenovirus that's the focus of this thesis, XVir-N-31, was also shown to induce ICD in an immunodeficient bladder cancer model as evidenced by enhanced release of HMGB1 and exosomal Hsp90 (Lichtenegger, Koll et al. 2019).

1.4. Adenoviruses

Adenoviruses are a family of non-enveloped, icosahedral viruses with double-stranded DNA genome. Currently, there are more than 120 species of adenoviruses identified, which can infect a variety of host species including, but not limited to, humans, monkeys, rats, and reptiles. Human adenoviruses belong to the genus Mastadenovirus, consisting of 51 species which can infect hosts like humans, monkeys, and rats. Human adenoviruses are generally not associated with severe disease in humans upon infection, with the most common manifestations of infection being respiratory diseases, gastroenteritis or adenoviral keratoconjunctivitis (Russell 2009, Kulanayake and Tikoo 2021).

Human adenoviruses are sub-divided into seven species based on their capacity of agglutinating erythrocytes of humans, rats, or monkeys. These species are further categorised into different types, formerly called serotypes, depending on serological cross-neutralisation. Lately genome sequencing is used to define new adenovirus types. There are currently 104 HAdV genotypes known. Different species also exhibit different clinical properties, such as, species B1, C and E cause respiratory disease, in contrast species B, D and E infect mainly the eyes (Russell 2009). Species B2 leads to infections of the kidney and urinary tract, whereas species F are responsible for gastrointestinal infections. Species C, types 2 and 5 are the most used adenoviruses for gene therapy and virotherapy approaches (Braithwaite and Russell 2001).

Adenoviruses are highly immunogenic. The virus capsid and the viral DNA exhibit strong pathogen-associated molecular patterns (PAMPs) that can be detected by host pathogen recognition receptors (PRRs) to trigger an inflammatory response. Cells infected with adenoviruses exhibit immunogenic cell death (ICD) and release PAMPs, damage-associated molecular patterns (DAMPs), tumour-associated antigens (TAA) and neoantigens into the tumour microenvironment, and effectively trigger an anti-tumour response in addition to anti-viral response (Fig-1.1). This characteristic of adenoviruses makes them a lucrative option for cancer immunotherapy to induce host immune response against infection and tumour.

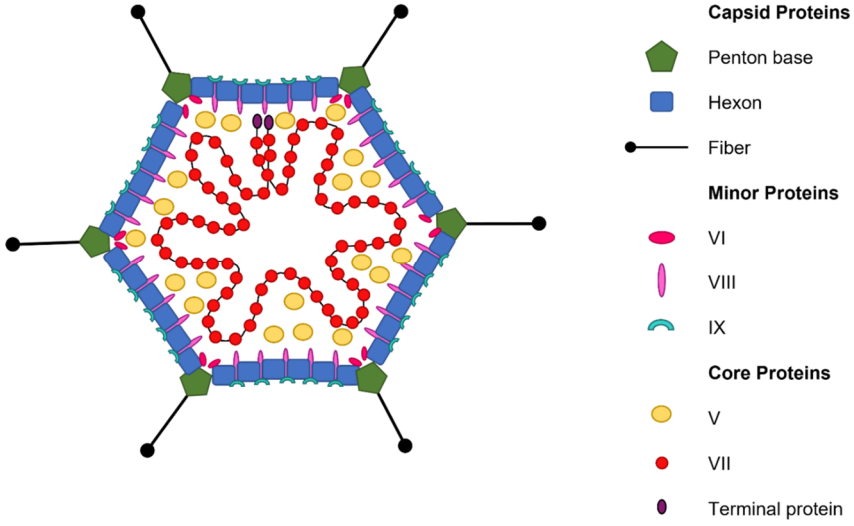

Figure 1.2. *A schematic representation of adenoviral structure and its components.*

Figure adapted from Russell 2009 (Russell 2009).

1.4.1. Adenoviral genome

Adenoviruses are DNA viruses with a double stranded DNA genome of approximately 30-40kb in length covered by an icosahedral capsid, with no envelope (~70 to 100 nm in diameter in size) (Kennedy and Parks 2009). Human Adenovirus serotype, which is the most well characterised one, has a genome of ~36kb. The capsid contains three major capsid proteins, hexon, fibre and penton, and several minor proteins such as VI, VIII, IX, IIIa, IVa2. Inside the virus core, structural components like V, VII, Mu, IVa2 and terminal protein (TP) are associated with the double stranded DNA, and the 23K virion protease, which plays a key role in the assembly of the virion (Russell 2009). The structure of the adenovirus is shown in the figure- 1.2.

The dsDNA genome is linear and flanked by inverted terminal repeats, which serve as the origin of replication. The Adenoviral genome encodes on both the strands for specific genes and exhibit bi-directional transcription. The top strand which reads from rightwards direction during transcription is called r-strand, and the bottom strand which reads leftwards is called l-strand (1977, Zhao, Chen et al. 2014). The adenoviral transcription follows a complex pattern with 8 different transcription units being transcribed from both DNA strands by RNA polymerase II and III. This complex transcription, alternative splicing, and multiple polyadenylation sites give rise to multiple transcripts from each transcription units, also leading to multiple protein isoforms (Braithwaite and Russell 2001).

The adenoviral infection is categorised in two phases- early phase and late phase. The genes are likewise categorised into three groups - early, intermediate, and late genes- based on the temporal pattern of their expression. The adenoviral genome consists of five early transcription units (E1A, E1B, E2, E3 and E4) which are necessary for viral replication and late gene activation, two intermediate transcription units (IX, IVa2) encoding for components of viral capsid, and a major late unit that gives rise to five families of late mRNAs, all of which form viral capsid proteins (Braithwaite and Russell 2001). An overview of adenoviral genome is shown in the figure-1.3.

Figure 1.3. *Genome organisation of human Mastadenovirus type C.*

Detailed organisation of the human Mastadenovirus type C wildtype genome. The genes depicted on the top of the line represent the genes transcribed rightwards from the upper strand, r-strand. The genes depicted beneath the line represent the genes transcribed leftwards from the lower strand, l-strand. Boxes represent viral genes (Mantwill, Klein et al. 2021).

E1A region

E1A is the first transcriptional unit to be expressed after the adenoviral genome enters the cellular nucleus and its activity is imperative in the early stages of infection. It is transcribed from the E1A promoter at the left end of the r-strand of the genome. E1A promoter contains inverted terminal repeats, an enhancer region, and binding sites for several crucial transcription factors, most notably, E2F1 binding site in the enhancer region (Berk 1986).

Extensive deletion analyses have led to the conclusion that E1A is indispensable for viral replication and deletions in E1A lead to highly attenuated viruses. E1A products have also been demonstrated to regulate several cellular promoters either by transactivation or repression (Braithwaite and Russell 2001, Ben-Israel and Kleinberger 2002). It is thought to display a transcription factor like activity to control cellular gene promoters to promote a conducive environment for viral replication. Five different proteins are encoded from the E1A region by alternative splicing- 9S, 10S, 11S, 12S and 13S. Among these, 13S and 12S are the most

important proteins. Under experimental conditions, both proteins can carry out the necessary biological functions required by E1A (Braithwaite and Russell 2001).

E1A products contain 4 conserved regions- CR1, CR3, CR3 and CR4. E1A13S is the largest transcript and the only transcript with all 4 conserved regions (CR). E1A12S lacks the CR3 domain. These conserved regions are crucial for the transcription factor binding and interactions with other cellular proteins. CR2 allows the binding with cellular pocket protein Retinoblastoma (RB) and allows for the release of the transcription factors E2F proteins and initiates gene transcription from cells controlled by RB/E2F cascade, leading to cell cycle progression and S-phase induction. RB/E2F pathway and its role in cell cycle progression have been described in detail in further chapters. Adenoviruses with a mutation in the CR2 domain of E1A can, thus, only replicate in cells with mutated RB (Bressy and Benihoud 2014). The CR3 domain is needed for the transactivation of viral late genes, and viral promoters such as E2-early promoter. The CR2 domain also possesses transactivation activity, but at a much lower extent compared to E1A13S (Berk 1986). The CR3 region has also been shown to recruit p300 to E4-promoter (Pelka, Ablack et al. 2009). These aspects of different binding partners for different CRs facilitate the generation of vectors for oncolytic virotherapy, allowing for cancer specificity.

E1B region

The E1B gene is transcribed from the left end of r-strand, adjacent to E1A. E1B promoter also possesses several binding sites for transcription factors, located in a closely packed region allowing the transcription factors to interact with each other, but is devoid of any E2F binding sites (Berk 1986). Two different proteins are generated by the E1B gene upon alternative splicing. E1B19k protein is homologous to Bcl-2 family of apoptotic proteins and exhibits anti-apoptotic activity by blocking both p53-dependent and p53-independent apoptotic pathways.

E1B55k protein's major documented function is to facilitate the transport of viral late mRNAs to ribosomes for translation. It also forms a complex with E4ORF6, and they both can, independently or together, bind to p53 and interfere with the activation of promoters by p53 and facilitate p53 degradation (Braithwaite and Russell 2001). The role of E1B55kD in cell death regulation is exploited in E1B55kD deleted viruses that can be used for the treatment of cancers. E1B55k-E4ORF6 also allows the translocation of Y-box binding protein 1 (YB-1)

from the cytosol into the nucleus. YB-1 acts as a transcription factor for the E2-late promoter which contains three YB-1 binding sites and stimulates the transcription from E2-late promoter (Holm, Bergmann et al. 2002). This complex is also shown to activate DNA replication by stabilising E1A and amplifying the activation of E2F1 (Dallaire, Schreiner et al. 2016).

E2 region

The E2 region is located on the l-strand with leftwards transcription. This region contains two promoters- E2-early and E2-late. E2-early is active during both early and late stages, however its activity is overshadowed by E2-late in the late phase. E2-early promoter contains 2 key binding sites for E2F1 aligned in the opposite direction to each other. Binding of E2F1 at these sites, TATA-Box binding protein (TBP), and activating transcription factor (ATF) are required for the E2-early promoter activation. The promoter activation is further enhanced by E4orf6 stabilisation of E1A (Swaminathan and Thimmapaya 1996). E2-late promoter on the other hand is E2F-independent. It contains 3 binding sites for YB-1 for its activation (Holm, Bergmann et al. 2002).

The protein products of E2-region are solely involved in viral DNA replication and regulation of viral DNA synthesis. The products include DNA polymerase, a primase (terminal protein) and a DNA-binding protein (DBP-E2A) which helps in denaturation of the template ahead of replication fork. E2B protein serves as DNA polymerase as well as primer for the DNA synthesis initiation (Braithwaite and Russell 2001).

E3- region

Adenoviral E3 region is located on the r-strand and the promoter region overlaps with the E2-early promoter on the opposite strand. E3 promoter does not contain any E2F binding sites. It has been speculated that it's close proximity to E2-early promoters and transcription factors binding sites could affect E3-transcription (Berk 1986). Nine distinct transcripts originate from the E3 region with various roles in modulation of antiviral immune responses by the host. Despite the high number of transcripts arising from this region, it is not indispensable for viral replication (Braithwaite and Russell 2001). It is for this reason that E3 region is deleted in adenoviruses to introduce transgenes in gene therapy and virotherapy approaches.

E4 region

The E4 region is located on the far right end of the l-strand of adenoviral genome, along with E2-early genes. E4 promoter, alike E3 promoter, does not contain any E2F binding sites but is induced by E1A through activation of transcription factors such as p50E4F and ATF. Its activity is also negatively regulated by E2A. A negative feedback loop of E4orf4 in complex with Protein phosphatase 2A (PP2A) regulates the E4 promoter through dephosphorylation of transcription factors, including E1A, leading to decreased transactivation of E1A on the E4 promoter gene (Täuber and Dobner 2001).

E4 region contains several open reading frames with 5 of them containing their own start codons. So far, 7 distinct transcripts have been identified from E4 region. The gene products have been shows to display an array of activities like regulation of viral DNA synthesis, inhibition of cellular protein synthesis, regulating mRNA shuttling, and cell death. E4orf6 regulates viral gene expression and viral DNA replication in complex E1B55k as mentioned before. E4orf6/7 stabilises E2F1 by forming complexes and enhance gene expression from E2-early promoter (Braithwaite and Russell 2001).

Intermediate, late genes and Major late promoter

Intermediate genes are regulated by two promoters, IX and IVa2, which become active after initiation of DNA replication. These proteins, which encode minor components of the virus particle, are expressed at low levels in early phase of infection, but their levels increase gradually with the duration of the infection. Both the proteins also act as transcriptional factors for the major late promoter (MLP) (Tribouley, Lutz et al. 1994, Zhang and Imperiale 2003). Late genes are present on the r-strand and are transcribed rightwards from the major late promoter (MLP). These genes mainly encode for the structural components of the virus particle, like hexon and fiber and is majorly controlled by E1A.

1.4.2. CDK4/6/RB/E2F pathway- Interplay of cell cycle regulation and adenoviral lifecycle

Cell division is a very tightly regulated process, with multiple control mechanisms to ensure the generation of two identical cells from a parental cell. To prevent accumulation and propagation of DNA damage and mutations during cell division, several cell cycle checkpoints operate as DNA surveillance mechanisms. Cell cycle progression happens sequentially through

the gap 1 (G1), synthesis (S), gap 2 (G2) and mitotic (M) stages. This transition from one phase to the next is tightly regulated via a complex signalling network involving consecutive expression of different cyclins and CDKs in a timely manner (Matthews, Bertoli et al. 2022). Before S-phase, a window occurs during which the cell commits to initiate DNA replication and enters the cell cycle. This G1/S transition is the key mechanism that controls cell division and supresses uncontrolled cell proliferation (Matthews, Bertoli et al. 2022).

The key regulator of cell cycle progression is CDK activity. CDK4 and CDK6 complexes are formed in the cells upon receiving mitotic stimuli and bind with cyclin D1. These activated CDK4/6-cyclin D1 complexes can then phosphorylate pocket proteins such as RB, p107, and p130 and inactivate them. In quiescent cells, these pocket proteins bind to transcription factors such as members of E2F family of proteins and repress S-phase entry (Matthews, Bertoli et al. 2022). The growth suppressive properties of RB could be largely attributed to its binding with E2F proteins. This inactivation by CDK4/6 leads to hypo phosphorylation of the pocket proteins, leading to the release of E2Fs from the pocket proteins. The now free E2Fs can subsequently act as transcriptional activators/repressors and initiate transcription of genes involved in cell cycle progression, such as cyclin A, cyclin E and CDK2. Cyclin A and cyclin E interact with CDK2, further phosphorylating RB and other cell cycle mediators allowing the cell to pass the restriction point and progress to S/G2 phase. Thereafter, CDK1 is activated by cyclin A and cyclin B ensuring the cell cycle progression to mitosis (Pan, Sathe et al. 2017).

Adenoviral replication involves a closely intertwined mechanism with the cell cycle regulation. They exploit the cell cycle machinery to interfere with cellular gene expression and utilise it for the progression of adenoviral life cycle. It has been described in literature that adenoviruses require S-phase induction for optimal viral replication, and that cells in G0/G1 phase can provide ideal environment for adenoviral replication (Flint and Shenk 1989, Goodrum and Ornelles 1997). The established model is that the adenoviral E1A protein interferes with RB/E2F complexes and replaces E2F by binding to RB, leading to the release of E2F transcription factors and allowing G1 to S transition (Nakajima, Masuda-Murata et al. 1987). A simplified overview of the interaction of adenoviral replication and RB/E2F cascade is shown in figure-1.4.

A lot of research has been performed to understand the replication machinery of adenoviruses, and most of the breakthrough discoveries occurred in the late 80s and early 90s,

with E2F's role in adenoviral biology being unravelled. The E1A gene is the master regulator of viral replication as it possesses transactivating abilities to almost all viral genes. It has been shown that the CR2 domain of E1A is crucial for its interaction with RB/E2F. E1A-E2F interactions are not direct and pRB/p107 can serve to facilitate these interactions (Fattaey, Harlow et al. 1993). It has also been speculated that E1A CR1 and E2Fs may bind to the same region on pRB, and CR2 binds independently on a different region (Fattaey, Harlow et al. 1993).

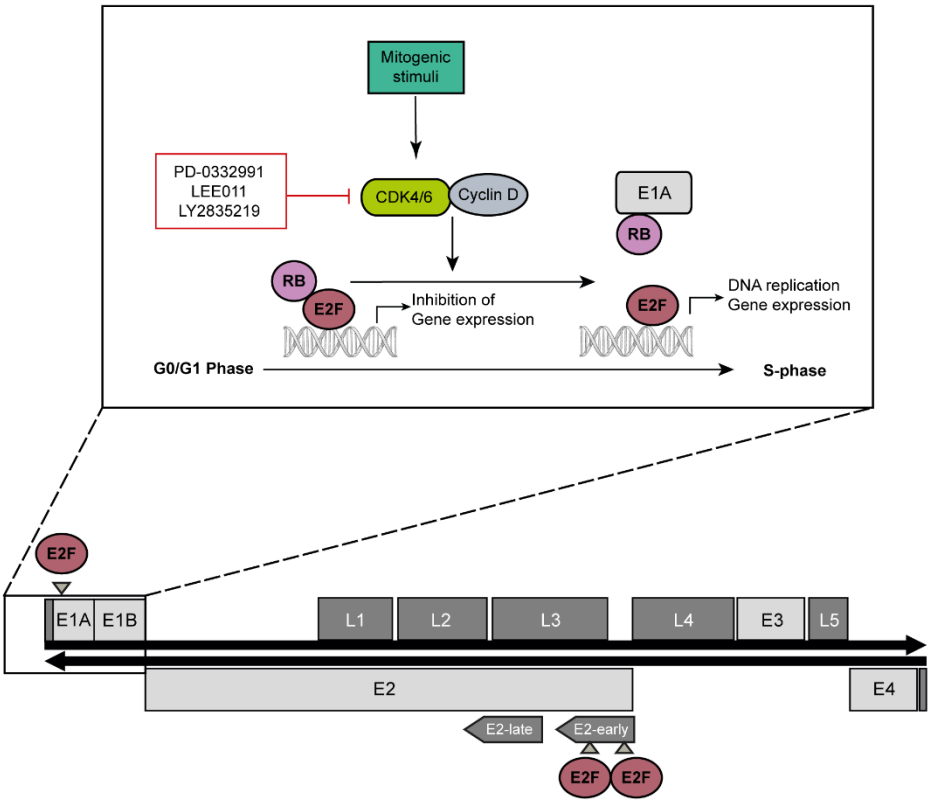

Figure 1.4. *Cell cycle regulation by CDK4/6 and interplay with adenoviral life cycle.*

Regulation of the cell cycle by pocket proteins of RB family, E2Fs, CDKs, and cyclins allowing G1/S transition in the cells- CDK4/6 inhibitors (Palbociclib(PD-0332991), Abemaciclib (LY2835219), and Ribociclib (LEE011)) are shown on the left side. Adenoviral E1A replaces E2F1 by binding with RB, leading to E2F-release. These released E2Fs can thus bind on the E2F binding sites on the adenoviral E1A and E2-promoters (grey triangles) and lead to viral gene expression and DNA replication.

The overview of E1A region and its binding sites with other proteins are shown in figure-1.5. The Adenoviral E2- region possesses two E2F binding sites arranged in a palindrome which are considered indispensable for adenoviral replication (Swaminathan and

Thimmapaya 1996). It also contains additional binding sites for TBP and ATF proteins, which together with E2Fs, regulate the transcription. It has been demonstrated that E1A modulation of E2-early gene requires the activity of a E4 gene product, which was later found, and characterised to be E4orf6/7 (Neill, Hemstrom et al. 1990, Helin and Harlow 1994).

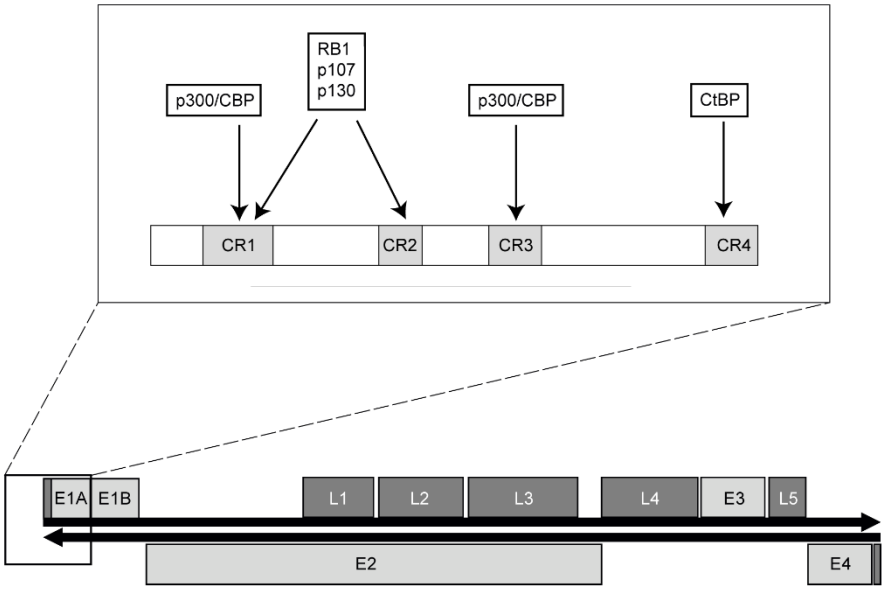

Figure 1.5. *Overview of Adenoviral E1A protein and its binding domains with major interacting proteins.*

The E2F family of transcription factors were initially discovered in context with their activity in the E2-region and were eventually characterised as cellular transcription factors (Kovesdi, Reichel et al. 1986, Kovesdi, Reichel et al. 1987). The described 'E2F' activity is in 2 components- E2F proteins, and their distant relatives- DP family of proteins. E2Fs form heterodimers with DP-1 proteins which are collectively required for its activation of the E2-early promoter (Cress and Nevins 1994, Helin and Harlow 1994, O'Connor and Hearing 1994). E1A protein, which is a major transactivator of E2-genes, acts along with TBP, ATF and E2Fs in a coordinated interaction and complex formation for the activation of E2-early promoter. More recently, it has been demonstrated that E1A can directly interact with E2F/DP1 complexes through a direct interaction with DP1 leading to the complex recruitment at the E2F-regulated promoters (Pelka, Miller et al. 2011).

In addition to E1A, the adenoviral E4orf6/7 protein also mediates the binding of the E2F-DP1 complex at the inverted binding sites at the E2-early promoter sequence by providing a dimerization interface to two adjacent E2F heterodimers. (Raychaudhuri, Bagchi et al. 1990,

Helin and Harlow 1994). Furthermore, it has been shown that the binding of E4orf6/7, and the binding of RB to E2F are mutually exclusive, suggesting that E4orf6/7 may mimic RB in its activity (O'Connor and Hearing 1994). Interestingly, E4orf6/7 also shows transactivating properties at the E2-promoter, but at a much lower level compared to E1A, by direct interaction with E2F/DP1 (Hardy, Engel et al. 1989, Reichel, Neill et al. 1989, Obert, O'Connor et al. 1994, Swaminathan and Thimmapaya 1996). In the absence of the E1A gene products, it has been demonstrated that the expression of the E4orf6/7 protein is sufficient to displace RB protein family members from E2Fs to activate E2-promoter (O'Connor and Hearing 2000). E4orf6/7 can also transactivate the E2-promoter even in the absence of ATF, possibly by promoting E2F-binding at the promoter and stabilising the transcription complex (Nevins 1992, Swaminathan and Thimmapaya 1996). The E4 protein has also been shown to induce an infection-specific DNA-binding activity of E2F upon DNA band shift assays, which was not observed with E1A (Hardy, Engel et al. 1989). Abridging the above findings, E1A and E4 both can interact with E2F proteins and have distinct roles in promoter activation independent of each other.

Babiss et al in 1989 have shown that the relation between E2F activity and E2A expression could only be observed in the early phases of infection but not in late phases, suggesting that E2F may not be required for E2-promoter activity 24hrs after infection (Babiss 1989). E1A protein is shown to stabilise E2F1 protein levels in late phase of infection to maintain cell viability until the completion of viral life cycle (Seifried, Talluri et al. 2008). This suggests that E2F proteins may have varied activities in different phases of infection. Although canonically E2F1-3 proteins have been described as activators, studies have demonstrated that they possess phase-dependent repressor function in certain biological processes such as cellular differentiation and myeloid development (Chong, Wenzel et al. 2009, Trikha, Sharma et al. 2011). However, detailed analyses into the role of E2F proteins in different phases of viral life cycle have not been performed so far.

While the focus of adenoviral gene regulation has largely been on the transactivating properties of E1A on the E2-promoter, little is known about the interaction the other way around. Chang et al have demonstrated that the DNA Binding Protein (DBP) encoded from E2A promoter can influence transcription from E1A, E2A and major late promoters in a plasmid based analysis (Chang and Shenk 1990). The major late promoter showed greater response upon activation by DBP than by the E1A protein, indicating that DBP may have a major role in activation of late gene expression.

E2F1 protein has been the predominant transcription factor of interest in the adenoviral context so far. However, some groups have studied the role of other E2F family proteins in adenoviral life cycle. Recently, it was demonstrated that E4orf6/7 facilitates nuclear localisation of E2F4 protein upon adenoviral infection and binding to the E2-early promoter confirming that E2F4 transactivates this viral early promoter region along with E4orf6/7 (Schaley, Polonskaia et al. 2005). It has also been demonstrated that E1A enhances E2F4 promoter occupancy (Pelka, Miller et al. 2011). While the regulation of E2-early promoter by a complex interaction of multiple transcription factors has been extensively studied, very little is known about the interaction of other E2F proteins with adenoviral genome leaving gaps in the knowledge about the role of E2F proteins on other adenoviral regions, and the individual roles of the E2F proteins other than E2F1 in adenoviral life cycle.

1.4.3. Adenoviruses in Oncolytic virotherapy

Adenoviruses are one of the best studied viruses for gene therapy and virotherapy approaches. They have many advantages in oncolytic therapy, such as their ability to their tropism. Them being double stranded DNA viruses gives a relative ease in their genetic manipulation and they are also comparatively easy to produce in large scale with high purity. They have a high capacity of transgene incorporation, nearly 6kb in non-replicating vectors and 2 kb in oncolytic vectors, to allow for therapeutic transgene expression (Cunliffe, Bates et al. 2020). Oncolytic adenoviruses (OAdV) have been among the earliest OVs to be tested in clinical trials. For example, Onyx-015, an E1B55k mutant adenovirus for selective replication in p53 dysfunctional tumour cells, has been investigated extensively. Even though their efficiency as monotherapy has been limited so far, these studies have demonstrated that administration of OAdVs is well tolerated and safe (Peter and Kuhnel 2020, Mantwill, Klein et al. 2021). A major advantage that OAdVs offer over traditional therapeutics is that they are also effective in tumour stem cells, which enables them to completely eliminate tumours and lower the chances of recurrence (Mantwill, Klein et al. 2021). Increase in release of immunogenic compounds such as HMGB1, Hsp90 have been observed upon oncolytic adenovirus therapy in both *in vitro* and in patients (Farrera-Sal, Moya-Borrego et al. 2021), suggesting that ICD is also a crucial mechanism of action in the therapy.

Replication-competent adenoviruses which are made tumour-specific by introducing genetic modifications are referred to as conditionally replicating adenoviruses (CrAds). So far,

4 different strategies are implemented to render adenoviruses tumour specific and achieve conditional replication. The first strategy is to replace the E1 promoter with cancer-specific promoters such as the prostate specific antigen promoter or the telomerase promoter, to activate viral gene transcription. An example for this type of OAdVs is the Adenovirus CG0070 in which E1A expression is regulated by the cellular E2F1 promoter. The other three strategies involve modifications of the adenoviral early transcription units E1A and E1B to render them dependent upon the cancer cell (Mantwill, Klein et al. 2021). Delta-24, which is also the most widely used backbone for oncolytic adenoviruses, is an example of the OAdVs with E1A deletions. A deletion of 24 base pairs in the CR2 region of adenoviral E1A renders it unable to bind to pRB, and thus cannot release E2F in the cells to initiate replication. Hence it can only replicate in cells with RB dysregulation where E2F is not dependent on RB, which is found in a lot of cancer cells (Mantwill, Klein et al. 2021).

The safety and tolerance of oncolytic adenoviruses have been established in clinical trials so far. However, the *in vivo* efficacy has been limited due to inefficient tumour transduction or immune reactions. Thus, more strategies are employed to enhance oncolytic virotherapy, for example, by combining oncolytic virotherapy with existing cancer treatments such as chemotherapeutic agents or targeted therapies.

1.4.4. The oncolytic adenovirus XVir-N-31

The oncolytic adenovirus used in this study, referred to as XVir-N-31, was first described in 2011 by Holzmuller et al (Holzmuller, Mantwill et al. 2011). The construct contains several deletion sites, and arming strategies to make it cancer-specific and increase infectivity. It contains a deletion in the CR3 domain of E1A region, hence it doesn't produce E1A13S. This leads to attenuated transactivation on E2-early promoter mediated by E1A13S, thus making it dependent on E2-late promoter for E2-gene expression and replication. As mentioned in earlier sections, E2-late promoter contains three YB-1 binding sites and relies on YB-1 for its activation. The lack of E1A13S proteins also leads to a reduction in transactivation of E4 genes, particularly E4orf6, which along with E1B55k plays a crucial role in the nuclear translocation of the transcription factor YB-1 from cytosol. This renders the virus dependent on nuclear YB-1 for its replication. YB-1 can only activate the viral gene expression, and subsequent replication, if it is already present in the nucleus, which is the case for several cancers (Holm, Bergmann et al. 2002, Holm, Lage et al. 2004). Thus, the virus is made cancer-

specific by being nuclear YB-1 dependent. In addition to these changes, XVir-N-31 also lacks the E1B19k protein which is an anti-apoptotic protein. Additionally, 2681 bp were deleted in the E3-region, making the virus susceptible to host inflammatory response, meanwhile providing space for transgene incorporation, for example, PD-L1 antibody (Lichtenegger, Koll et al. 2019). To improve the viral entry into the cell, the fibre gene encodes for an additional arginyl-glycyl-aspartic acid (RGD) motif which can facilitate better viral entry into the cells irrespective of the CAR levels in the host cell (Holzmuller, Mantwill et al. 2011). A schematic of the genetic changes in XVir-N-31 is shown in the figure-1.6.

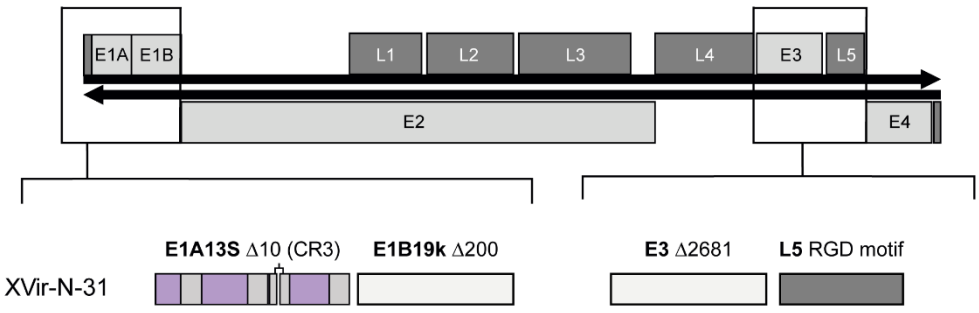

Figure 1.6. *Overview of the structure of the oncolytic adenovirus XVir-N-31.*

A minimal schematic with major adenoviral genes of ADWT is shown in the top panel of the figure. The bottom panel shows the schematic of XVir-N-31 with the changes in comparison with ADWT.

1.4.5. Enhancing Oncolytic Virotherapy with combination therapies

Oncolytic adenoviruses are highly immunogenic and are well tolerated in patients, with limited side effects. However, in terms of efficacy, there is a need for improvement as genetically modified viruses demonstrate reduced replicative ability (data not shown). Several strategies can be implemented to improve the efficiency of various aspects upon infection, such as introduction of transgenes in the viral genome like GM-CSF, improving viral tropism by introducing an RGD motif on the fiber knob. Apart from these modifications in the viral genome, combination therapy approaches are implemented to enhance the oncolytic activity of the viruses, with existing therapies such as chemotherapeutics, targeted therapies, or immunotherapies (Mantwill, Klein et al. 2021).

Some studies have reported that combining oncolytic viruses with chemotherapeutics could enhance viral replication and cell lysis, even though the mechanism wasn't clearly understood. In previous studies by our group, it was shown that YB-1 gets translocated to nucleus in response to irradiation and stress induced by chemotherapy, and a triple therapy with trichostatin, irinotecan and oncolytic adenoviruses could enhance the viral replication (Bieler, Mantwill et al. 2006). It is hypothesised that the topoisomerase I inhibitor irinotecan causes DNA breaks which leads to translocation of YB-1 into the nucleus resulting in activation of viral replication via the E2 late promoter. Alike chemotherapy, radiation can also induce nuclear translocation of YB-1 leading to enhanced viral replication and higher viral yield (Bieler, Mantwill et al. 2006).

As described earlier, adenoviral life cycle is intrinsically intertwined with the molecular mechanisms of the host cell. Using targeted therapies for specific molecules/pathways, the biology of the virus could be exploited to create a feasible replicative environment for oncolytic adenoviruses. The ability of OVs to turn cold tumours into hot tumours makes them a lucrative treatment option in ICI refractors tumours as OVs make tumours susceptible and eligible to ICIs. It was also previously observed that oncolytic adenoviruses (OAdV) work best in immunologically cold tumours (Breitbach, Lichty et al. 2016, Taipale, Tähtinen et al. 2018). To further enhance the immunogenicity of the OVs, several combination therapy regimens with immunotherapy have also been tested. It was observed by Woller et al that OAdV infection could overcome resistance to PD-1 immunotherapy in mice (Woller, Gurlevik et al. 2015). A broader T-cell response and neoepitopes were also observed and the combination approach has inhibited the tumour spread in a CD8+ T-cell dependent manner. In a melanoma model treated with the OAdV ONCOS-102 in combination with checkpoint inhibitor, Pembrolizumab, enhanced immune infiltration has been observed (Kuryk, Møller et al. 2019).

Aside from immune checkpoint blockade, other targets have been explored in combination therapies. Some of the examples of studied targeted therapeutics include mTOR inhibitors (RAD001, Rapamycin) which inhibit mTOR kinases that are involved in cell proliferation, autophagy, apoptosis, immune cell differentiation among other functions, or inhibitors of histone deacetylases that inhibit HDACs which regulate transcription of genes, (Trichostatin, Valproic acid). Studies have shown that small molecule inhibitors also enhance virotherapy by increasing viral replication or tumour cell but unfortunately the molecular mechanisms are not thoroughly investigated. Monoclonal antibodies directed against molecules such as epithelial growth factor receptor (EGFR), cetuximab or anti-vascular

endothelial growth factor (VEGF) antibody bevacizumab showed promising outcomes were observed *in vivo* (Bressy and Benihoud 2014). mTOR kinase is a key protein which is frequently activated in tumours. It has been shown that combination of mTOR inhibitor rapamycin with oncolytic virotherapy led to an increase in enhanced viral replication, and cytotoxicity due to rapamycin induced increase in autophagy (Comins, Simpson et al. 2018). Similar results have also been seen with combining oncolytic viruses with mTOR inhibitor Everolimus (Homicsko, Lukashev et al. 2005). Other kinase inhibitors have also been studied in combination with oncolytic viruses, like, aurora B kinase inhibitor AZD1152, MEK inhibitor CI1040, Chk1 inhibitor UCN-01, all resulting in increased viral replication and cytotoxicity (Bagheri, Shiina et al. 2011, Connell, Shibata et al. 2011, Libertini, Abagnale et al. 2011). Collectively, these studies demonstrate that combination therapies with oncolytic viruses and targeted therapies could be a potentially successful therapy strategy.

1.4.6. Combining the oncolytic adenovirus XVir-N-31 with CDK4/6 inhibitors

The dissociation of RB from E2F is crucial in controlling G1 to S transition, and is part of a complex signalling cascade (Matthews, Bertoli et al. 2022). Dysregulations in this signalling pathway are found in multiple cancers. Thus, targeting these proteins with small molecule inhibitors proves as an attractive strategy for therapy in cancers. Several inhibitors targeting the components of CDK4/6 signaling network have been developed over the years. Next generation CDK4/6 inhibitors were much more refined with selected activity towards CDK4/6 and include Palbociclib (PD-0332991 from Pfizer), Abemaciclib (LY-2835219 from Eli Lilly) and Ribociclib (LEE011 from Novartis). All three of these drugs have different pharmacokinetic properties and clinical toxicities despite similar functioning mechanisms (Finn, Aleshin et al. 2016, Braal, Jongbloed et al. 2021). These inhibitors target the CDKs in RB positive tumour cells to induce cell cycle exit and reduce cell proliferation by cytostatic activity and are largely inactive in RB negative cells making the RB-expression a prerequisite for the therapy. They have shown success in preclinical studies both *in vitro* and *in vivo* in several cancers, like, melanoma, glioma, breast cancer, pancreatic cancer, and metastatic bladder cancer (Pan, Sathe et al. 2017, Iwata 2018). CDK4/6 inhibitors have shown success in clinic, with the major breakthrough being the approval by the FDA for the treatment of Hormone Receptor (HR)-positive and Human Epidermal Growth Factor Receptor 2 (HER2)-negative breast cancer. However, acquired resistance remains a concern, limiting their success.

This encourages the exploration of combinatorial approaches since CDK4/6i have tolerable safety profile.

In previous studies by Jana Annika Koch from our group, we have tried to enhance the oncolytic activity of XVir-N-31 by combining with targeted therapies via small molecule inhibitors (Koch 2021). Connell et al had demonstrated that the Chk1 inhibitor UCN-01 could enhance the effects of oncolytic virotherapy by increasing DNA damage and viral genome replication, leading to an enhanced cytotoxicity in the combination therapy (Connell, Shibata et al. 2011). It was observed by our group that XVir-N-31 showed increased viral genome replication, particle formation and virus-induced cell death upon combination with the Chk-inhibitor UCN-01. However, these effects could not be observed upon combination with AZD-7762, a Chk1 inhibitor with improved specificity, suggesting that the enhanced oncolytic activity by UCN-01 is possibly due to off-target effects of the compound. UCN-01 was also reported to potently inhibit the proteins CDK4 and 6 (Ashwell and Zabludoff 2008). Hence, CDK4/6 inhibitors were used in combination with XVir-N-31 to explore their potential as a combination therapy.

Three specific CDK4/6 inhibitors, Palbociclib, Abemaciclib and Ribociclib, were used in combination with XVir-N-31 and bladder cancer cell lines, and a potent enhancement in oncolytic activity was observed. It was observed that XVir-N-31 showed synergy with CDK4/6 inhibitors in bladder cancer cells that had functional RB-protein. This synergy was also observed in glioblastoma and a xenograft model of sarcoma. In a previously published study by our group, it was showed that functional RB protein is required for the activity of CDK4/6 inhibitors (Sathe, Koshy et al. 2016). A remarkable factor in the observed synergy was that the viral genome replication and particle formation were enhanced upon CDK4/6i even at lower MOIs.

At a molecular level, CDK4/6i leads to reduction in RB and E2F1 protein levels. However, RB levels are partially restored as a resistance mechanism at day-2 after treatment. An increase in protein level was also observed with E2F3 and 4. However, upon combining with adenoviral infection, it was observed that E2F1 levels started recovering 12hrs past infection and completely restored by 24hrs, while the RB levels remained downregulated. As described in the earlier chapter, E2F proteins are crucial for adenoviral gene regulation and transcriptional activation of E1A and E2-early regions. Hence, it comes as a surprise that we observe an enhancement in adenoviral replication in the absence of E2F proteins. It is also quite

interesting that the virus overrides the CDK4/6i mediated downregulation of E2F1 by restoring the E2F1 protein levels within 24hrs (Koch 2021). It has been published earlier that the adenoviral E1A protein stabilised E2F1 levels to keep the cell viable for successful completion of adenoviral life cycle (Seifried, Talluri et al. 2008). The synergy observed upon reduction of RB and E2F1 levels with CDK4/6i raised questions about the roles of these proteins in adenoviral replication. This prompted us to investigate the mechanisms driving the synergy between oncolytic adenoviruses and CDK4/6 inhibitors, and also the role of RB and E2F proteins in adenoviral life cycle, which forms the major focus on this thesis.

1.5. JAK-STAT pathway in Bladder cancer

The JAK-STAT signalling pathway is composed of two main components- Janus Kinases (JAKs) and signal transducer and activator of transcription (STAT). It is one of the most important pathways regulating immune mechanisms in cells. The functions of JAK-STATs encompass a wide array of cellular functions, such as, haematopoiesis, immune regulation, inflammation, tissue repair, adipogenesis, and apoptosis. Hence it is of no surprise to find that it is also widely dysregulated in cancers, since immune dysregulation is one of the hallmarks of cancer (Owen, Brockwell et al. 2019).

JAKs are transmembrane tyrosine kinase molecules belonging to the Receptor Tyrosine Kinase (RTK) family comprising of 4 members- JAK1, JAK2, JAK3 and TYK2. JAK1, JAK2 and TYK2 are expressed ubiquitously whereas JAK3 is predominantly found in haematopoietic cells. Together, these molecules can conduct signal transduction of approximately 60 different cytokines, hormones, and growth factors such as interferons, interleukins, erythropoietin, thrombopoietin, prolactin, and growth hormone (Xiu, Ma et al. 2016). STATs are downstream targets of JAKs, comprising of 7 members- STAT1, STAT2, STAT3, STAT4. STAT5a, STAT5b and STAT6. They play a crucial role in cytokine-mediated signalling, with STAT3 and 5 showing wide range of functions compared the rest of the STATs.

Mechanistically, the JAK-STAT pathway is quite simple in its activation and regulation. A variety of ligands such as cytokines and chemokines, can bind to JAKs leading to their activation. Activation of JAKs lead to their dimerization and thus, facilitating transphosphorylation. The activated JAKs can then interact with, and phosphorylate their key substrates, STATs, leading to dimerization of STATS forming homo, or heterodimers. These

STAT dimers are then translocated to the nucleus where they can initiate signalling at their target genes either by activation or by repression (Xin, Xu et al. 2020). Despite the relatively simplistic nature of pathway activation, events such as selective dimerization, negative pathway regulation, and post-translational modifications of pathway members have characterized the JAK-STAT pathway a complex cascade to understand with many regulatory processes still poorly understood (Xin, Xu et al. 2020).

Activation of JAK-STAT pathway in chemo resistant bladder cancer cells has been demonstrated. Particularly, JAK2 and STAT3 activation was observed suggesting that JAK2 and STAT3 are perhaps involved in tumour recurrence by acquiring resistance to chemotherapy in bladder cancer (Ojha, Singh et al. 2016).

STAT family of proteins have been shown to be dysregulated in many human cancers such as lung cancer, kidney cancer, cervical cancer and they're also associated with poor prognosis (Guo, Yang et al. 2009, Takemoto, Ushijima et al. 2009, Tong, Wang et al. 2017). Dysregulation in STAT3 activation in bladder cancers has been shown in multiple studies with elevated STAT3 levels observed in bladder cancer tissues. More specifically, activated STAT3 has been shown to predominantly localize in the nucleus of cancer cells indicating an increased active-STAT3 (Mitra, Pagliarulo et al. 2009, Shen, Gu et al. 2013, Degoricija, Situm et al. 2014). Furthermore, the nuclear localization of p-STAT3 was observed to be more pronounced in invasive cancer tissues when compared to non-invasive and early-stage cancer tissues suggesting that the higher nuclear localization of p-STAT3 in invasive bladder tumors might be of prognostic importance. Ho et al., have created a transgenic mouse model of invasive bladder cancer by targeting an active dimerized form of STAT3 to the basal cells of bladder epithelium (Ho, Lay et al. 2012). When exposed to carcinogens, the transgenic mice directly developed invasive carcinoma from carcinoma in situ highlighting the possible role of STAT3 in bladder cancer progression. Collectively, evidence suggests that the higher nuclear localization of p-STAT3 in invasive bladder tumors might be of prognostic importance and it is of interest to monitor STAT3 role in bladder cancer disease progression. What is also of interest is that STAT3 is shown to be highly expressed and activated in Bladder cancer stem cells when compared to bladder cancer non-stem cells (Yang, He et al. 2017).

Several studies have studied the prognostic significance of p-STAT3 in bladder cancers. It has been shown that higher p-STAT3 levels were associated with poorer survival (Mitra, Pagliarulo et al. 2009). High STAT3 activation levels are also correlated with invasiveness,

higher grade, and stage of the disease (Chen, Cen et al. 2008, Yang, Shen et al. 2017). From the above-mentioned studies, it could be concluded that STAT3 activation plays a major role in the disease progression in bladder cancers, thus making it an interesting target for therapy in advanced and muscle-invasive bladder cancers.

Several small molecule inhibitors targeting JAKs are already in the clinic for various immune- mediated illnesses, such as, auto-immune disorders and myelofibrosis. Inhibitors against STAT3 have showed preclinical success in various cancers and have successfully been tested in phase-I clinical trials for safety and efficacy in solid tumours (Xin, Xu et al. 2020).

In a CRISPR/dCas9 screening performed by our group to study resistance mechanisms upon CDK4/6 inhibiton in bladder cancer, it was found that the components of JAK-STAT pathway may have a role in mediating acquired resistance (Tong, Sathe et al. 2019). Inhibitors against STAT3 and JAKs could potentially be used to overcome acquired resistance upon CDK4/6 inhibition. It was also observed that combining JAK inhibition with oncolytic viruses could enhance viral replication and cell lysis, in oncolytic herpes simplex virus and vesicular stomatitis virus (Ghonime and Cassady 2018, Patel, Dash et al. 2019). This could possibly be mediated by modulation of interferon signaling upon JAK inhibition. This is an encouraging finding to further explore combination therapies with JAK and STAT inhibitors along with oncolytic adenoviruses.

1.6. Aim of the study

Oncolytic virotherapy is a rapidly expanding mode of therapy in the treatment landscape of cancers. Oncolytic adenoviruses, in particular, have shown remarkable safety profile in clinical trials so far. A major limiting factor for their success is their limited replicative ability in cancer cells which results in incomplete tumour elimination and probably also limited effects on stimulation of the immune system. One way to overcome this drawback is by implementing combination therapy strategies which enhance viral replication and cell killing ability. Our group has earlier demonstrated that the oncolytic adenovirus XVir-N-31 shows remarkable synergy in combination with CDK4/6 inhibitors in bladder cancer (Koch 2021). This strategy also proved to be successful in glioblastoma and sarcoma in other studies in our group (PhD thesis, M. Ehrenfeld and PhD thesis, S. Schober, yet unpublished). As CDK4/6 inhibitors suppress RB/E2Fs, and from established knowledge, it is understood that adenoviruses need RB and E2F for their life cycle, this synergy comes as a surprise. Thus, a thorough investigation of molecular mechanisms underlying this synergy is important in identifying this obviously novel regulatory mechanisms involved in adenoviral life cycle. Understanding this mechanism might result in the design of novel adenoviral therapy strategies with improved efficacy.

In this study, we aimed to:

I. Investigate the dose and time dependency of Palbociclib treatment for the enhancement in oncolytic activity.
II. Investigate the MOI dependency on the adenoviral gene expression upon Palbociclib treatment.
III. Study the functional effects on the cells upon CDK4/6 inhibition by assessing apoptosis and cell death.
IV. Perform temporal analysis of enhancement in viral gene expression upon Palbociclib treatment.
V. Investigating the role of E2F family of proteins in adenoviral replication by using siRNA mediated knockdown.
VI. Studying the importance of E2F-binding sites in adenoviral genome, and the availability of E2Fs, for adenoviral replication using novel adenoviral constructs.
VII. Characterizing JAK-STAT pathway components as therapeutic targets in Bladder cancer as monotherapy, and in combination with oncolytic adenovirus XVir-N-31.

2. Materials and methods

2.1. Materials

2.1.1. Adenoviruses

Table 2.1. Adenoviruses

Name	Producer
ADWT-RGD-dE3	Klaus Mantwill, Klinikum rechts der Isar der TUM, Germany
ADWT/E2Fm	Klaus Mantwill, Klinikum rechts der Isar der TUM, Germany
ADWT/2xE2Fm	Klaus Mantwill and Maximilian Ehrenfeld, Klinikum rechts der Isar der TUM, Germany
ADWT/Trap	Klaus Mantwill, Klinikum rechts der Isar der TUM, Germany
XVir-N-31	Klaus Mantwill, Klinikum rechts der Isar der TUM, Germany

2.1.2. Antibodies

Table 2.2 Antibodies

Name	Cat. no.	Dilution	Producer
E1A	Sc-25	1:100	Santa cruz
E2A		1:100	Kindly provided by M. Dobbelstein, Göttingen University, Germany
E2F1	3742	1:1000	Cell Signaling Technology
E2F3(PG37)	3E2F04	1:1000	Thermo Fisher Scientific
E2F4	sc-398543	1:1000	Santa cruz
GAPDH (14C10)	2118	1:1000	Cell Signaling Technology
Hexon	ABIN2686029	1:1000	Antibodies online
HRP conjugated rabbit-anti-goat	P0449	1:1000	Dako
Peroxidase-conjugated anti-mouse IgG	715-036-150	1:10,000	Dianova

Peroxidase-conjugated anti-rabbit IgG	711-036-152	1:10.000	Dianova
Rb (D20)	9313	1:1000	Cell Signaling Technology
Phospho Rb (Ser 780) (D59B7)	8182	1:1000	Cell Signaling Technology
YB-1 (EP2708Y)	ab76149	1:500	Abcam

2.1.3. Buffers and solutions

Table 2.3. Buffers and solutions

Buffer	**Composition**
Chemiluminescence reagent A	0.1M Tris-HCl (pH 8.5) 2.5mM Luminol 0.4mM p-Coumaric acid
Chemiluminescence reagent B	0.1M Tris-HCl (pH 8.5) 0.18% H_2O_2
DNA Lysis buffer	10mM Tris-HCl (pH 8) 100mM NaCl 25mM EDTA (pH 8) 0.5% SDS
Immunoblotting primary antibody dilution buffer	5% BSA in TBS 0.02% Sodium azide
Immunoblotting blocking solution	5% non-fat milk powder in TBST
Protein loading buffer (4x)	0.25M Tris-HCl (pH 6.8) 8% SDS 0.04% Bromophenol blue 40% Glycerin 100µl 1M DTT to 500µl prior to use
SDS page running buffer (10x)	25nM Tris 192mM Glycine 0.1% SDS (w/v)
SDS protein lysis buffer (1%)	10mM Tris-HCl (pH 7.2)

	1% SDS 1mM Na-orthovanadate one Mini-Protease Inhibitor tablet 10µl/ml phosphatase inhibitor prior to use
Separating gel buffer	1.5M Tris/HCl pH 8.8
SRB staining solution (0.5%)	0.5% SRB (w/v) in 1% acetic acid
Stacking gel buffer	0.5M Tris/HCl pH 6.8
TBE (10x)	1M Tris 1M Boric acid 0.02M EDTA
TBS (10x)	0.5M Tris pH 7.6
TBS-T	0.1% Tween-20 in TBS (1x)
TCA (100%)	0.3M TCA in 22.7ml dH_2O
TE (0.1x)	0.1% TE (100x, pH 8)
Transfer buffer (10x)	25nM Tris 192mM Glycine
Transfer buffer (1x)	10% Transfer buffer (10x) 20% Methanol
Tris base (10mM)	1% Tris Base (1M)
Virus resuspension buffer	20mM Tris 25mM NaCl
Virus storage buffer	20 mM NaCl 25 mM Tris 2.5 % Glycerol

2.1.4. Cell lines

Table 2.4. Cell lines

Cell lines	**Source**
253J	Kindly provided by W. Schulz, Heinrich-Heine-University, Düsseldorf, Germany
639V	Kindly provided by W. Schulz, Heinrich-Heine-University, Düsseldorf, Germany

647V	Leibniz Institute DSMZ- German collection of microorganisms and cell cultures, Braunschweig, Germany
EJ28	Cell Lines Service GmbH
HEK-293	American type culture collection, Manassas, VA, USA
J82	LGC Standards Ltd.
RT112	Leibniz Institute DSMZ- German collection of microorganisms and cell cultures, Braunschweig, Germany
SD	Kindly provided by W. Schulz, Heinrich-Heine-University, Düsseldorf, Germany
T24	American type culture collection, Manassas, VA, USA
UMUC3	American type culture collection, Manassas, VA, USA
UMUC6	Kindly provided by W. Schulz, Heinrich-Heine-University, Düsseldorf, Germany

2.1.5. Cell culture media

Table 2.5. Cell culture media

Medium	**Composition**
Culture medium for cells cultured at 5% CO2	RPMI 10% FBS 1% NEAA 1% PS
Culture Medium for cells cultured at 10% CO_2	DMEM 10% FBS 1% P/S
Freezing Medium	50% RPMI or DMEM 40% FBS 10% DMSO
Infection medium for cells cultured at 5% CO2	RPMI 1% NEAA 1% PS
Infection medium for cells cultured at 10% CO_2	DMEM 1% P/S

2.1.6. Chemicals, reagents, and enzymes

Table 2.6. Chemicals, reagents, and enzymes

Material	**Source**
100% Ethanol	Sigma-Aldrich Chemie GmbH
70% Ethanol	GrüggemannAlcohol Heilbronn GmbH, Heilbronn, Germany
Acetic Acid	Sigma-Aldrich Chemie GmbH
Ammonium persulfate (APS)	Sigma-Aldrich Chemie GmbH
Boric acid	Sigma-Aldrich Chemie GmbH
Bovine serum albumin (BSA)	Sigma-Aldrich Chemie GmbH
Bromophenol blue	Serva
Calcium chloride ($CaCl_2$)	Merck Chemicals GmbH
Chloroform	Sigma-Aldrich Chemie GmbH
Color Prestained Protein Standard, Board Range	New England Biolabs
Complete mini protease inhibitor	Roche
Dimethyl sulfoxide (DMSO)	Sigma-Aldrich Chemie GmbH
Dithiothreitol (DTT)	Cell Signaling
Dulbecco´s Modified Eagle´s Medium (DMEM)	Biochrom
Ethidium bromide (10mg/ml)	Sigma-Aldrich Chemie GmbH
Ethylene diamine tetra acetic acid (EDTA, 0.5M)	AppliChem
Foetal bovine serum (FBS)	Biochrom
Fluoroshield with DAPI	Sigma-Aldrich Chemie GmbH
FuGENE HD Transfection Reagent	Promega Cooperation
Glucose	Sigma-Aldrich Chemie GmbH
Glycine	Sigma-Aldrich Chemie GmbH
GoTaq qPCR master mix	Promega Cooperation
GoTaq Green PCR master mix	Promega Cooperation
Hydrogen chloride (HCl)	Merck Chemicals GmbH
Isopropanol	Sigma-Aldrich Chemie GmbH

Lipofectamine RNAimax	Invitrogen
Magnesium chloride (MgCl)	Sigma-Aldrich Chemie GmbH
Methanol	Sigma-Aldrich Chemie GmbH
Opti-MEM	Invitrogen
Penicillin Streptomycin (P/S; 100x)	Sigma-Aldrich Chemie GmbH
Phenol Chloroform Isoamyl Alcohol (PCI)	Sigma-Aldrich Chemie GmbH
Phosphate buffered saline (PBS, 1x, 10x, 20x)	Biochrom
Phosphatase inhibitor Mix II	Serva Electrophoresis GmbH
Phusion High-Fidelity PCR Master Mix	Thermo Scientific
Precision plus protein standard	BioRad
Proteinase K	Qiagen
Potassium chloride (KCl)	Merck Chemicals GmbH
Skimmed milk powder	Sigma-Aldrich Chemie GmbH
Sodium acetate	Merck Chemicals GmbH
Sodium azide	Sigma-Aldrich Chemie GmbH
Sodium chloride (NaCl)	Merck Chemicals GmbH
Sodium dodecyl sulfate (SDS)	Sigma-Aldrich Chemie GmbH
Sodium orthovanadate	Sigma-Aldrich Chemie GmbH
Sodium phosphate dibasic	Merck Chemicals GmbH
Sulforhodamine B (SRB)	Sigma-Aldrich Chemie GmbH
Tetramethyl ethylene diamine (TEMED)	Carl Roth
Trichloroacetic acid (TCA)	Sigma-Aldrich Chemie GmbH
Tris(hydroxymethyl)-aminomethane	Merck Chemicals GmbH
Triton X-100	Sigma-Aldrich Chemie GmbH
Trypan blue (0.5%)	Biochrom
Trypsin/EDTA	Biochrom
Tween-20	Serva Electrophoresis GmbH

2.1.7. Commercial kits

Table 2.7.Commercial kits

Kit	Cat. No	Source
Caspase -Glo 3/7 Assay	G8090	Promega
CellTiter-blue Cell Viability Assay	G8080	Promega
DNase I digestion Kit	AMPD1	Sigma-Aldrich Chemie GmbH
High-Capacity cDNA Reverse Transcription Kit	4368813	Thermo Scientific
Liquid DAB + Substrate Chromogen System	K3468	Dako
mirVANA miRNA Isolation Kit	AM1560	Thermo Scientific
HiSpeed Plasmid Midi Kit	12643	Qiagen
Pierce BCA Protein assay	23225	Thermo Scientific

2.1.8. Disposable equipment

Table 2.8. Disposable equipment

Equipment	Source
Amersham hybond-P PVDF-Membrane	GE Healthcare
Cell culture plates (96-well, 24-well, 12-well, 6-well, 10cm, 15cm)	Corning Incorporated
Cell culture plates (24-well)	Techno Plastic Products AG
Cell lifter	Sigma-Aldrich Chemie GmbH
Cell lifter with 2-position blade	Sarstedt, Incorporated
Conical tubes Falcon (15ml, 50ml)	Greiner GmbH
Cryogenic vials Nunc (1.8ml)	Thermo Scientific
Gel Saver II – Tips 1-200µl	Kisker Biotech GmbH
Glass coverslips	Corning Incorporated
Hard-shell PCR plates (96-well)	BioRad
Lens cleaning paper	The Tiffen company
Needles (27 Gauge)	BD Biosciences
PCR reaction tubes (0.5ml)	Biozym Scientific

Pipette tips with/without filter	Sarstedt
Reaction tubes (0.5ml, 1.5ml, 2ml)	Sarstedt
Serological pipettes (5ml, 10ml, 25ml)	Greiner Bio-One International AG
Slides, microscope	Merck Chemicals GmbH
Sterile filter Nalgene (0.25µm, 0.4µm)	B. Braun Melsungen AG
Syringes	B. Braun Melsungen AG
White polystyrene plates (96-well)	Corning Incorporated

2.1.9. Multiple use equipment

Table 2.9. Multiple use equipment

Equipment	**Source**
Analytic balance AT250	Mettler Toledo
Autoclave Sytec DX-65	Systec GmbH
Avanti JXN-30 Ultracentrifuge	Beckman Coulter
Biological safety cabinet Herasafe KS12	Thermo Scientific
BVC professional laboratory fluid aspirator	Vacuubrand GmbH
Centrifuge 5430R	Eppendorf GmbH
Centrifuge 5810R	Eppendorf GmbH
Centrifuge ROTINA 35R	Hettich
ChemiDoc XRS Imaging System	BioRad
ChemiDoc MP Imaging System	BioRad
CO_2 incubator HERA Cell240	Thermo Scientific
CO_2 incubator HERA Cell240i	Thermo Scientific
Cold light source Leica L2	Leica Microsystems GmbH
Countess II FL automated cell counter	Thermo Fisher
Cryogenic freezing container, 1 Deg C	Nalgene
Electrophoresis power supply EPS 601	Amersham Pharmacia Biotech
Glassware	Schott AG
Heating and drying oven Heraeus FunctionLine B6	Thermo Scientific
Heating and drying oven Heraeus FunctionLine UT20	Thermo Scientific

Heating block thermostat BT100	Kleinfeld Labortechnik
Ice machine Manitowoc	Manitowoc Ice
Intellimixer RM-2L	Elmi Ltd. Laboratory Equipment
Magnetic Stirrer	Heidolph Instruments GmbH
Microcentrifuge 5430R	Eppendorf GmbH
Microcentrifuge QikSpin QS7000 personal	Edwards Instrument Co.
Micropipettes Pipetman	Gilson Inc.
Micropipettes	Eppendorf
Microplate reader Vmax Kinetic	Molecular Devices
Microscope AxioVert 135	Carl Zeiss
Microscope AxioVert A1	Carl Zeiss
Microscope camera AxioCam ERc 5s	Carl Zeiss
Microscope EVOS M5000	Invitrogen
Mini protean system	BioRad
Mini trans-blot cell transfer system	BioRad
Mini-protean tetra cell gel system	BioRad
Minishaker IKA MS2	IKA Works Inc.
Multilabel plate reader Victor X3	Perkin Elmer
Neubauer chamber	LO Laboroptik
Orbital shaker K15	Edmund Buehler GmbH
Perfect blue gelsystem Mini M	PEQLAB Biotechnologie GmbH
pH Meter 691	Metrohm
Power supply PowerPac HC	BioRad
Pressure cooker	Fissler & Fissler
Spectrophotometer Nanodrop 2000c	Thermo Scientific
Stereo microscope Stemi DV4	Carl Zeiss
Thermal cycler C1000 CFX96	BioRad
Thermal cycler iCycler iQ Real-time PCR detection system	BioRad
Thermal cycler MJ Research PTC-200	BioRad
Trans-Blot Turbo Transfer System	BioRad
Vortex-Genie 2	Scientific Industries

Water bath W350	Memmert
Water purification system, Purelab	ELGA Lab water

2.1.10. Plasmids

Table 2.10. Plasmids

Plasmid	**Source**
pE2-early-luc-Trap	Klaus Mantwill
pE2-early-luc-TrapM	Klaus Mantwill

2.1.11. Primers

Table 2.11. Primers

Name	Company	Forward primer	Reverse Primer
β-actin	Eurofins	TAAGTAGGTGCA CAGTAGGTCTGA	AAAGTGCAAAGAA CACGGCTAAG
E1A12S	Eurofins	CGACGAGGATGAA GTCCTGTGTCTG	CTCAGGATAGCAG GCGCCAT
E1A13S	Eurofins	TGTTTGTCTACAG TCCTGTGTCTG	CTCAGGATAGCAG GCGCCAT
E1B55k	Eurofins	CCTGGCCAGTGTTT GAGCAT	CCCGTTCAGGTTCA CCTTGG
E2-early	Invitrogen	CCGTCATCTCTAC AGCCCAT	GGGCTTTGTCAGA GTCTTGC
E2-late	Apara Bioscience	CTTCCTAGCGACT TTGTGCC	GTCAGAGTGGTAG GCAAGGT
E2F1	Life Technologies	ACGCTATGAGAC CTCACTGAA	TCCTGGGTCAA CCCCTCAAG
E4Orf6	Metabion	TCC CTC CCA ACA CAC AGA GT	GAC AGG AAA CCG TGT GGA AT
Fiber	Eurofins	AAGCTAGCCCTGC AAACATCA	CCCAAGCTACCAG TGGCAGTA
GAPDH	Eurofins	TGGCATGGACTGT	ACTGGCGTCTTCA

		GGTCATGAG	CCACCATGG
Hexon	MWG Biotech AG	GGCCATTACCTTTGA CTCTTC	GCATTTGTACCAGGAA CCAGTC
RB	Life Technologies	AGCAACCCTCCTA AACCACT	TGTTTGAGGTATC CATGCTATCA

2.1.12. Programs and softwares

Table 2.12. Programs and softwares

Program	**Website**
Adobe Illustrator	https://www.adobe.com/de/products/illustrator.html
Adobe Photoshop	https://www.adobe.com/de/products/photoshop.html
Bio-Rad CFX Manager	BioRad, Hercules, CA, USA
cBioPortal	https://www.cbioportal.org/
Compusyn	www.combosyn.com/
ImageJ	https://imagej.nih.gov/ij/
Image Lab	BioRad, Hercules, CA, USA
Microsoft Office	https://www.microsoft.com/de-de/microsoft-365

2.1.13. siRNAs

Table 2.13. siRNAs

siRNA	**Source**
Negative control siPOOL	siTOOLs Biotech GmbH, Planegg, Germany
siE2F1 pool	siTOOLs Biotech GmbH, Planegg, Germany
siE2F3 pool	siTOOLs Biotech GmbH, Planegg, Germany
siE2F4 pool	siTOOLs Biotech GmbH, Planegg, Germany

2.1.14. Small molecule inhibitors

Table 2.14. Small molecule inhibitors

Name	**Target**	**Stock conc.**	**Dissolvent**	**Company**
PD-0332991	CDK4/6	10mM	Water	MedChemExpress

Palbociclib				
BBI608 Napabucasin	STAT3	10mM	DMSO	Selleckchem GmbH
Ruxolitinib	JAK1/2	10mM	DMSO	Selleckchem GmbH
Stattic	STAT3/5	10mM	DMSO	Selleckchem GmbH

2.2. Methods

2.2.1. Cell culture, maintenance, and cryopreservation

Cells were cultured under sterile conditions in laminal flow safety cabinets. Cell lines were grown in 10-cm plates and maintained under sub-confluent conditions with daily monitoring and ensured that they were used for experiments in early passages. Cell lines were cultured in either RPMI medium at 37°C and 5% CO_2 or DMEM medium at 37ºC and 10% CO_2 as per cell line guidelines. Upon reaching 60-70% confluency, cells were split by aspirating cell culture medium, washing with PBS containing 5% 0.5M EDTA, and incubating with trypsin at 37°C until the cells were detached from the surface. Fresh medium was added to neutralise the trypsin, and cells were collected in a falcon tube and spun for 5 min at 300rcf. The cell pellet was resuspended in fresh medium and fraction of cells was seeded in fresh 10-cm plates as recommended by cell line manufacturers. For seeding, cell counting was performed using Countess II FL automated cell counter. Depending on the experiment, 0.2-1x10^6, 0.5-3x10^5, 0.125-1x10^5 were seeded in 10cm, 6-well, or 12-well formats, respectively.

For cryopreservation, cells were dissociated from plates in PBS and trypsin as described above. After centrifugation of cells, the cell pellet was re-suspended in 1ml of freezing medium and transferred into cryovials. Cells were frozen using a freezing container and stored at −80°C for 1-2 days, before transferring to liquid nitrogen. While thawing of cells, the cryovial was thawed in a water bath at 37°C to ensure quick thawing, and then cells were added to a tube containing fresh medium, centrifuged and sub-cultured as described above.

2.2.2. Adenoviral production and preservation

Virus production from G2 stocks was performed using HEK-293 cells. A lower passage of HEK-293 cells were seeded in 20x 15-cm plates and grown till 80% confluency and were infected with 20 MOI of corresponding G2 stock of the adenoviral construct. The G2 stock was diluted in 4ml medium and applied onto the cell layer after aspirating the growth medium and incubated at 37°C for 1hr with gently swirling every 15mins. After 1 hour, 10 ml of growth medium was carefully added onto the cells and the cells were incubated at 37°C for 2 days. After 2 days, cells were observed under the microscope for change in morphology and cytopathic effect and are collected carefully into tubes and centrifuged at 1000rcf for 10 mins. The supernatant was discarded and the pellet from 20 plates was resuspended in 8-10ml resuspension buffer. Intact viruses within the cells were released by subjecting the pellet to repeated freeze thaw cycles three times, and the lysates were stored at -80°C until caesium chloride purification.

The lysates were thawed and centrifuged at 3000rcf for 15 minutes to pellet the cell debris. The supernatant was collected in a fresh tube and incubated with 100U/ml of benzonase and 2mM MgCl2 for 2hrs at 37°C to digest any free cellular DNA in the solution. The purification of virus concentrate was performed by caesium chloride density gradient method. In two ultra-centrifuge tubes, 17ml of a 1.33g/ml caesium chloride solution was pipetted and carefully layered with 9ml of a 1.45g/ml caesium chloride solution. The virus solution was added carefully on top of these two layers of caesium chloride solutions, and then centrifuged at 100,000rcf for 3hrs at 10°C in Avanti JXN-30 ultracentrifuge. The virus particles appear as a visible white band at the interface which is removed using a syringe and needle. A second round of caesium chloride centrifugation is performed to increase the purity by centrifuging again at 100,000rcf for 18hrs. The purified virus band was extracted using a syringe and the salt residues were removed using PD-10 desalting columns. The freshly produced and purified virus was stored in buffers, aliquoted and stored at -80°C.

2.2.3. Adenoviral infection

Cells were seeded for infection in 10cm, 6- or 12-well plates as per the assay requirements and followed up with small molecule inhibitor treatment or transfections as mentioned in the experimental design. 24hrs post treatment/transfection, cells were infected with viruses in the desired MOIs in 2mL, 400µL, or 250µL serum-free medium for 1h respectively and incubated at 37°C for 1hr, with gently swivelling plates every 15mins. Growth medium (2mL or 1mL)

was then added to the cells with and without inhibitors. Cells were processed for further analysis at specific time points after virus infection.

2.2.4. Small molecule inhibitors

Inhibitor stock solutions were prepared as per the concentrations mentioned and in corresponding solvents as per the table 2.1.14. Working solutions were prepared freshly before use in cell culture medium. For inhibitors dissolved in DMSO, highest concentration of DMSO was used as a control.

2.2.5. Serum starvation

Cell culture medium supplemented with serum was aspirated from the wells to be subjected to serum starvation. Fresh medium without serum was added to the wells and cells were grown for 24hrs. After infection, medium with serum was added to the wells for continued growth of cells after infection.

2.2.6. Cell proliferation assays

Cell viability was assessed by either Cell Titer-Blue assay or sulphorhodamine-B assay (Skehan, Storeng et al. 1990). Cell Titer-Blue assay was used to detect cell proliferation upon small molecule inhibitor treatment. 500-700 cells were seeded in 96-well plates and treated with increasing concentrations of the inhibitors on the following day. Cell viability was measured after 72hrs as per manufacturer's protocol using 560nm and 580nm excitation and emission wavelengths respectively. All treatments were performed in triplicate.

Sulphorhodamine-B assay was used to assess virus-induced cell death in combination with small molecule inhibitors. It was also used to measure cell viability upon small molecule inhibitor treatment as monotherapy where mentioned. 0.25-0.5x10^5 cells were seeded and treated with desired concentrations of inhibitors one day after seeding. 24hrs post treatment, cells were infected with desired multiplicity of infection (MOI) of the indicated viruses. The wells were replenished with the inhibitors post infection. Four days after infection (dpi), cells were washed with PBS and fixed with 10% Trichloroacetic acid (TCA) for 1h at 4°C. Cells were washed with cold water and stained with 0.5 % Sulforhodamine B (SRB) for 30min at room temperature (RT), followed by washing with 1% acetic acid to remove excess of SRB. The plates were then allowed to dry to completely remove excess acetic acid. Dried SRB was dissolved in 10mM tris base and quantified by photometric measurement using a multilabel plate reader at 590nm. All treatments and infections were performed in triplicate.

2.2.7. Live cell counting by trypan blue staining

$2x10^6$ were seeded in 10-cm plates and treated with increasing concentrations of the inhibitors the following day. Medium was aspirated and cells were harvested with PBS and trypsin, centrifuged at 300rcf for 5 mins and stained with Trypan Blue. Stained cells were visualized and quantified using Invitrogen EVOS M5000 microscope and live cells were quantified by counting 10x optical fields.

2.2.8. Caspase 3/7 activity

To determine caspase-dependent apoptosis after treatment with Palbociclib, 2000 cells were seeded per well in 96-well plates. 24hrs post seeding, cells were treated with increasing concentrations of the inhibitors for indicated amount of time. Caspase-Glo 3/7 (Promega G8091) and Cell Titer-Blue (Promega G8081) assays were conducted in parallel according to the manufacturer's instructions. The caspase 3/7 activity was quantified from the Caspase-Glo assay was normalised to the number of living cells present in each condition as determined by Cell Titer-Blue assay.

2.2.9. Viral genome replication

Viral DNA replication was determined by a qPCR directed against fiber DNA. 0.5x10^5 cells were seeded in 6-well plates and treated with inhibitors as per the experimental design. Cells were then infected with indicated viruses at desired MOIs. Inhibitors were replenished in the medium after infection for combination treatment conditions. Cells were harvested at 4-72hpi as per experimental design. The medium was aspirated from the wells and cells were washed with PBS once. Cells were lysed using 200µl DNA lysis buffer, and lysates were digested with 3µl proteinase K for 2-24h at 56°C.

DNA was isolated from the lysates using phenol chloroform method. 200µl of phenol chloroform isoamyl alcohol was added to the lysates and vortexed for 30-60 seconds. The mixture was incubated on ice for 5mins and centrifuged at 16000rcf for 5mins at 4°C to allow phase separation. The upper phase was transferred to a fresh tube and 200µl of chloroform was added to remove phenol residues. The samples were mixed carefully by vortexing, incubated on ice for 5mins, and centrifuged at 16000rcf for 5mins at 4°C. The upper phase was transferred to a fresh tube and mixed with 800µl of DNA precipitation buffer (100% EtOH and 3M sodium acetate) and a drop of glycogen to facilitate DNA precipitation. Tubes were inverted thoroughly and centrifuged at 16000rcf at 4°C for 30mins to pellet the precipitated DNA. The supernatants were discarded, and the DNA pellets were washed with 75% EtOH at room temperature for 10

mins and centrifuged at 7500rcf for 5 mins at 4°C. The EtOH supernatant was discarded, and the pellets were airdried in an incubator at 37°C until the pellets become colourless. The dried pellet was then resuspended in 50-100µl of 0.1x TE buffer and the samples were incubated at 40°C on a thermomixer with gentle shaking until the DNA is completely dissolved. DNA concentrations were measured with Nanodrop 2000 and samples for diluted to 10 ng/µl for further use.

2.2.10. Gene expression analysis

0.5x10^5 cells were seeded in 6-well plates and treated with inhibitors as per the experimental design. Cells were then infected with indicated viruses at desired MOIs. Inhibitors were replenished in the medium after infection for combination treatment conditions. Cells were harvested at corresponding time points as per experimental design. The medium was aspirated from the wells and cells were washed with cold PBS once. Cells were lysed using 500µl mirVana RNA lysis buffer and stored at -80°C until further use.

RNA was extracted using phenol-chloroform method. 50µl of RNA homogenising additive was added to the lysates and incubated on ice at 10 mins. 500µl of acid phenol chloroform was added to the lysates and mixed thoroughly by vortexing. The samples were centrifuged at 16000rcf for 5 mins at 4°C for phase separation. The upper phase was transferred to a fresh tube and 500µl of isopropanol was added and mixed thoroughly by inverting the tubes. Samples were incubated for 10mins on ice, and then centrifuged at 16000rcf for 30 mins at 4°C. The supernatants were discarded, and the pellets were washed twice carefully with 75% EtOH for 10 mins on ice, and then centrifuged at 7600rcf for 5 mins at 4°C. EtOH was discarded, and pellets were dried in an incubator at 37°C until it turned colourless, but not completely dry. Pellet was resuspended in 20-50µl of RNase free H2O and incubated at 56°C on a thermomixer to facilitate RNA dissolution. RNA concentration was measured using Nanodrop 2000, and the samples were stored at -80°C until further use.

DNase digestion and Reverse transcription:

DNase digestion was performed after RNA isolation to remove any DNA remnants using Amplification grade DNase I. 1µg of RNA was digested in DNase for 15 mins at room temperature and the reaction was stopped by adding inactivating the DNase by adding stop solution and incubating at 70°C for 10 mins. This DNA-digested RNA is further used for reverse transcription.

RNA samples were reverse transcribed to cDNA using the cDNA reverse transcription kit, Applied Biosystems. 1µg of RNA was used for reverse transcription of viral genes, and 2µg of RNA was used for cellular genes with random primers. A master mix containing deoxynucleoside triphosphates (dNTPs), reverse transcriptase, RNase inhibitor, and random hexamer primers was prepared as per the table 2.15. This was added to the DNase digested RNA samples and incubated in a thermocycle using the program. These samples were then further diluted to 10ng/µl for further use in qPCR.

Table 2.15. Master mix- reverse transcription

Ingredient	**Amount (1x)**
RT buffer (10x)	2µl
dNTP mix (25x, 100mM)	0.8µl
RT random primer (10x)	2µl *
Reverse Transcriptase	1µl
RNAse inhibitor	0.8µl
RNA	2µg
H_2O	upto 20µl

*For RT of viral genes, gene specific primers were used (forward primers for genes on l-strand, and reverse primers for the genes on r-strand) at a concentration of 0.1µM instead of random hexamers were used.

Table 2.16. Reverse transcription program

Step	**Temperature**	**Duration**	**Process**
1	25°C	10 min	Initiation
2	37°C	120 min	Elongation
3	85°C	5 min	Inactivation

2.2.11. Real-time PCR

Real time PCR was performed to determine viral genome replication on the isolated DNA samples, and to assess gene expression in the reverse transcribed cDNA samples. The protocol for master mix is mentioned in the table 2.17. The reactions were performed in 96-well qPCR-compatible plates by mixing 10µl of master mix and 5µl (50ng) of either DNA or cDNA from

previous steps. Non template controls were included by adding nuclease free H_2O instead of nucleic acid samples. Plates were sealed with film, briefly centrifuged, and analysed on Real-Time PCR detection system by BioRad using the corresponding programmes in the genes. The quantification was performed relatively using comparative CT method. For viral genome replication analysis, the CT values of samples were normalised to reference gene and values from 4hpi. For viral gene expression analysis, values were normalised to either reference gene alone, or to reference gene and untreated control sample values as mentioned in the figure legends.

$$\Delta CT = CT\ (gene\ of\ interest) - CT\ (house\ keeping\ gene)$$

$$\Delta\Delta CT = \Delta CT\ (treated\ sample) - \Delta CT\ (control\ sample)$$

$$relative\ normalised\ gene\ expression = 2^{-(\Delta\Delta CT)}$$

$$SD\ \Delta CT = SD\ \Delta\Delta CT = \sqrt{CQ\ SD\ (gene\ of\ interest)^2 + CQ\ SD\ (house\ keeping\ gene)^2}$$

$$SD\ UP = \Delta\Delta CT - 2^{-(\Delta\Delta CT - SD\ \Delta\Delta CT)};\ SD\ DOWN = \Delta\Delta CT - 2^{-(\Delta\Delta CT + SD\ \Delta\Delta CT)}$$

As the housekeeping gene Actin was used and the samples were normalised to their 4hpi values.

Table 2.17. Master Mix for qPCR

	Target gene master mix	Housekeeping master mix
GoTaq qPCR Master Mix	7.5	7.5
Forward primer (1:10)	0.75	0.75
Reverse primer (1:10)	0.75	0.75
Ultra-pure H_2O (DNase/RNase free)	1	1
Total [µl]	**10**	**10**

Table 2.18.qPCR Programme for Fibre

Step	**Temp.**	**Duration**	**Process**
1	94°C	120 sec	Initiation
2	94°C	15 sec	Denaturation
3	60°C	15 sec	Annealing
4	72°C	15 sec	Polymerase activity (go to step 2, 45x)

Table 2.19. qPCR Programme for viral genes

Step	Temp.	Duration	Process
1	94°C	90 sec	Initiation
2	94°C	15 sec	Denaturation
3	58°C	15 sec	Annealing
4	72°C	15 sec	Polymerase activity (go to step 2, 45x)

Table 2.20. qPCR Programme for cellular genes

Step	Temp.	Duration	Process
1	95°C	120 sec	Initiation
2	95°C	15 sec	Denaturation
3	60°C	30 sec	Annealing
4	72°C	60 sec	Polymerase activity (go to step 2, 40x)

2.2.12. Viral particle formation by hexon titre test

Infectious viral particle formation was measured by a hexon titre test. Cells were seeded, treated, and infected as mentioned in 'Viral genome replication' section. At 3dpi, the medium and the attached cells were collected in a 15mL falcon to ensure that all the viral particles within the cells and that are released in the medium are collected. Viruses within the cells were released by repeated freeze-thaw cycles for 3 times, followed by centrifugation at 1600rcf at RT. The supernatants containing the virus particles are transferred to fresh tubes and viral particle determination was performed in HEK-293 cells. $2x10^5$ HEK-293 cells were seeded per well in 24-well plates. The supernatants from the previous step were serially diluted (10^0 – 10^{-4}) and HEK-293 cells were infected immediately after seeding in duplicates for each dilution. At 2 dpi, the wells that do not show obvious cytopathic effect were fixed by aspirating the medium from the wells and drying, and adding 100% ice-cold methanol for 10 mins at -20°C. Cells were then washed twice with 1%BSA-PBS and incubated with 250µl of the goat-anti-hexon primary antibody (AB), diluted 1:500 in 1%BSA-PBS, for 1h at 37°C. The primary

antibody was removed by aspiration and cells were washed again with 1% BSA-PBS for three times. Goat-anti-rabbit secondary antibody was diluted to 1:1000 in 1% BSA-PBS and added to the wells, and the cells were incubated for 1h at 37°C. The wells were washed twice with 1% BSA-PBS to remove the secondary antibody and stained with 250µl of DAB solution. The infected cells turn brown upon adding DAB solution, which can then be counted under the microscope at the desired dilution using 5x magnification and the titer is calculated as follows:

$$Titer\ [pfu/ml] = \frac{average\ number\ of\ positve\ cells/fields * fields/well}{volume\ of\ diluted\ virus\ used\ per\ well\ (ml) * dilution\ factor}$$

2.2.13. Protein expression analysis by western blotting

The expression levels of cellular and viral proteins were measured by immunoblotting. Cells (0.5-2x10^6 cells) were seeded in 10-cm plates. For cellular protein analysis, the cells were treated with the inhibitors on the following day of treatment. For viral protein analysis, cells were infected with viruses on the following day upon seeding and lysates were at the indicated time points.

Protein lysates were prepared on ice at the indicated time points. The medium was aspirated from the wells and the cells were washed three times with ice-cold PBS to ensure that all the residues were removed from the wells. The PBS was then aspirated thoroughly before adding 400-500µl of 1% SDS lysis buffer containing proteinase and phosphatase inhibitors and collected into microfuge tubes. Shear forces were applied to the samples using a 27-gauge needle to breakdown DNA molecules and remove the viscosity, and the samples were centrifuged for 30 min at 30,000rcf at 4°C. The supernatant was collected in a fresh tube and stored at -80°C until further use.

Protein concentrations in the lysates were determined by BCA assay according to the manufacturer's protocol. A standard series was prepared and 112.5µl of working reagent (mixture of solution A and B in 50:1 ratio) were pipetted into 96-well plate. 12.5µl of the standards or samples were added to the wells in duplicates and the plate was incubated at 37°C for 30 min. The absorbance was measured at 562nm, and the protein concentrations of the samples were calculated using the standard curve. Subsequently, the equal concentrations were adjusted with lysis buffer and a mixture of 4x protein loading buffer and DTT was added to the adjusted samples followed by boiling of the samples for 10 min at 100°C.

The samples were then further used in SDS gel electrophoresis. The percentage of the separating gels was decided based on the desired separation of the target proteins, for example, 6, 8, 10, 12 or 15% gels. The gel compositions are mentioned in the table 2.21. The separating gel was poured into the assembled gel casting chamber without any leakages, and isopropanol was added on top to ensure uniform surface. Upon polymerization, isopropanol was discarded the gel surface was gently rinsed with water. Then, stacking gel was poured on top and either a 8-well or 10-well comb were inserted. The polymerised gels were assembled in the gel electrophoresis unit and the samples were loaded onto the wells. Protein ladder was loaded on a well for reference. 1x SDS buffer was added to the electrophoresis tank and run at 90V until the samples enter the separating gel and continued at 150V.

Table 2.21.Separating and stacking gel

	Separation gel (10%)	Stacking gel
ddH_2O	1.5ml	1.4ml
30% Acrylamide	3.3ml	0.5ml
Separation buffer (pH 8.8)	5ml	-
Stacking buffer (pH 6.8)	-	2ml
10% APS	100µl	40µl
TEMED	10µl	4µl
Total [ml]	**10ml**	**4ml**

The samples were run until the dye front reaches the bottom of the gels and the proteins were then transferred on to a PVDF membrane. The membrane was soaked in methanol for 2-5min to activate it, followed by rinsing off methanol in blotting buffer. Sponges were soaked in 1x blotting buffer. The gel plate was removed from the electrophoresis unit and the stacking gel was cut out and discarded. The separating gel was then incubated in blotting buffer for few minutes to remove the residues of SDS buffer. The membrane, gel was assembled between two layers of filter papers and the soaking sponges, and the transfer was carried out in cold 1x blotting buffer for 2h at 100V. Upon completion of transfer, the membrane was then blocked for non-specific binding by incubating in a blocking solution made of 5% milk in TBST for 1h.

The membranes were washed 3-times in TBST upon blocking and incubated with appropriate dilutions of primary antibodies against desired proteins at 4°C overnight. The primary

antibodies residues were removed by washing the membrane with TBST and incubated with corresponding secondary antibody diluted in the blocking solution for 30-60 mins at RT. The membranes were washed thoroughly with TBST, and the proteins were detected using the ECL reaction. Chemiluminescent signals were detected by Chemidoc MP imaging system. The antibody information is described in detail in the table 2.2.

2.2.14. siPOOL transfection

siRNA mediated transient gene knockdowns were performed as per siTools Biotech protocols using reverse transfection method in 6-well plates. A 50nM siRNA prediluted stock was prepared and mixed with OptiMEM for a final concentration of 1nM. RNAiMax transfection reagent was mixed with OptiMEM concurrently. These two solutions were combined by mixing thoroughly in 1:1 ratio and vortexing briefly, followed by a short centrifugation and incubation at 5 min at RT. The mix was transferred to the empty wells in 6-well plates. Cells were harvested, counted, and added to the plates. The cells were gently mixed by pipetting and incubated at 37°C. Viral infection was performed 24hrs after transfection, and the cells were harvested at corresponding time points for further experimental analysis.

2.2.15. Plasmid production and transfection

For the plasmids and empty vectors, corresponding glycerol stocks were amplified in 10 or 100mL LB medium with 0.1% ampicillin overnight at 37°C until the medium turned cloudy. Following day, the grown bacteria were harvested by centrifugation at 3000rcf for 10mins, and a Qiagen mini- or midi-prep was performed according to the manual. The eluted plasmid concentration was measured using nanodrop and stored at 4°C for further experiments.

0.5-1x10^5 cells per well were seeded in 6-well plates overnight. Following day, the required concentration of plasmid DNA was mixed with FuGENE® HD transfection reagent according to the manufacturer's protocol The mixture was incubated at room temperature for 5-10 mins, and gently added to the wells dropwise, and the cells were incubated at 37°C. In case of small molecule inhibitor treatment after transfection, the treatment was performed 6-8hrs after transfecting the plasmid. Viral infection was performed 24hrs after transfection, and the cells were harvested at corresponding time points for further experimental analysis.

2.2.16. Transcriptomics analysis by RNA-Seq:

Library preparation for bulk-sequencing of poly(A)-RNA was done as described previously (Parekh, Ziegenhain et al. 2016). Briefly, barcoded cDNA of each sample was generated with

a Maxima RT polymerase (Thermo Fisher) using oligo-dT primer containing barcodes, unique molecular identifiers (UMIs) and an adaptor. 5'-ends of the cDNAs were extended by a template switch oligo (TSO) and full-length cDNA was amplified with primers binding to the TSO-site and the adaptor. NEB UltraII FS kit was used to fragment cDNA. After end repair and A-tailing a TruSeq adapter was ligated, and 3'-end-fragments were finally amplified using primers with Illumina P5 and P7 overhangs. In comparison to Parekh et al. (2016), the P5 and P7 sites were exchanged to allow sequencing of the cDNA in read1 and barcodes and UMIs in read2 to achieve a better cluster recognition. The library was sequenced on a NextSeq 500 (Illumina) with 57 cycles for the cDNA in read1 and 16 cycles for the barcodes and UMIs in read2. Data was processed using the published Drop-seq pipeline (v1.0) to generate sample- and gene-wise UMI tables (Macosko, Basu et al. 2015). Reference genome (GRCh38) was used for alignment. Transcript and gene definitions were used according to the GENCODE version 38. Differential expression analysis was performed using DESeq2 method (Love, Huber et al. 2014). Gene ontology and KEGG pathway analyses were performed on R Studio.

2.2.17. TCGA analysis

The Cancer Genome Atlas (TCGA) analysis was performed by using the cBioPortal website (www.cbioportal.org). Indicated altered parameters were identified in the TCGA dataset, and the survival analysis was performed.

2.2.18. Statistics

All experiments were performed at least three times unless stated otherwise. Graphs were plotted using Microsoft excel depicting the arithmetic mean ± standard deviation (S.D.) or standard error of the mean (S.E.) as mentioned in the corresponding figure legends. Statistics for comparisons between two conditions were performed by two-tailed Student's t-test using the 'Data analysis' function on Microsoft Excel. $p<0.05$ was defined as significant. * represents $p<0.05$. ** represents $p<0.01$. *** represents $p<0.001$. ns = not significant.

3. Results

3.1. Analysis of oncolytic virotherapy in combination with CDK4/6 inhibitors

CDK4/6 pathway plays a crucial role in cell cycle progression from G1 to S-phase. The RB/E2F pathway which is downstream of CDK4/6 is also crucial for adenoviral replication as evidenced by decades of research into adenoviral biology. It was a serendipitous discovery by our group that CDK4/6 inhibitors enhance replication and cell killing ability of adenoviruses Type 5 (Koch 2021), whereas in principle, they should induce antagonistic mechanisms. Thus, we intended to reveal the molecular mechanisms/factors driving this synergy, to understand the underlying biology. The primary focus of this dissertation research has been to elucidate the mechanisms driving this synergy, and to investigate the roles of E2F proteins in the adenoviral life cycle.

3.1.1. Palbociclib monotherapy does not affect cell death via apoptosis

In a vast majority of studies, CDK4/6 inhibitors induce cell cycle arrest or senescence to an extent, but only in single reports, apoptosis (Goel, DeCristo et al. 2018). Also, replication of adenoviruses relies on a viable host cell (Seifried, Talluri et al. 2008). Since CDK4/6 inhibitors degrade RB, we wanted to explore whether a potential increase in free E2F might lead to an increase in apoptosis. In order to characterize our cellular system used in this respect, we examined apoptosis and cell viability upon treatment with Palbociclib using Trypan Blue staining, and caspase 3/7 activity. No cell death was observed upon Palbociclib treatment, which is plausible since Palbociclib is cytostatic, not cytotoxic (Ingham and Schwartz 2017). We observed a reduction in caspase 3/7 activity in T24 and UMUC3 cells in a dose-dependent manner which could be explained by decrease in E2F1 protein levels upon CDK4/6i (Fig-3.1) which has been reported to be involved in regulation of apoptosis (Ginsberg 2002). These results and the results from other groups consolidate that monotherapy with CDK4/6 inhibitors does not induce apoptosis.

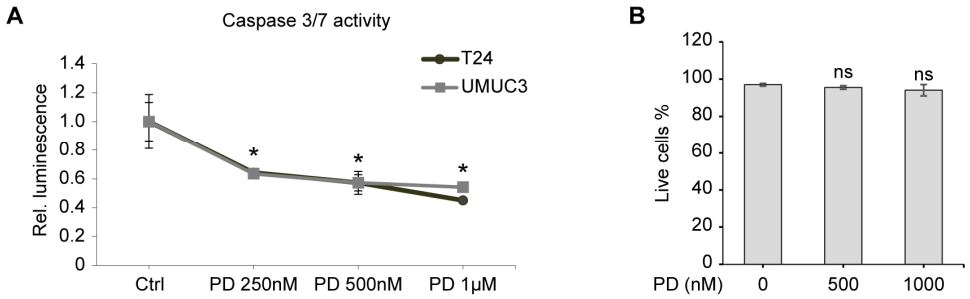

Figure 3.1. *Palbociclib treatment does not induce apoptosis.*

(a) Caspase 3/7 activity was assessed in T24, and UMUC-3 cells treated with increasing concentrations of Palbociclib for 24 hrs as a surrogate marker for apoptosis. Data is shown as luminescence relative to untreated control. (b) Live cell counting was performed by Trypan blue staining in T24 cells treated with indicated concentrations of Palbociclib for 24 hrs. Data is shown as live cell percentage among total cells (Mean ± SE). $p<0.05$.

3.1.2. Serum starvation of cells prior to infection increases adenoviral replication

It has been shown earlier that adenoviruses replicate better under synchronized cell cycle conditions and G0/G1 phase (Ben-Israel and Kleinberger 2002). To determine whether this applies also to our cellular system and the oncolytic adenoviruses, cells were synchronized before infection by serum starvation for 24hrs. DNA was extracted at 24hrs post infection and viral genome replication was assessed by qPCR for fiber DNA. Serum starvation induced a strong increase in viral genome replication accompanied by reduction in RB and phospho-RB levels, as seen via western blotting. While this confirms the published findings that adenoviruses show enhanced replication under G0/G1 arrest, it also suggests that the enhanced replication might be an RB-dependent mechanism (Fig-3.2). The RB dependency is substantiated by the fact that we do not observe an enhancement in the adenoviral activity upon CDK4/6i in RB-negative cells (Koch 2021), emphasising that RB protein is a key element for this combination strategy.

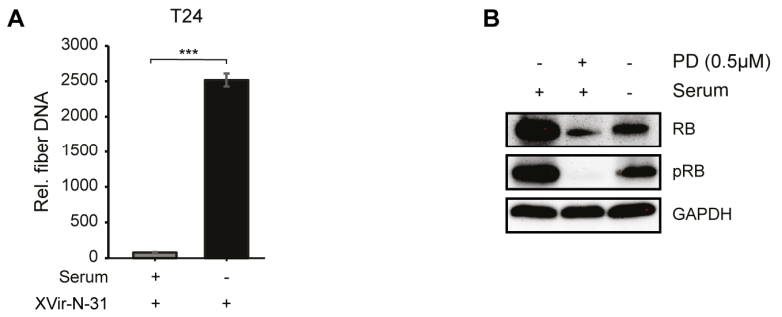

Figure 3.2. *Cell synchronisation by serum starvation induces adenoviral replication.*

(a) T24 cells subjected to serum starvation for 24 hrs prior infection with XVir-N-31 (MOI 50) and viral replication was assessed by qPCR against fiber DNA at 24 hpi. Data is represented relative to fiber DNA at 4hpi as the baseline. Error bars S.D. (b) Protein expression was assessed by western blotting in T24 cells subjected to 24 hrs of serum starvation. GAPDH was used as internal control.

3.1.3. Viral replication enhancement is independent of the timing of CDK4/6 inhibition

The primary effect of CDK4/6 inhibition on cancer cells is G0/G1 arrest (Goel, DeCristo et al. 2018). Since we also observed an enhancement in viral genome replication upon cell cycle synchronisation in our cell system, it was crucial to investigate whether the enhancement upon CDK4/6i is solely because of the G0/G1 arrest. To assess this, T24 cells were treated with Palbociclib with 3 different treatment timings - 24 hrs before infection, 6 hrs before infection, and concurrently with infection, and the cells were then infected with either ADWT or XVir-N-31. Surprisingly, viral genome replication was enhanced in all three timepoints in both ADWT and XVir-N-31 (Fig-3.3). This provides strong evidence that the observed effects of CDK4/6i on adenoviral replication are not simply due to cell cycle synchronisation by it, but possibly regulated by a deeper molecular mechanism.

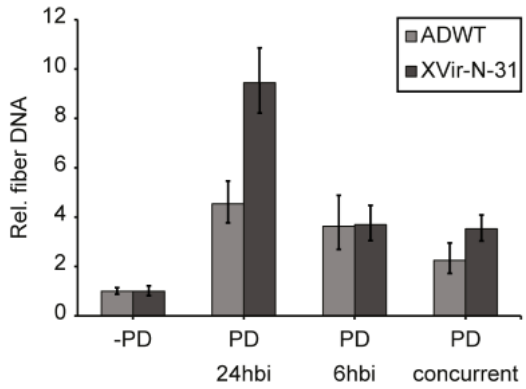

Figure 3.3. *Enhancement of viral genome replication by Palbociclib is independent of treatment duration.*

Viral replication was assessed in T24 cells that were treated with 500nM Palbociclib for either 24 hrs or 6 hrs before infection, or concurrently with infection with ADWT or XVir-N-31 (MOI 50). Fiber DNA was quantified at 24 hpi by qPCR. Error bars S.D.

3.1.4. The effect of CDK4/6i on virus-induced cell death is dose-dependent

The next question we asked was if there is a dose dependent threshold in this combination therapy. T24 cells were treated with increasing concentrations of Palbociclib for 24hrs and infected with MOI 50 of either ADWT or XVir-N-31. Cell viability was measured on day-4 of infection by sulphorhodamine-B assay. It was observed that the enhancement begins at a PD concentration of 50-100nM (Fig-3.4a). Interestingly, cell proliferation in the monotherapy setting was only inhibited from 250nM Palbociclib onwards. At a molecular level, this response to Palbociclib concentration was also observed with dose-dependent decrease in RB protein levels. Thus, the synergy correlates with the reduction of RB protein level in a linear kinetic (Fig-3.4b), underlining that the complete elimination of RB protein is not essential rather only a reduction in the levels is sufficient for the synergy.

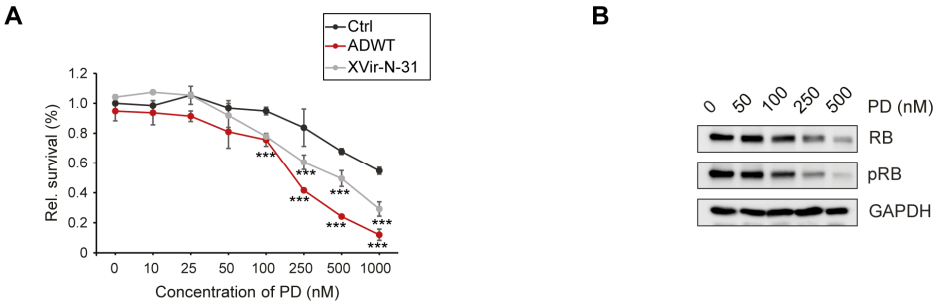

Figure 3.4. *Effect of Palbociclib on virus induced cell killing shows a linear kinetic.*

(a) Cell proliferation was determined in T24 cells that were treated with increasing concentrations of Palbociclib for 24 hrs and infected with ADWT (MOI 50) and XVir-N-31 (MOI 50). Cell viability was measured at 4 dpi by sulphorhodamine B assay. Error bars S.D. $p<0.001$. (b) Protein expression was assessed by western blotting in T24 cells subjected to treatment with increasing concentrations of Palbociclib for 24 hrs. GAPDH was used as internal control.

3.1.5. The effect of CDK4/6i on viral gene expression is not MOI-dependent

Since the effect of CDK4/6i on viral replication is dependent on Palbociclib concentration, we examined the critical threshold of virus is required to observe this effect, which is an important factor from a clinical perspective. To assess this, T24 cells were treated with 500nM Palbociclib for 24hrs before infection and cells were infected with increasing MOIs of XVir-N-31 ranging from MOI 1 to 250. It was observed that a drastic enhancement in viral gene expression was observed in E1A12S and hexon irrespective of the MOIs used, even at lower MOIs where the expression levels in untreated cells were negligible (Fig-3.5). Concurrently, this effect was also observed on viral genome replication where critically low amounts of XVir-N-31 could also successfully replicate in the presence of CDK4/6i (Koch et al. 2022, manuscript under review). This was also confirmed by hexon staining demonstrating higher viral particle production in the presence of CDK4/6i with low viral load. Thus, we conclude that CDK4/6i provide a conducive cellular environment for viral replication and enable viral replication even with low viral load.

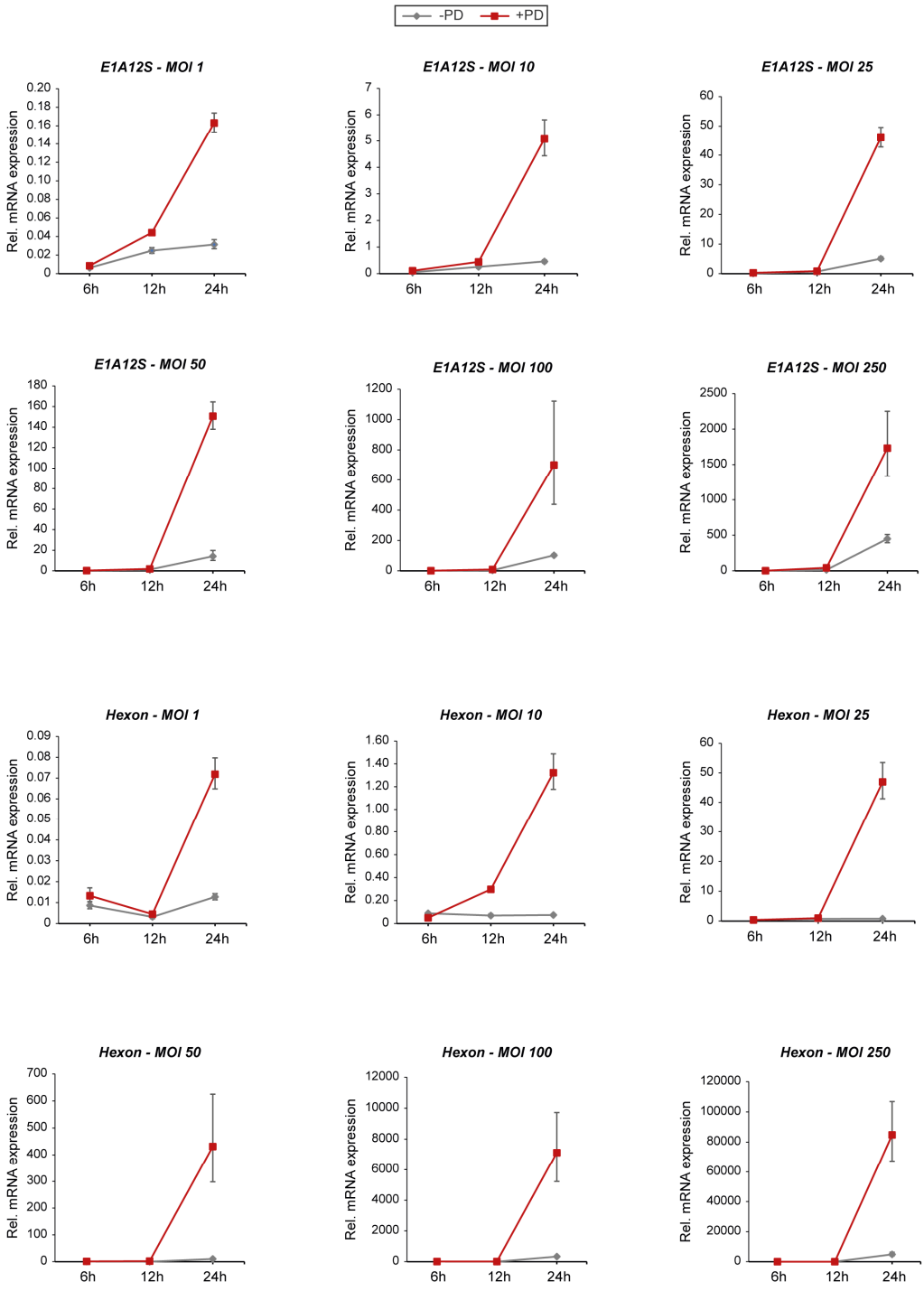

Figure 3.5. *The effect of Palbociclib on viral gene expression is MOI-independent.*

Viral gene expression was evaluated in T24 cells treated with 500nM Palbociclib 24 hrs before infection with indicated MOIs of XVir-N-31. RNA was extracted at indicated time points, cDNA was generated by gene-specific reverse transcription, and qPCR was performed for E1A12S and Hexon genes. Error bars S.D.

3.1.6. Viral gene expression is increased by CDK4/6i at early time points

Since it is established from previous results that the viral replication enhancement is mediated by Palbociclib by unknown mechanisms, the focus is directed to deduce these underlying molecular mechanisms involved in the process. Initially, a detailed time kinetic of viral gene expression was performed upon Palbociclib treatment with both ADWT and XVir-N-31 to determine when exactly in the viral life cycle does the shift occur. Hence, we used a time kinetic spanning both early and late infections including very early time points of 4 and 8 hrs in ADWT. 6hrs was chosen as the earliest timepoint for XVir-N-31 owing to its slower action compared to ADWT. A panel of early and late transcripts were used to detect which genes are affected by CDK4/6i. T24 cells were treated with 500nM Palbociclib for 24hrs and infected with MOI 50 of either ADWT or XVir-N-31. RNA was extracted over a time course, and cDNA was generated for qPCRs by gene-specific reverse transcription. In ADWT, it could be observed that several early transcripts expression levels were increased as early as 8hrs after infection upon Palbociclib treatment (Fig-3.6a). For hexon, there was already a highly significant increase in expression by 16hrs post infection. Similar trend was observed with XVir-N-31 as well (Fig-3.6b). These results imply that the effects of CDK4/6i on viral replication occur during very early stages of infection, perhaps even before the initiation of viral transcription. It also suggests that CDK4/6i presumably changes the molecular milieu of the cells to initiate early gene expression and replication of the adenoviruses

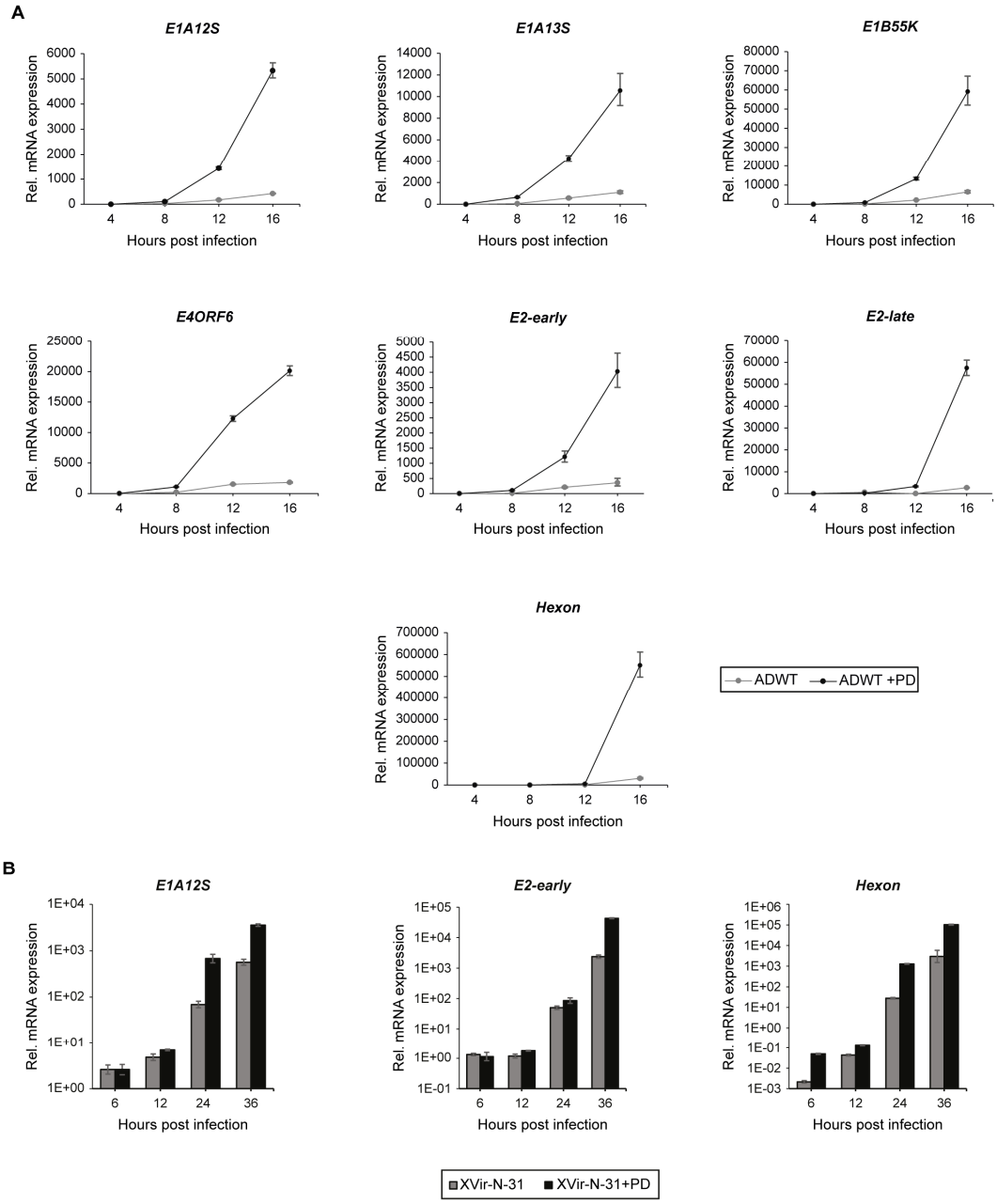

Figure 3.6. *Enhancement in viral gene expression upon CDK4/6 inhibition is observed at early time points.*

(a)Viral gene expression was evaluated in T24 cells treated with 500nM Palbociclib 24 hrs before infection with indicated ADWT (MOI 50). (b) Viral gene expression was evaluated in T24 cells treated with 500nM Palbociclib 24 hrs before infection with indicated XVir-N-31 (MOI 50). RNA was extracted at indicated time points, cDNA was generated by gene-specific reverse transcription, and qPCR was performed for the denoted viral transcripts. Data is represented on log-scale for 3.6B to represent the drastic differences in a legible manner.Error bars S.D.

3.1.7. CDK4/6 inhibition does not affect YB-1 expression

YB-1 is a transcription factor that plays pivotal role in initiating viral replication by mediating transcription of DNA-polymerase from E2- region. Since transcription from E2-region is enhanced at very early time points, it was of interest to investigate whether Palbociclib treatment affects YB-1 levels in the cells, thus triggering an earlier gene expression from E2-region. To assess whether the observed synergy upon CDK4/6i is due to modulation of YB-1 expression, YB-1 protein levels were examined upon Palbociclib treatment. T24 and UMUC3 cells were treated with 500nM Palbociclib and protein lysates were collected at 24hrs post treatment. No effect on YB-1 levels were observed upon CDK4/6i in both these cell lines (Fig-3.7). In an independent experiment, it could also be confirmed by immunofluorescence that CDK4/6i by Palbociclib does not affect the nuclear translocation of YB-1 from cytoplasm in T24 and UMUC-3 cells (Koch et al. 2022, manuscript under review). These results affirm that the observed synergy of CDK4/6i and adenoviruses is independent of YB-1.

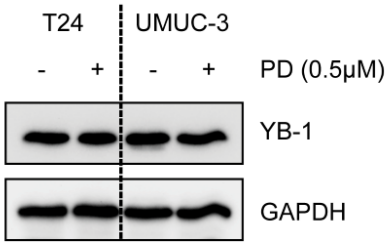

Figure 3.7. *YB-1 protein levels are unaffected by Palbociclib treatment.*

Protein expression of YB-1 was analysed via western blotting at 24 hrs after treatment with Palbociclib in T24 and UMUCV-3 cells. GAPDH was used as internal control.

3.1.8. RB and E2F1 levels increased in a time-dependent manner upon adenoviral infection and CDK4/6i

Further, the focus was directed to identify the changes in cellular environment by analysing the transcriptional changes occurring in RB and E2F1 after adenoviral infection and CDK4/6i, since RB-E2F pathway is implicated in adenoviral replication and modulated by CDK4/6i. Upon monotherapy with Palbociclib, no changes in mRNA levels of RB and E2F1 were observed in the indicated concentration. Adenovirus infection positively altered mRNA levels of both RB and E2F1, which were further enhanced by its combination with CDK4/6i,

in a time-dependent manner (Fig-3.8). This effect was not visible at early time points of infection at 6hrs, but at highest level at 24hrs after infection. However, at protein level, E2F1 was recovered partially at 12hrs post infection, and completely by 36hrs post infection, whereas RB remained downregulated in combination therapy (Koch et al. 2022, manuscript under review). The mRNA and protein level changes indicate that adenoviruses can regulate RB and E2F1 levels even in the presence of CDK4/6i and override the effect of CDK4/6i, and that adenoviruses can stabilise E2F1 protein even under the influence of CDK4/6i. This further hinted that the synergy might be mediated by either RB/E2F1 together as a complex or by either one of the proteins. To investigate this, in the further experiments, attempts were made to elucidate the individual role of E2Fs in adenoviral life cycle.

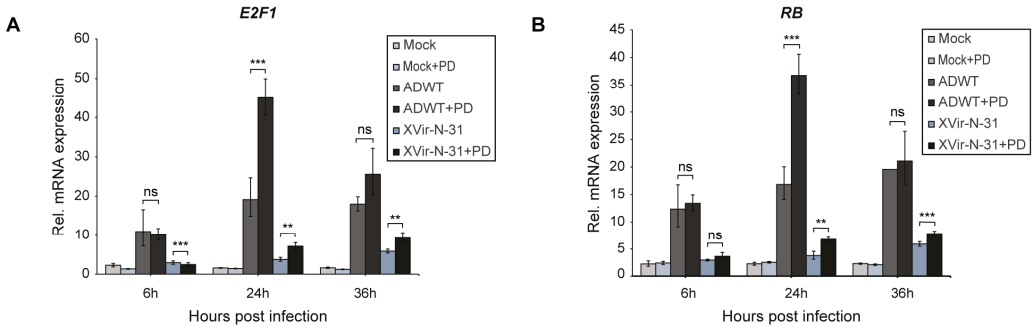

Figure 3.8. *Combination therapy of adenovirus and Palbociclib induces RB and E2F1 transcript expression.*

T24 cells were pre-treated for 24hrs with 0.5µM Palbociclib and infected with ADWT or XVir-N-31 (MOI 50) (a, b) RNA was extracted at indicated time points and cDNA was generated by reverse transcription using random primers. Cellular gene expression was analysed by qRT-PCR at indicated time points for the genes E2F1 (a) and RB (b). Data is presented as relative mRNA expression compared to the housekeeping gene beta-actin. n=3, Error bars S.D. $p<0.05$.

3.2.Investigating the role of RB-E2Fs and E2F binding sites on adenoviral replication

3.2.1. E2F knockdown does not affect viral life cycle

In our previous studies, it was noted that Palbociclib treatment affects the protein levels of E2Fs. While levels of E2F1 are decreased upon CDK4/6i, E2F3 and E2F4 levels are increased (Koch 2021). It is suggested in literature that in the absence of E2F1, other E2Fs show compensatory activity and can take over the roles of E2F1 (Kong, Chang et al. 2007).

Hence, we wanted to determine whether any of the E2Fs E2F1, E2F4, and E2F4 affect viral replication directly.

For this purpose, siRNAs using siPOOL technology were used. Since siPOOLs contain a cocktail of 30 single siRNAs targeting same protein, the knockdown is considered highly reliable (Hannus, Beitzinger et al. 2014). First, the efficiency of the siRNAs was tested by qPCR and western blotting 24hrs after transfection in T24 cells with siRNAs against E2F3 and E2F4. As seen in fig.3.9, the knockdown by siPOOLs was highly efficient and resulted in complete reduction in transcript and protein levels in T24 cells.

In the next step, viral genome replication and particle formation were tested upon siRNA-mediated knockdown of E2F1, E2F3 and E2F4. For this purpose, T24 cells were transfected with siRNAs while seeding to ensure maximum transfection efficiency, and then infected with ADWT or XVir-N-31 24hrs after transfection. Viral genome replication was observed 24hrs after infection by fiber qPCR, and particle formation, 72hrs after infection by hexon titer test. Knockdown of E2F1, E2F3 and E2F4 did not result in an increase in viral genome replication. In hexon titer test, it appeared that there was slight increase in viral particles upon E2F4 knockdown, but it was statistically insignificant (Fig-3.10). These results show that the protein levels of individual E2Fs are not the direct contributing factors for the enhanced viral replication in the combination therapy.

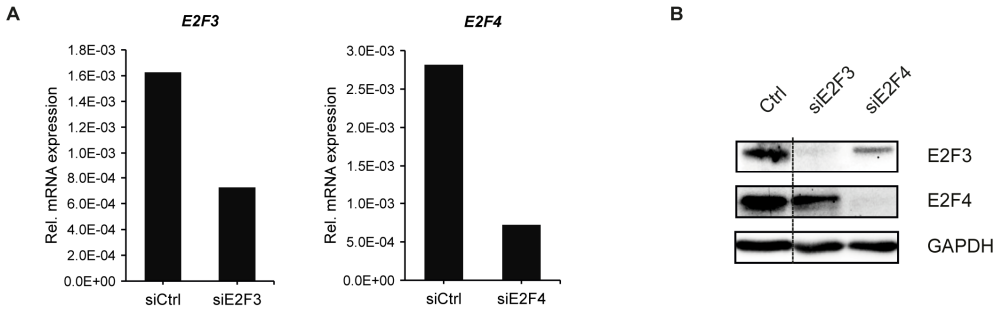

Figure 3.9. *E2F3 and E2F4 are efficiently knocked down by siPOOL siRNAs.*

siRNA mediated knockdown of E2F3 and E2F4 was performed in T24 cells by reverse transfection with siPOOL. Knockdown was confirmed by (a) qPCR and (b) western blotting at 24hrs.

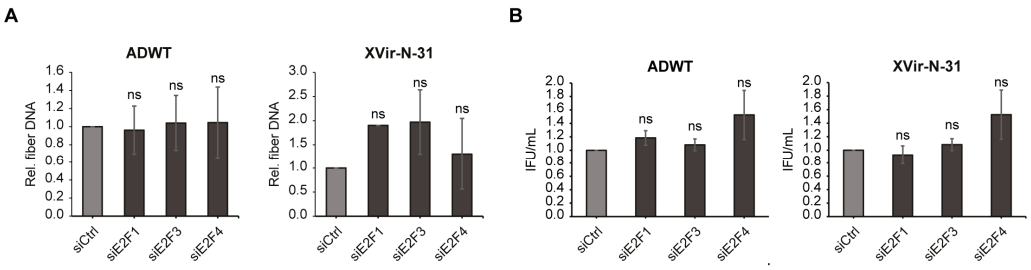

Figure 3.10. *Knockdown of siE2F1, 3 and 4 does not affect viral genome replication and particle formation.*

siRNA mediated knockdown of E2F1,3 and 4 was performed with siPOOL technology in T24 cells for 24hrs and infected with ADWT or XVir-N-31 (MOI 50). (a) Viral genome replication was analyzed at 24hpi. n=4. (b) Viral particle formation was determined by a hexon titer test and represented as infectious units per milliliter (IFU/ml). n=4, mean ± SE.

3.2.2. E2F1 knockdown by siPOOL leads to increase in adenoviral E1A expression

We further investigated whether E2F1 knockdown affects viral protein expression levels. T24 cells were reverse transfected with siPOOL against E2F1 and infected with ADWT (MOI 50), and protein lysates were extracted over a time course of 24hrs. Western blotting was performed to detect cellular protein levels of RB and E2F1 and adenoviral E1A. Interestingly, E2F1 downregulation mediated by knockdown was completely abrogated by adenoviral infection, and a strong recovery of E2F1 was detected at 24hrs. This is accompanied by downregulation of RB at 24hrs. These results correlate with the effects seen upon combination therapy with CDK4/6i. On the adenoviral protein side, strong increase in E1A expression was observed at early time points, suggesting that E2F1 protein availability might have a role in regulation of early viral gene expression (Fig-3.11).

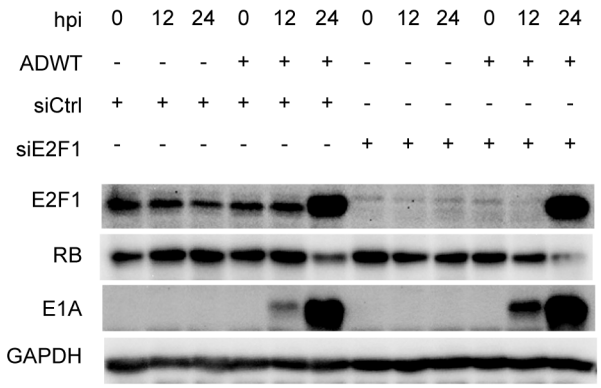

Figure 3.11. *E2F1 knockdown upon siRNA is abrogated upon adenoviral infection.*

siRNA mediated knockdown of E2F1 with siPOOL technology in T24 cells for 24hrs and infected with ADWT (MOI 50). Protein expression was detected by western blotting.

Independently, the role of RB- family of pocket proteins was observed with a similar approach. It was observed that knockdown of RB, but not RBL1 (p107) and RBL2 (p130) led to a marginal increase in viral genome replication (Koch et al. 2022, manuscript under review). This implies that probably only RB protein has a direct role in viral replication at a protein level, but not other pocket proteins of RB family, or E2F transcription factors.

3.2.3. Sequestering of E2F proteins leads to increase in viral replication

Since individually manipulating the E2F protein levels did not affect the viral genome replication, and it is difficult to control the potential compensatory activity of E2Fs in such a condition, alternate approaches have been implemented to study the role of E2Fs on adenoviral replication.

As a first approach, a plasmid-based promoter analysis was performed. An E2-early promoter plasmid was cloned with a luciferase reporter fused with E2F binding sites, wildtype and mutated. These E2F binding sites have been described to 'trap' the free active E2Fs (He, Cook et al. 2000). This resulted in two plasmids, the pE2-early-luc-Trap with wildtype E2F binding sites, and pE2-early-luc-TrapM with mutated E2F binding sites. T24 cells were then transfected with either of the plasmids and treated with 500nM Palbociclib 6hrs after transfection. Cells were infected with ADWT 18hrs after treatment. Luciferase transactivation

and viral genome replication were assessed in these cells. It was observed that the introduction of E2F-trap cassette led to a reduction in the promoter activation, as demonstrated by reduced luciferase activity, emphasizing the importance of E2Fs for E2-early promoter activity (Fig-3.12a). In addition, Palbociclib treatment did not have an effect on this construct. Since the mutated E2F-trap site cannot bind to E2Fs, the activation of E2-early promoter by E2F was not affected. In contrast, an increase in viral genome replication was observed in ADWT upon introduction of E2F-trap cassette compared to the mutated-trap construct (Fig-3.12b).

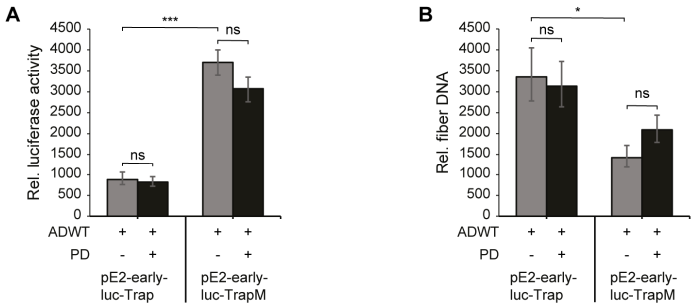

Figure 3.12. *Trapping E2F proteins by plasmids induces adenoviral replication.*

T24 cells were transfected with a plasmid containing 10 E2-early motifs with 20 E2F binding sites (pE2-early-luc-Trap) or with mutated E2F binding sites (pE2-early-luc-TrapM) and were infected with ADWT (MOI 50) 24hrs post-transfection. (a)Luciferase activity was measured to detect promoter activity. Error bars. S.E. (b) viral genome replication was assessed by fiber qPCR. Error bars S.D. $p<0.05$

To further characterize these E2F binding sites in the viral context, and their role on viral genome replication, the E2F-trap cassette was cloned into the adenoviral E3 region, to generate a new viral construct ADWT/Trap. T24 cells were infected with ADWT or ADWT/Trap at different MOIs and viral replication was observed at early and late time points. It was observed that viral replication was significantly increased in ADWT/Trap, particularly at low MOIs compared to ADWT (Fig-3.13a). It was also observed that the effect was seen at a maximum level at early time points of replication i.e., 18hrs, and the differences diminished at later time points (Fig-3.13b). These results with the trap plasmids and trapping virus suggest that the unavailability of E2Fs is not detrimental for viral life cycle. In fact, the viruses replicate better in the absence of E2Fs at early time points suggesting that E2F availability may not be indispensable in adenoviral life cycle and E2Fs might have a repressive activity in the early phase of adenoviral life cycle.

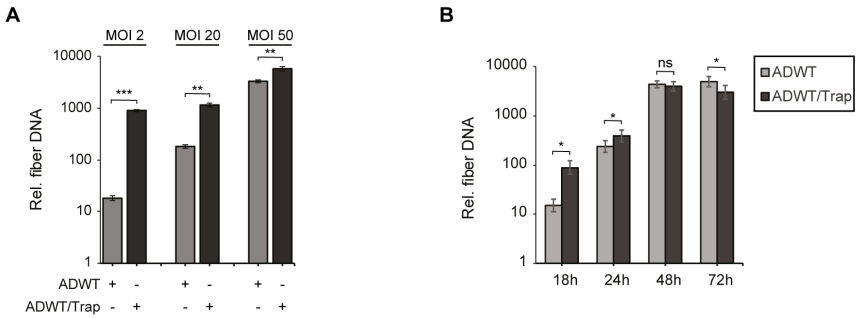

Figure 3.13. *Trapping the available E2F proteins leads to increase in adenoviral replication.*

Viral genome replication was assessed in T24 cells infected with ADWT/Trap or ADWT by fiber qPCR (a) at indicated MOIs and (b) at indicated time points with MOI 10. n=3. Error bars S.D. $p<0.05$.

3.2.4. Mutations in E2F-binding sites in adenoviral E2-region reduces adenoviral replication and gene expression

The previous set of experiments were focused on availability of E2F proteins at adenoviral promoters. Since the binding of E2Fs to the adenoviral promoters is an important aspect of adenoviral replication, attempts were made to elucidate the role of E2F binding sites on adenoviral replication. A mutated adenovirus, ADWT/E2Fm, was generated with two point mutations in its E2F-bindings sites at E2-early promoter, and viral genome replication and gene expression were assessed.

T24 and UMUC-3 cells were infected with either ADWT or ADWT/E2Fm and viral genome replication was analyzed. A drastic reduction in viral genome replication was detected in ADWT/E2Fm compared to ADWT, which substantiates the fact that the E2F-binding sites are crucial for E2-early promoter activity, and thus, adenoviral replication (Fig-3.14).

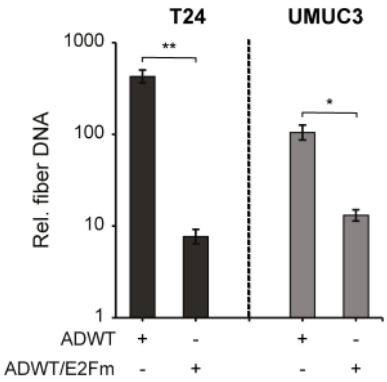

Figure 3.14. *Mutation in E2F-binding sites of adenoviral E2- early region reduces viral replication.*

Viral genome replication was assessed upon E2F-binding site mutation in E2-early promoter in T24 and UMUC-3 cells that are infected with ADWT or ADWT/E2Fm (MOI 10) at 24hpi by qPCR against fiber DNA. Error bars S.D. $p<0.05$.

Next, viral gene expression was assessed for early and late viral genes in a detailed time kinetic. A decrease in E2-early expression was observed, which was expected. Surprisingly, E1A levels were decreased upon mutations in E2-early promoter (Fig-3.15a). This decrease in E1A levels would affect the transactivation of late viral genes, which was confirmed by reduced hexon levels. This also reflected in the reduced protein levels of E1A, E2A and hexon as seen by western blotting (Fig-3.15b). This effect of E2-early promoter mutation on E1A levels was unexpected. E1A enhancer region also possesses an E2F-binding site. We thus speculated that the mutation in E2-early promoter might lead to an increased pool of free available E2Fs which might bind at E1A enhancer region and act as a repressor, and thus suppressing E1A expression. We speculated that this effect could be reversed by Palbociclib treatment, which would result in enhanced E1A expression in ADWT/E2Fm.

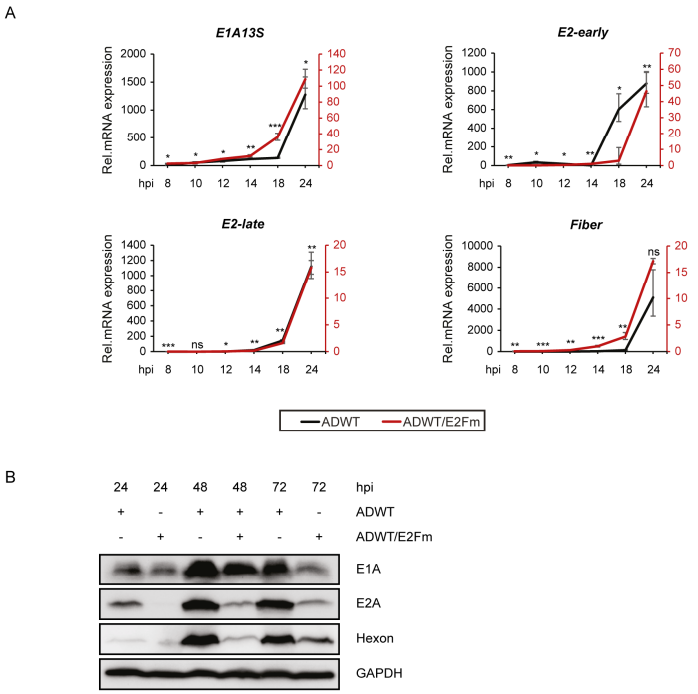

Figure 3.15. Mutation in E2F-binding sites of adenoviral E2- early region reduces viral gene expression and protein levels.

(a) Viral gene expression was studied in T24 cells infected with viruses ADWT or ADWT/E2Fm (MOI 10) at indicated time points after infection. RNA was extracted at indicated time points, cDNA was generated by gene-specific reverse transcription, and expression was assessed by qPCR for the viral E1A13S gene, E2-early transcripts, E2-late transcripts, and fiber gene. Data is represented as relative mRNA expression compared to the reference gene beta-actin. n=3, Error bars S.D. $p<0.05$. (b) Protein expression was analyzed by western blotting in T24 cells infected with ADWT and ADWT/E2Fm (MOI 10) at indicated time points. One representative blot is shown of three independent experiments.

3.2.5. CDK4/6i enhances viral gene expression in ADWT/E2Fm

To determine the effect of E2F-binding sites mutation on the response to CDK4/6 inhibition, T24 cells were pretreated with 500nM Palbociclib for 24hrs and infected with ADWT/E2Fm. RNA was extracted over a time course and viral gene expression was assessed for early and late genes. The analysis showed that the viral gene expression increased consistently in a time-dependent manner, as is observed with ADWT and XVir-N-31, confirming that the effect of Palbociclib on adenoviral life cycle is independent of E2-early promoter region (Fig-3.16a). It was also observed that the ADWT/E2Fm responds much better to Palbociclib treatment compared to ADWT, as evidenced by higher fold changes in response (Fig-3.16b). This confirmed the hypothesis that E2F binding at E1A could have a repressive activity which could be reversed by Palbociclib treatment.

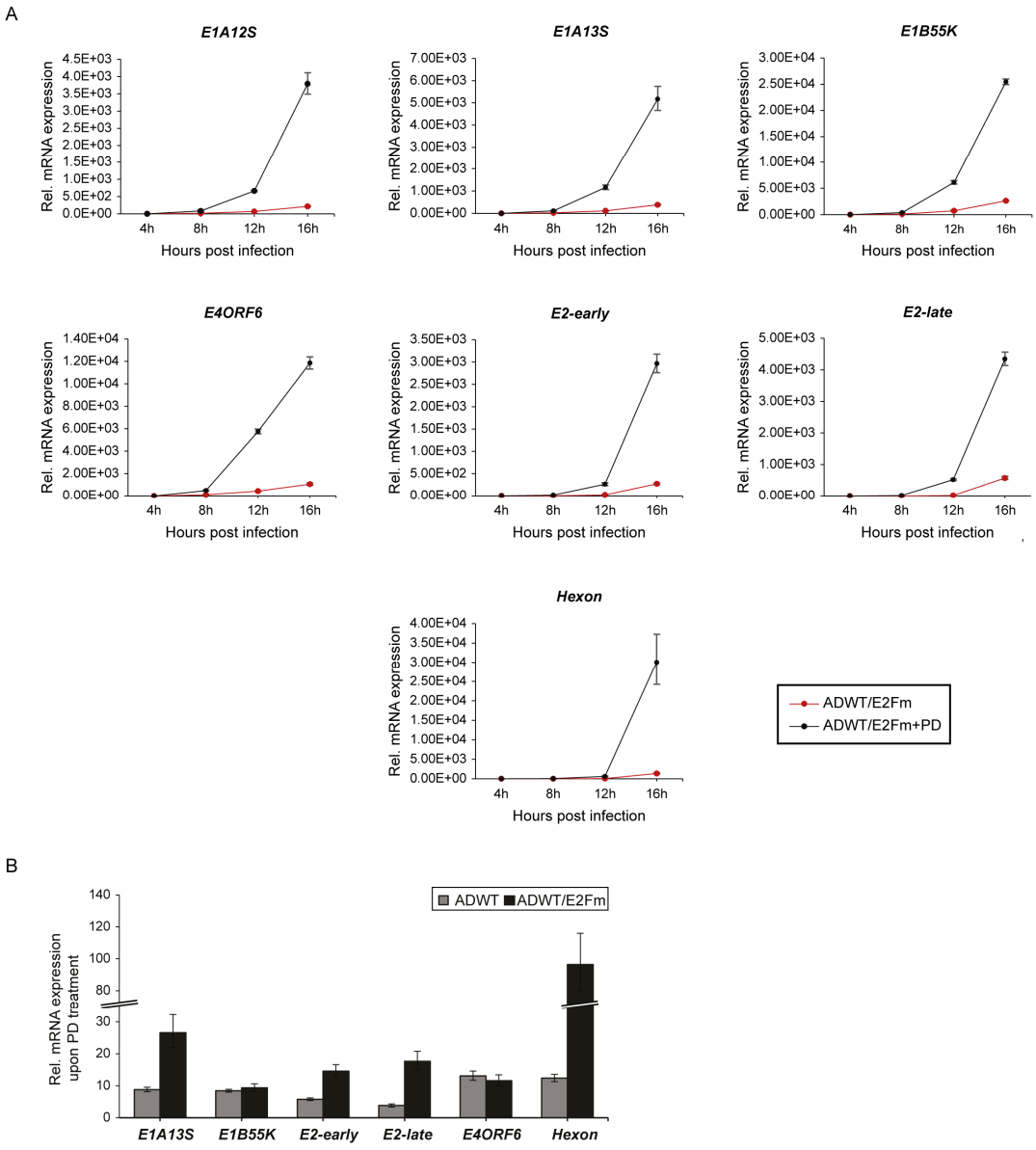

Figure 3.16. *Palbociclib treatment enhances viral gene expression in ADWT/E2Fm.*

(a): Viral gene expression was studied in T24 cells pretreated with 0.5µM Palbociclib and infected with ADWT/E2Fm (MOI 50). RNA was extracted at indicated time points, cDNA was generated by gene-specific reverse transcription, and expression was assessed by qPCR for the indicated viral transcripts. Data is represented as relative mRNA expression compared to the reference gene beta-actin. n=3, Error bars S.D. $p<0.05$. (b) Viral gene expression for indicated genes were assessed by qRT-PCR in T24 cells pre-treated with 0.5 µM Palbociclib and infected with ADWT and ADWT-E2Fm (MOI 50) at 20hpi. Data is represented as the fold increase relative to untreated control. n=3, Error bars S.D.

3.2.6. Compensation of E1A levels restores gene expression in ADWT/E2Fm

Since the mutations in E2-early promoter reduce E1A levels, which would in turn reduce viral gene expression by reduced transactivation, it is difficult to assess the role of E2F-binding site mutations on E2-early promoters alone. We tried to compensate for the diminished E1A by introducing E1A plasmids in T24 cells. T24 cells have low transfection and infection efficiency, and it is hard to ensure that same cells are both transfected and infected. Since this was too difficult to establish, this approach was abandoned as the results did not give any biological insights (data not shown).

To overcome this disadvantage, HEK-293 cells were used, which contain the entire adenoviral E1 region integrated in its genome. HEK-293 cells were infected with either ADWT or ADWT/E2Fm and viral gene expression was studied over a span of 48hrs. The levels of E2-early and hexon transcript levels were reduced at early time points after infection. However, towards the late stages of infection, the transcript levels from ADWT/E2Fm reached up to similar levels as of ADWT (Fig-3.17). This suggests that while E2F-binding maybe important for adenoviral life cycle, it is possibly not indispensable.

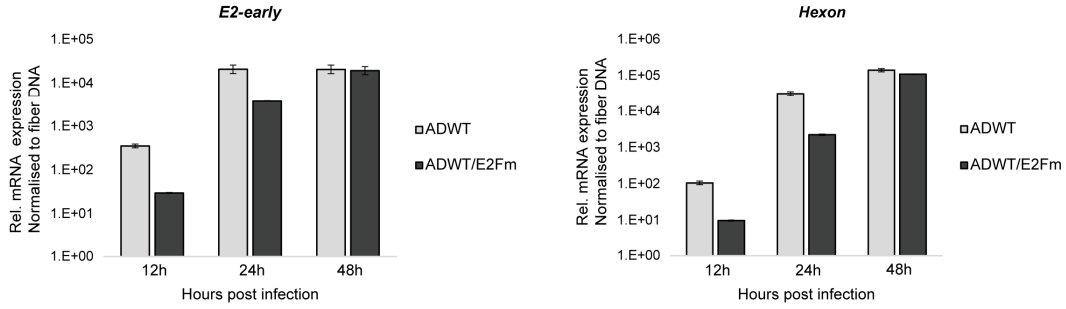

Figure 3.17. *Compensation of E1A protein levels restores viral gene expression of ADWT/E2Fm.*

Viral gene expression of the transcripts E2-early and hexon were assessed in HEK-293 cells infected with either ADWT or ADWT/E2Fm (MOI 1) by qRT-PCR. Data is represented as the viral transcripts relative to incoming fiber DNA at 4h. Error bars S.D.

To summarise the results upon E2F proteins manipulation,

- Knockdown of E2F-1,3 and 4 proteins does not affect viral replication.
- E2F1 knockdown leads to enhanced expression of E1A at 12hrs, and recovery of E2F1 is observed at 24hrs upon ADWT infection.

- The introduction of E2F-trapping sites via plasmids led to reduction in E2-early promoter activity, but increased replication.
- Trapping on E2Fs by additional E2F binding sites led to an increase in adenoviral genome replication.
- Mutation in E2F binding sites of E2-early promoter led to a reduction in E1A levels.
- When E1A levels are compensated, the gene expression from ADWT/E2Fm is nearly the same as ADWT.
- CDK4/6 inhibition on ADWT/E2Fm leads to an increase in viral gene expression, and the fold increase is much higher compared to ADWT, possibly by the reversal of E2F's repressive effect on E1A enhancer region.

The ADWT/Trap results also suggest that adenoviruses can replicate earlier and better when E2Fs are unavailable. In literature, E2F1 has been described to have a canonically activator role. Since the observed results and proposed hypothesis is contradictory to published literature, it is imperative to show the excess binding of E2F1 at E1A-enhancer region. To prove this, a chromatin immunoprecipitation was performed by our group, and it was proved that there is indeed higher E2F1-binding at the E1A-enhancer region in ADWT/E2Fm compared to ADWT (Koch et al. 2022, manuscript under review). Hence, we next directed our focus to understand the E2F-binding site at E1A-enhancer region.

3.2.7. Mutation in E2F binding sites in E1A-enhancer does not affect E1A expression

To characterize the E2F-binding site in E1A-enhancer region, a new adenoviral construct was generated (Maximilian Ehrenfeld, PhD thesis, 2022, unpublished). This construct, named ADWT/2x-E2Fm, possesses mutations in E2F-binding sites of E1A-enhancer region, and in E2-early promoter region. Replication analysis by this construct has been described elsewhere (Maximilian Ehrenfeld, PhD thesis, 2022, unpublished). In this thesis, the focus was on the gene expression of early and late genes upon the complete disruption of E2F binding at both the early gene regions. It was observed that ADWT/2xE2Fm exhibits unusual characteristics of viral entry, a 10x more entry into the cells as compared to ADWT at comparable MOIs, which is puzzling (data not shown). Hence a 10 times lower MOI of ADWT/2xE2Fm was used in the following experiments as compared to ADWT. UMUC3 cells were infected with either MOI 10 of ADWT or MOI 1 of ADWT/2xE2Fm and viral gene

expression for early genes was assessed at 24 hrs after infection. As seen in the figure 3.18, the expression was E2-early transcripts were downregulated in ADWT/2xE2Fm compared to ADWT, which is expected because of the mutations in E2-early promoter. However, the expression of E1A was not affected at all despite the mutation at E1A-enhancer, effectively abrogating the effect seen in ADWT/E2Fm. This strengthens the hypothesis that RB/E2F as complex or just E2F proteins alone act as a repressor at E1A-enhancer region predominantly in the early phases of infection.

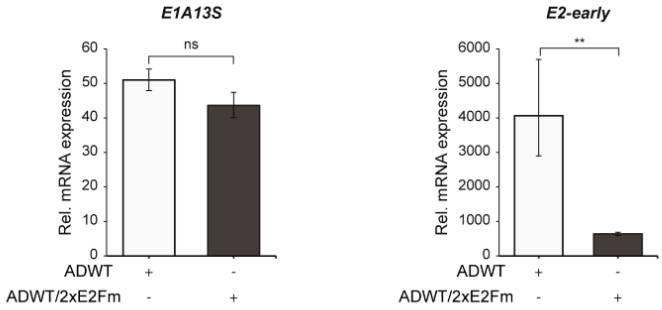

Figure 3.18. *Mutations in E2F-binding sites of E1A enhancer does not affect E1A expression.*

Viral gene expression was assessed in UMUC-3 cells infected with either ADWT (MOI 10) or ADWT-2xE2Fm (MOI 1) at 24hpi. Data is represented as the viral transcripts relative to incoming fiber DNA at 4h. Error bars S.D.

3.2.8. CDK4/6i enhances viral gene expression in ADWT/2xE2Fm

Furthermore, the effects of Palbociclib treatment of viral gene expression were assessed in ADWT/2xE2Fm. UMUC3 cells were pretreated with 500nM Palbociclib for 24hrs and infected with ADWT/2xE2Fm. Viral gene expression was assessed at 24hrs after infection. It could be observed that despite the mutations in E2F-binding sites at E1A enhancer and E2-early promoter, the virus still responds quite strongly to Palbociclib treatment, and an enhancement was observed in viral genes E1A13S, E2-early and hexon (Fig-3.19). These results suggest that, while RB/E2F may have a role in mediating adenoviral replication and be the link between CDK4/6i and adenoviral life cycle, there might be additional mechanisms involved that are regulating this synergy.

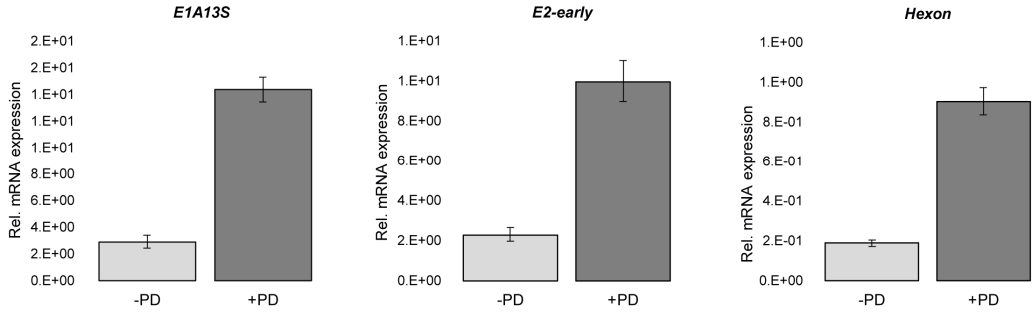

Figure 3.19. *Palbociclib treatment enhances viral gene expression in ADWT/2xE2Fm.*

UMUC-3 cells were treated with 0.5µM Palbociclib and infected with ADWT/2xE2Fm (MOI 1). RNA was extracted at 24hpi, and cDNA was generated by gene specific reverse transcription and qPCR was performed for indicated genes. Error bars S.D.

3.3. Transcriptomics analysis upon Palbociclib treatment at 8hrs and at 24hrs

In this study, so far, several adenoviral mutated constructs were studied in combination with Palbociclib treatment. One common aspect that all the constructs show despite their mutation status is that they all respond strongly to Palbociclib treatment and show enhanced replication and gene expression. This could also be observed in an E1-deleted construct (data not shown), emphasizing that the adenoviral response to CDK4/6i is E1-independent.

Concurrently, it was also observed that ADWT and XVir-N-31 respond strongly to Palbociclib treatment even when treated 6hrs before infection or in parallel to infection. This suggests that the molecular changes responsible for synergy can potentially be already observed at 6-8hrs of Palbociclib treatment, since that is when the viral internalization would complete, and the virus would start early gene expression. Hence, we decided to study the molecular changes that occur at a transcriptomic level at 8hrs after treatment of Palbociclib. Since most of the experiments are performed with 24hr- priming of Palbociclib, we also investigated the transcriptomics changes at 24hr treatment of Palbociclib as well. Common dysregulated genes and transcription factors at this time point would give an insight into the mechanisms regulating the synergy.

T24 cells were treated with 1µM Palbociclib and lysates was extracted at 0hrs, 8hrs and 24hrs of treatment. RNA was isolated and subjected to single-end sequencing, and the data was analyzed as per DESeq2 standard protocol (Love, Huber et al. 2014). Differential gene

expression analysis was performed based on the normalized reads, for 8hrs vs 0hrs and 24hrs vs 0hrs. Log fold changes were corrected using the algorithm 'apeglm' to exclude the effect of biological and technical variation (Zhu, Ibrahim et al. 2019). Gene ontology and KEGG pathways were performed based on the shrunken log fold changes.

Upon gene ontology analysis, it was observed that the key terms detected were related to mostly cell cycle pathway with G2-M checkpoint, E2F targets, enriched in control upon 24hrs of treatment. This also reflected in the KEGG pathway analysis with the key enriched pathways in control after 24hrs of treatment were related to cell cycle and DNA replication. Interestingly, these results also looked very similar when the treatment duration was just 8hrs. E2F targets, cell cycle, and DNA repair related genes were enriched in control even within 8hrs of treatment with Palbociclib. In KEGG pathways, cell cycle, DNA replication and DNA repair related pathways were enriched at 8hrs of treatment already (Fig-3.20). Most significant of these observations is that E2F targets are dysregulated as early as 8hrs of treatment, implying the effect of Palbociclib on E2F proteins at very early time points, which was not known earlier based on our biochemical assays. This provides strong support to the hypothesis that E2F levels hinder adenoviral replication in the early time points, and reduction of E2F levels early on provides suitable environment for earlier and higher adenoviral gene expression and replication.

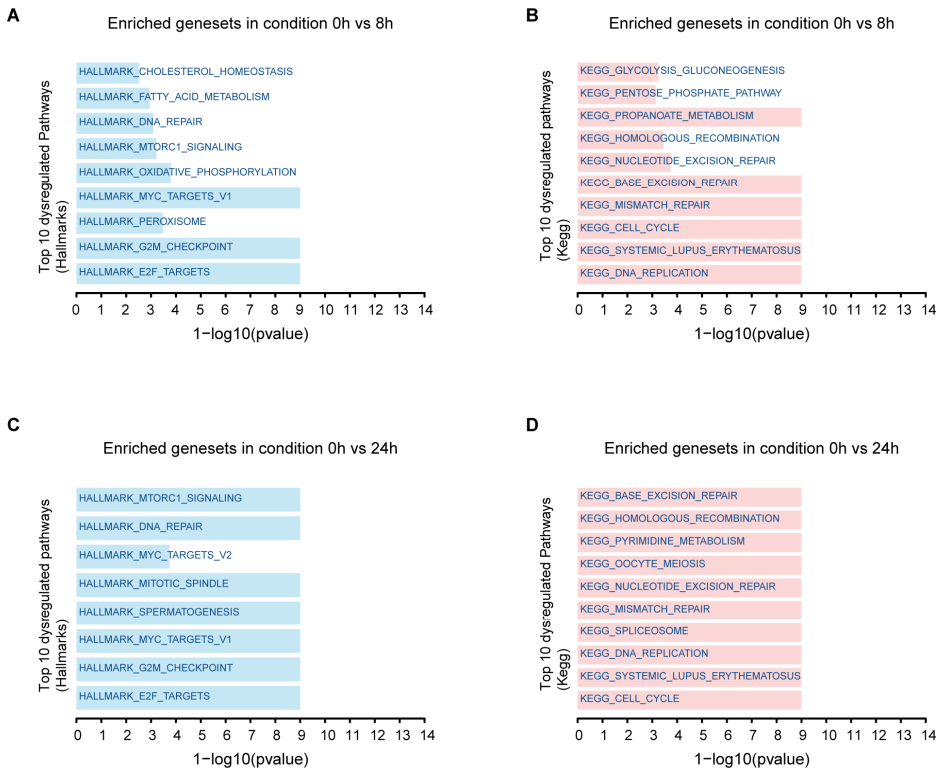

Figure 3.20. *E2F targets are dysregulated as early as 8hrs post Palbociclib treatment.*

Gene ontology (a,c) and KEGG pathway analysis (b,d) were performed in T24 cells that were treated with 1µM Palbociclib for (a,b) 8 hrs and (c,d) 24 hrs. For both the analysis, only the top 10 dysregulated terms enriched at 0 hrs compared to the respective time points have been shown in the image.

3.4. Characterizing JAK-STAT pathway components as therapeutic targets in Bladder cancer

The secondary focus of this thesis has been to characterize the components of JAK-STAT pathway components as therapeutic targets in bladder cancer. A detailed overview of JAK-STAT pathway and its significance in cancer has been described in the introduction.

3.4.1. JAK-STAT pathway is dysregulated in Bladder cancer

Activation of JAK-STAT signalling in bladder cancer has previously been shown by several studies, especially via protein levels and phosphorylation of STAT3/5. In this study, the aim was to characterise JAK and STAT proteins as potential targets for therapy. To

investigate the transcript profile of JAK-STAT proteins in bladder cancer, The Cancer Genome Atlas (TCGA) dataset was explored using a cohort consisting of 412 bladder cancer patients to identify the alterations in 4 JAK family proteins and 7 STAT family proteins. In 54% of the patients, alterations in the JAK-STAT proteins were observed with no effect on overall survival in patients (Fig-3.21a, b). Upon looking at individual elements, alterations in STAT3 were observed in 7%, STAT5A in 8%, STAT5B in 7% of patients, JAK1 in 8% and JAK2 in 15% of patients indicating that some of these genes are frequently altered in bladder cancer (Fig-3.21c). Interactions were observed between STAT3 and 5 with JAK1 and 2. Significant co-occurrence was observed between JAK2-STAT5A, STAT3-STAT5A and STAT3-STAT5B. Based on these results, an immunohistochemistry analysis was performed to study STAT3 expression in bladder cancer patients, and a higher STAT3 expression was observed (fig-3.21d). In a panel of bladder cancer cell lines, constitutive expression of JAK1 and 2, STAT3 and 5 were observed, prompting us to attempt inhibition of JAK-STAT pathway components. This was done at 2 levels, inhibition of JAK1/2, and inhibition of STAT3 using specific inhibitors.

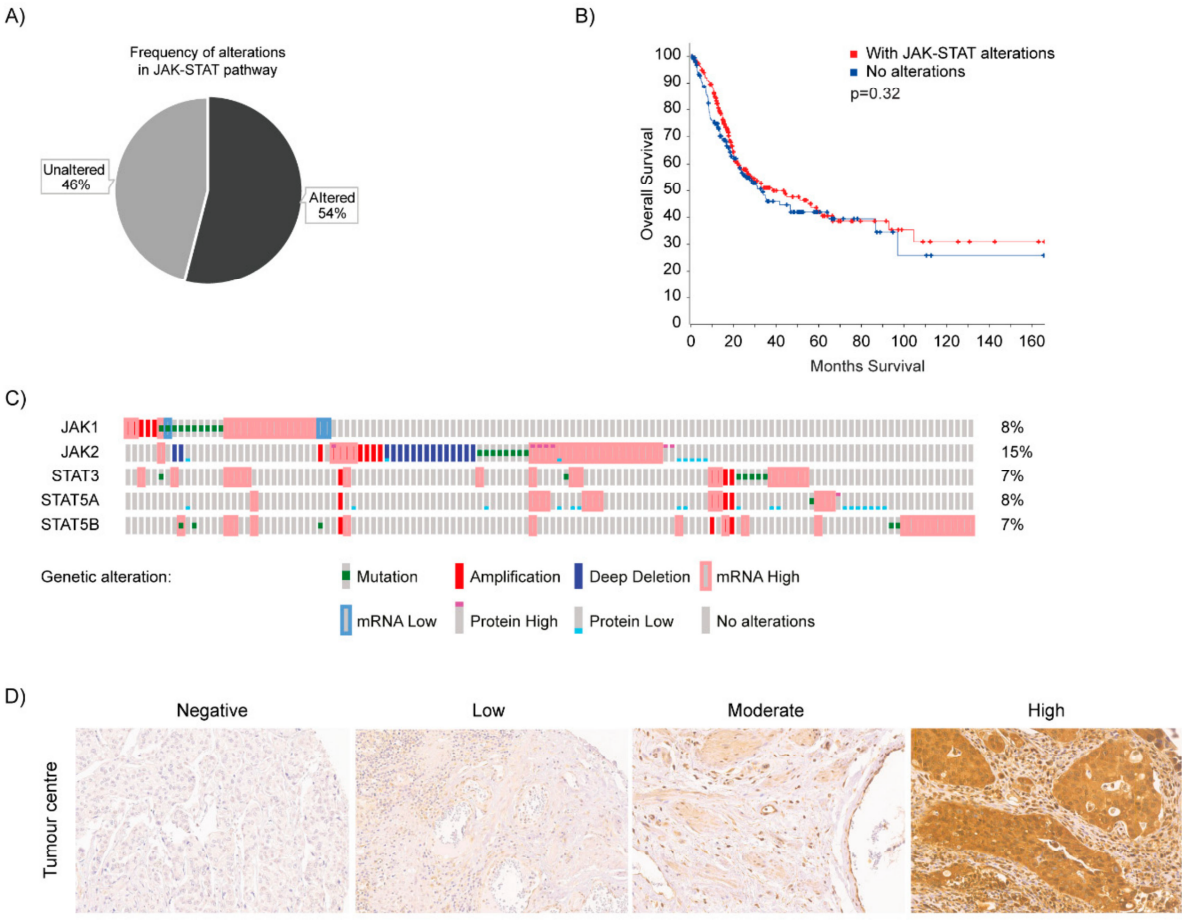

Figure 3.21. *JAK-STAT pathway components are dysregulated in Bladder cancer.*

(A) A TCGA cohort of 412 patients (413 samples) was analysed using cBioPortal. Components of JAK-STAT pathway were altered in 54% of bladder cancer specimens. (B) Overall survival is depicted by Kalpan-Meier plot among patients with and without alterations in JAK-STAT pathway in the TCGA cohort. (C) OncoPrint showing alterations in JAK1, JAK2, STAT3, STAT5A and STAT5B genes - indicating tumours altered with mutations (green bars), amplification (red bars), homozygous deletion (blue bars), high mRNA (red—outlined bars), mRNA low (blue-outlined bars), protein high (bars with red cap), protein low (blue-bottomed bars) and no alterations (grey bars). (D) Immunohistochemistry of bladder cancer patient tissues stained for STAT3- with various staining intensities categorised as- Negative (Score-0), Low (Score-1), Moderate (Score-2), High (Score-3). Tissue sections were imaged at 200X magnification.

3.4.2. STAT3/5, but not JAK1/2 inhibitors reduce cell proliferation in bladder cancer

JAK1 and 2 were inhibited using JAK1/2 inhibitor Ruxolitinib. Bladder cancer cell lines were treated with increasing concentrations of either of the compounds, and cell viability was assessed 72hrs post treatment by cell-titer blue assay. As seen in figure 3.22, JAK1/2

inhibition did not affect cell survival at all in bladder cancer cell lines, thus ruling out the proteins as potential therapeutic targets.

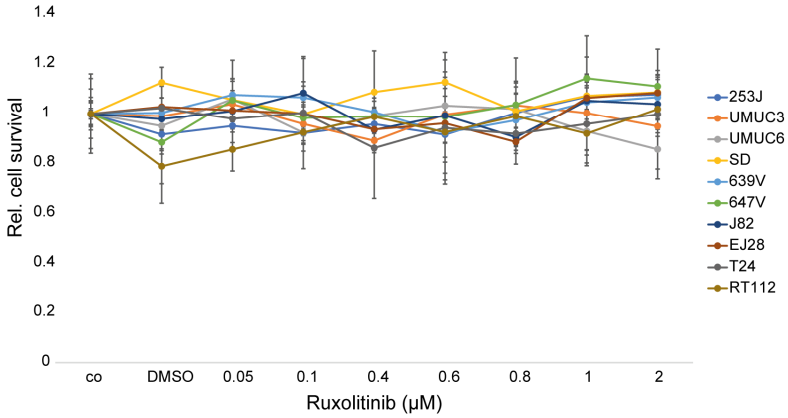

Figure 3.22. *JAK1/2 inhibition has no effect on cell viability in bladder cancer cell lines.*

A panel of 10 bladder cancer cell lines were treated with increasing concentrations of Ruxolitinib and cell viability was assessed at 72hrs post treatment by CellTiter-Blue® Cell Viability Assay. Data is represented as percentage of surviving cells relative to control. Error bars S.E. (Data from Eva Maria Baur)

Napabucasin, a STAT3 inhibitor and also a stemness inhibitor, was used to determine the effects of STAT3/5 inhibition *in vitro*. T24 and UMUC3 cells were treated with increasing concentrations of Napabucasin, and cell viability was measured 72h after treatment. STAT3 inhibition with Napabucasin led to a dose-dependent reduction of cell viability in bladder cancer cell lines (Fig-3.23). This also correlated with the data from our group with other STAT3 inhibitors Stattic and SH-4-54 (Hindupur, Schmid et al. 2020). Collectively, these results suggest that STAT3/5 inhibition could be a successful therapeutic strategy to be implemented in bladder cancer.

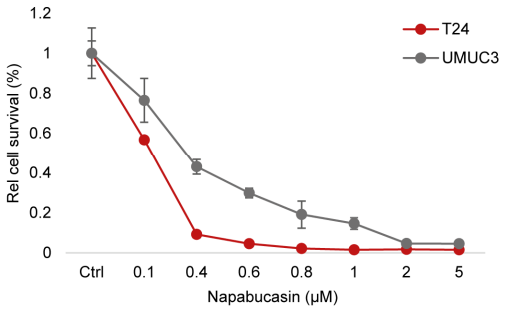

Figure 3.23. *STAT3 inhibition leads to reduced cell viability in bladder cancer cell lines.*

T24 and UMUC3 cells were treated with increasing concentrations with STAT3 inhibitor Napabucasin and cell viability was assessed at 72h post treatment by sulphorhodamine B assay. Data is represented as percentage of survining cells relative to control. Error bars S.E.

3.4.3. Both JAK1/2i and STAT3i enhance oncolytic virotherapy by XVir-N-31

Since the primary focus of this thesis has been studying the mechanisms involved in a successful combination therapy approach of CDK4/6i and XVir-N-31, we attempted to test whether the oncolytic XVir-N-31 shows enhancement in its efficiency upon combination with other targeted approaches like JAK1/2 inhibitors and STAT3 inhibitors. Principally, adenoviruses activate JAK-STAT pathway upon infection. A study demonstrated that vesicular stomatitis virus-based oncolytic virus shows enhancement in efficiency upon combination with JAK inhibitor Ruxolitinib (Patel, Dash et al. 2019). Hence, oncolytic adenovirus XVir-N-31 was combined with either JAKi Ruxolitinib or STAT3i and their effects on cell viability and viral replication were studied.

T24 and UMUC3 cells were treated with STAT3 inhibitors Napabucasin or Stattic for 24hrs, and then infected with XVir-N-31. Cell viability was assessed 4 days after infection by sulphorhodamine B assay. It was observed that STAT3 inhibition by either of the drugs enhanced virus induced cell death (Fig-3.24a, b). Viral replication was also assessed at 48 hrs after infection in T24 cells pretreated and infected with XVir-N-31. A significant increase in viral genome replication was observed upon the combination (Fig-3.24c). An increase in viral particle formation was also observed in the combination of XVir-N-31 and Stattic in T24 cells (Fig-3.24d). These results suggest that STAT3 inhibitors and XVir-N-31 could potentially offer a successful therapeutic regimen in clinic.

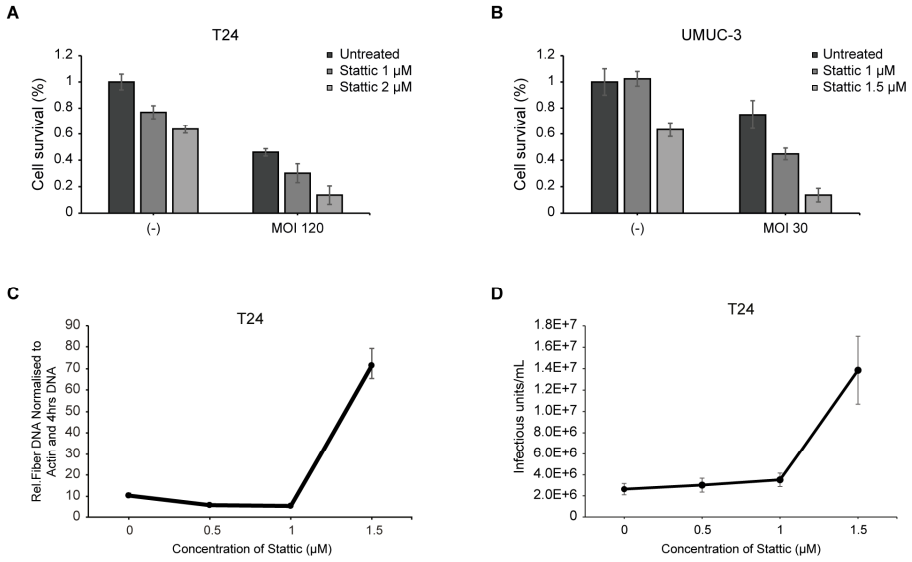

Figure 3.24. *STAT3 inhibition leads to enhancement of oncolytic activity of the oncolytic adenovirus XVir-N-31.*

(a,b) Cell viability was assessed by sulphorhodamine B assay in T24 (a) and UMUC3 (b) cells upon pretreatment with Stattic for 24 hrs, and infection with XVir-N-31 at indicated MOIs. Error bars S.E. (C) T24 cells were treated with increasing concentrations of Stattic and infected with XVir-N-31 (MOI 50) 24 hrs after treatment. Viral genome replication was analysed at 48h by fiber DNA Error bars S.D., and (D) the viral particles were measured by by hexon titre test and represented as infectious units/mL (IFU/mL).

Ruxolitinib does not affect cell viability at all in bladder cancer cell lines as shown earlier. Despite its lack of efficiency as monotherapy, we studied whether the drug could affect the efficacy of oncolytic adenoviruses. T24 cells were treated with Ruxolitinib in increasing concentrations for 24 hrs and cells were infected with XVir-N-31. Cell viability was assessed at 96 hrs after infection and viral genome replication was assessed at 24 and 48 hrs after infection. Surprisingly, an enhancement in virus-induced cell death was observed in T24 cells upon combination therapy (Fig-3.25a). This also reflected in the increase in viral genome replication at both 24 and 48 hrs post infection (Fig-3.25b). It is surprising to see that a compound which has no effect as monotherapy can lead to enhancement in the effectivity of oncolytic viruses. This can potentially open new avenues for therapy in oncolytic virotherapy, to employ more combination therapy strategies for successful clinical translation.

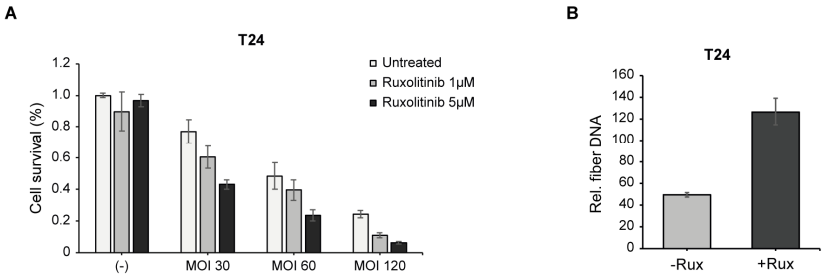

Figure 3.25. *JAK1/2 inhibition leads to enhancement of oncolytic activity of the oncolytic adenovirus XVir-N-31.*

(a) Cell viability was assessed by sulphorhodamine B assay in T24 cells upon pretreatment with Ruxolitinib for 24 hrs, and infection with XVir-N-31 at indicated MOIs. Error bars S.E. (b) T24 cells were treated with 5µM Ruxolitinib for 24 hrs and infected with XVir-N-31 (MOI 50. Viral genome replication was analysed at 48 h by fiber DNA Error bars S.D.

4. Discussion

4.1.Combination of oncolytic adenoviruses and CDK4/6i for therapy

In this study, we have studied molecular effects of CDK4/6 inhibitors on adenoviral replication, and the role of E2F binding sites in adenoviral genome. As discovered by our group earlier, CDK4/6 inhibition results in increase of virus-induced cell death and viral particle formation. It was also observed that there were more virus producing cells upon CDK4/6i (Koch 2021). These results are very encouraging from a clinical aspect, since lower MOIs of oncolytic viruses can be used in patients to achieve higher efficacy for tumour elimination. In this study, most of the experiments were performed on bladder cancer cell lines, but we have established in our group that the combination therapy strategy is successful in other solid tumour entities also, like paediatric sarcoma and glioblastoma. Considering the broad applicability of the therapy strategy, understanding the mechanisms behind the synergy would be beneficial so that the efficacy of the OVs can be enhanced by the newfound knowledge. To achieve this, studies were performed to understand both functional and molecular changes that occur in the cell upon combining OAdVs with CDK4/6i.

4.1.1. Functional and biochemical alterations upon CDK4/6i and oncolytic adenovirus infection

CDK4/6 pathway has multitude of functions in cells affecting several signalling proteins in the cascade (Bonelli, La Monica et al. 2019). Therefore, it was crucial to investigate whether CDK4/6i enhances viral replication by merely disturbing the signalling pathway.

E2F1 has implicated roles in apoptosis (Ginsberg 2002), and CDK4/6 inhibition could potentially lead to increase in free E2F1 protein levels which might induce apoptosis. To rule out enhanced cell death due to apoptosis, we measured cell death and apoptosis upon CDK4/6i and found that no increase in apoptosis or cell death was observed. This is also in line with previously published studies demonstrating that virus needs viable cell for its replication (Seifried, Talluri et al. 2008). We could also successfully show that the enhancement is not due to an increase in the levels of transcription factors such as YB1, which is known to facilitate adenoviral replication. It was also supported by parallel studies which demonstrated that CDK4/6i does not enhance the CAR protein expression, or an uptake of adenoviruses in combination (Lichtenegger, Koll et al. 2019).

It is an established fact that the dominant effect of CDK4/6 inhibition is G0/G1 arrest (Ingham and Schwartz 2017). Adenoviruses have been shown to ideally infect quiescent cells, and then drive the cells into S-phase (Nakajima, Masuda-Murata et al. 1987, Ben-Israel and Kleinberger 2002). However, we observed that the viruses show enhancement in replication even with concurrent treatment of CDK4/6i, thus ruling out the possibility that cell synchronisation via G0/G1 arrest is the reason behind the synergy in combination therapy.

A crucial aspect for oncolytic viruses in clinical implementation is their critical viral load. Insufficient viral load leads to unsuccessful replication and the viral infection would not successfully trigger the host immune system (Yang, Gu et al. 2021). A promising aspect of the combination therapy is that we can observe increase in viral gene expression, as seen in results with E1A and hexon transcript levels, even at low MOIs which show negligible gene expression in untreated condition. This was also supported by an increase in viral genome replication in lower MOIs as mentioned in the results section (Koch et al., 2022, Manuscript under review). This suggests that a critical amount of viral load is required to achieve successful infection and propagation of infection, and this critical threshold is lowered upon CDK4/6i. Based on these data, it is safe to conclude that CDK4/6i changes the cellular milieu so as to support adenoviral replication.

Subsequently, we also examined whether the response of oncolytic adenovirus to Palbociclib treatment is dose dependent. As shown in the results, the effect of CDK4/6i showed a linear kinetic in cell survival assay and correlated with reduction in the levels of RB protein. These data suggest that the effect of CDK4/6i on adenoviral replication might be an RB-dependent mechanism since we do not see the synergy in combination therapy in RB-negative cells. It has been reported earlier by our group as well as others that CDK4/6 inhibitors are only effective *in vitro* in RB-positive cells presumably due to inactive cyclin D-CDK4/6 complexes in RB-negative cells (Pan, Sathe et al. 2017). RB-family of proteins have been shown to be closely interrelated with adenoviral life cycle, by their interactions with adenoviral E1A. RB-family of pocket proteins, p107 and p130, have also been demonstrated to interact with E1A by the virtue of being binding partners to E2F proteins (Fattaey, Harlow et al. 1993, Liu and Marmorstein 2007, Ferreon, Martinez-Yamout et al. 2009). Previous results from our lab have shown that CDK4/6i can modulate the expression levels of E2F1, 3, and 4, and also modulate RB and p107 levels (Koch 2021). Based on this evidence, the focus was directed to characterise the roles of RB and E2F proteins in adenoviral replication since the results so far raised questions on their exact roles.

4.1.2. Molecular mechanisms upon CDK4/6i and oncolytic adenovirus infection

RB has been identified as a major factor in the combination therapy, based on previous results from our group. The combination therapy is only successful in RB-positive cells. In a CDK4/6 resistant cell line SK-N-MC, downregulation of RB led to increase in viral replication (Koch 2021). Since E2F proteins are also majorly dysregulated upon CDK4/6 inhibition, and we observed that the adenoviruses can restore the E2F1 levels that are downregulated by Palbociclib, hereon we focussed mainly on studying roles of E2F proteins, and E2F binding sites on adenoviral replication.

To evaluate the role of E2F proteins on adenoviral replication as individual proteins, we implemented siRNA mediated knockdown approach. In this study, only E2F1, 3 and 4 proteins were knocked down using siPool as shown in results, since these are the only E2Fs that are modulated by CDK4/6i (Koch 2021). It has earlier been shown that E2F4 translocation to nucleus is increased upon adenoviral infection, and E1A protein can interact with E2F4 and increase promoter occupancy of E2F4 (Schaley, Polonskaia et al. 2005, Pelka, Miller et al. 2011). We postulated that lack of E2F1 mediated by CDK4/6i maybe compensated by an increased protein level of E2F3 or E2F4. Surprisingly, knockdown of the tested E2F proteins had no effect on viral replication or particle formation. This could potentially be attributed to the compensatory activity exhibited by E2F proteins in the absence of one or more E2Fs (Kong, Chang et al. 2007). To test the effects of E2F proteins more accurately, one would have to knockout all E2F proteins which would be detrimental for cell survival. Since it would be difficult to achieve successful knockdown of multiple E2F proteins in a single cell using siRNAs, multiple E2F knockdown was not attempted. E2F proteins form heterodimers with DP1 at the DNA-binding sites, and E1A has been shown to interact with E2F/DP complexes (Pelka, Miller et al. 2011). Accordingly, it was also demonstrated earlier by our group that knocking down of DP1 did not induce viral replication (Johanna Krusche, Master's thesis).

Since the analysis of individual roles of E2F proteins did not give significant insight into the roles of single E2Fs in adenoviral life cycle, the focus was redirected to understand their binding and availability on adenoviral promoters. Adenoviral genome possesses E2F binding sites at E2-early promoter and at E1A enhancer regions. The two binding sites at E2-early promoter are considered indispensable for E2- transcription, and thus viral replication (Zajchowski, Boeuf et al. 1987). Upon introducing mutations in E2F-binding sites at the E2-

early promoter (ADWT/E2Fm), a reduction in replication was observed, which is expected since the expression levels of E2 are drastically reduced, as confirmed by qPCR and western blotting. Surprisingly, these mutations also led to decrease in E1A transcript and protein levels. A lot of studies performed on the adenoviral biology focussed on the role of E1A and its transactivation properties on other adenoviral genes. It has been well established that E1A is required for E2F-binding on the E2-early promoter (Babiss 1989). However, the interaction in the other direction is not completely understood. Previously published data suggested that DBP protein transcribed by E2-early region can affect the promoter activities of E1A promoter and major late promoter in plasmid-based assays (Chang and Shenk 1990). It has been, however, demonstrated that the viral genes behave differently in plasmid-based assays as compared to a viral infection (Manohar, Kratochvil et al. 1990, Rajan, Dhamankar et al. 1991). This reduction in E1A protein levels in the context of viral replication suggests that there might be a hitherto unknown mechanism of interaction between the E1A enhancer region and E2-early region mediated by E2F protein binding. Upon compensating for the lack of E1A protein, and thus reduced transactivation of all viral genes, it was observed that the viral genes could achieve similar expression levels in HEK-293 cells despite the mutations in E2-early promoter region. This strongly hints at an alternate mechanism of adenoviral E2-regulation which is independent of E2F-binding sites at E2-region.

We intended to investigate the role of E2F-binding at E1A-enhancer region by using the novel adenovirus construct ADWT-2xE2Fm. Interestingly, the mutations in E1A enhancer did not have an effect on E1A expression which raised questions about the role of E2F proteins at E1A-enhancer region. We hypothesised that E2F proteins bind excessively at E1A enhancer region upon mutations in E2-early region, and thus potentially act as a repressor. This would also explain the enhanced replication with CDK4/6i since E2F1 protein levels are decreased upon treatment with CDK4/6i. In the virus ADWT/2xE2Fm, the mutation at E1A enhancer thus inhibits E2F protein binding and allows for normal transcription from E1A region. Increased binding of E2F proteins at E1A region in ADWT/E2Fm as detected by chromatin immunoprecipitation assay also supports this hypothesis (Koch et al 2022, manuscript under review). It has been reported that adenoviral replication is suppressed by IFNɣ depending on a conserved E2F-binding site in the E1A-enhancer region, and additionally, adenovirus E2 expression possibly through enrichment of RB-pocket protein-E2F complexes at the E1A enhancer (Zheng, Stamminger et al. 2016). However, more studies need to be performed to

isolate complexes at both regions and study the transcription factor binding in detail to understand the transcription regulation from these regions.

The most interesting dataset for elucidating the role of E2F proteins comes from the trap mutant constructs. The trap plasmid and the trap adenovirus used do not specifically sequester a single E2F protein. They are designed to capture all the available E2F proteins within a cell (He, Cook et al. 2000). Upon luciferase reporter assay, it indeed confirms the role of E2F proteins in activating E2-early promoter, since we observe a reduction in promoter activity. This is complemented by an increase in viral replication. Since the plasmid-based assays differ compared to viral construct, the same E2F-trapping sequences were also incorporated into the viral genome to generate the adenovirus ADWT/Trap. Consolidating the trap-plasmid results, an increase in replication was observed upon ADWT/Trap infection. This is surprising, since so far, E2F proteins have only been shown to have activating roles on adenoviral promoters. Adenoviral promoter activation is tightly regulated by complex interactions between viral and cellular proteins. It has been published earlier that E2F-binding requires an interaction of E2F proteins with both E1A and E4Orf6/7 proteins(O'Connor and Hearing 1994). It is plausible that E2F activity is tightly controlled by these viral proteins to ensure the E2F proteins are only active for a brief window in adenoviral life cycle. Upon closely examining the time kinetics, it is evident that the ADWT/Trap virus replicates much faster than ADWT/TrapM as seen by much higher viral DNA produced in earlier time points. However, at later time points, both the viruses acquire same levels of viral DNA. This suggests that E2F proteins might have a repressive role in the initial time points of replication but are required in later time points as is supported by recovery of E2F1 protein at late phases of infection in multiple approaches. This hypothesis would then explain the enhancement in viral replication observed upon CDK4/6i. Since we also observe an earlier and much more rapid gene expression and replication of adenoviruses upon CDK4/6i, it could be hypothesised that the lack of E2F1 mediated by CDK4/6i can facilitate an earlier replication of the adenoviruses, as is also evidenced by ADWT/Trap data. The increase in E1A protein level upon E2F1 knockdown at early phases is in accordance with the other findings, and strongly supports that E2F proteins play a negative regulatory role in adenoviral life cycle. E2F proteins have been demonstrated to have a dual activator-repressor role in different phases of organogenesis and myeloid development (Chong, Wenzel et al. 2009, Trikha, Sharma et al. 2011). Hence, it is quite plausible that E2F proteins have dual role in viral life cycle.

As shown in results, all the tested viral constructs in this study respond strongly to CDK4/6i, irrespective of their mutation status. We also observe an increase in E1-deleted viruses upon CDK4/6i (data not shown). This strongly suggests that there might be additional mechanisms involved in the regulation of adenoviral replication apart from RB-E2F pathway. To understand the molecular alterations upon CDK4/6i in detail, transcriptomics was performed. It was unanticipated to see E2F protein targets among the dysregulated genes in GO and KEGG analysis as early as 8 hours after treatment. This strengthened our hypothesis that E2F proteins act as a repressor in early time points of viral replication. Viral replication and early gene expression initiates within the first 6-8 hrs of infection (Crisostomo, Soriano et al. 2019). As seen by viral gene expression time kinetics, a drastic increase is seen in viral gene expression levels well within the first 8hrs of infection. Since we also observe an enhancement in viral replication upon concurrent treatment with CDK4/6i with viral infection, it is presumably because of the early effects of CDK4/6i that we see an enhancement in viral activity. Adenoviral E2 region is mainly regulated by three components: E2Fs, ATF, and TBP (as explained in the Introduction)(Swaminathan and Thimmapaya 1996). Upon examining the dysregulated genes upon CDK4/6i, we do observe an increase in ATFs at 8hrs post infection (data not shown). This suggests that the mechanism is not solely driven by E2F proteins. Another possible mechanism might be related to DNA conformational change caused by E2F-binding. Cress et al have reported the DNA-bending capacity of the E2F transcription factor family (Cress and Nevins 1996). Three members of the E2F family, along with the DP1 protein, bend the DNA towards the minor groove, suggesting that DNA bending might be a characteristic of the entire E2F family. Upon introducing mutations at E2F-binding sites at adenoviral promoters, it is possible that other transcriptional factors binding sites would be exposed, which would otherwise be hidden due to E2F binding. One way to resolve this issue would be to perform EMSA assays at both the E2F binding sites and compare the protein complexes at these sites in mutated and wildtype viruses. It would reveal whether any new transcription factors bind at these sites in the absence of E2F-binding. Since the enhancement upon CDK4/6i is also seen in E1-deleted viruses, and E4orf6/7 protein is reported to substitute for the transactivation activity of E1A in its absence (O'Connor and Hearing 2000), it is possible that the synergy-causing factors are associated with E4 region rather than E1A or E2 region. More studies need to be performed to understand the role of E4orf6/7 protein in the context of combination therapy. However, the data presented in this thesis so far, hints at a strong repressive activity of E2F proteins in early time points of adenoviral replication, and a possible hitherto unknown mechanism regulating the E1 and E2 regions of adenoviral genome.

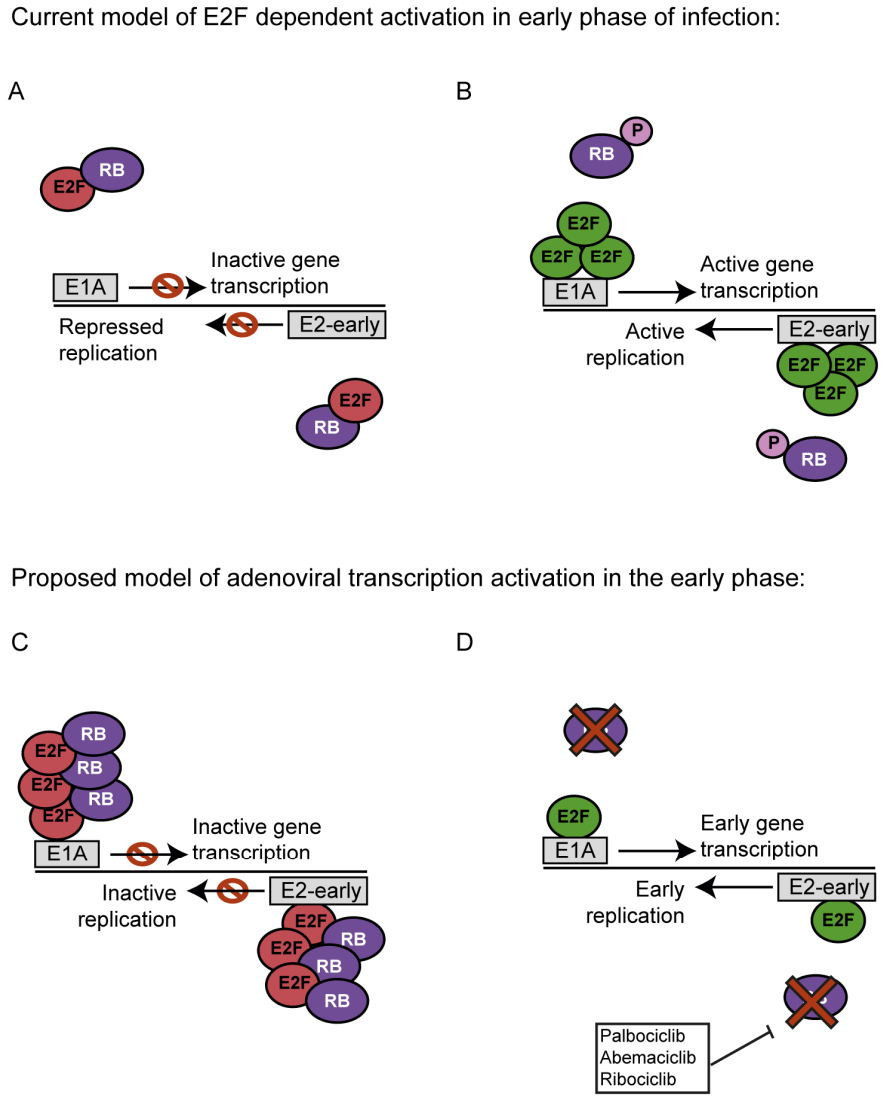

Figure 4.1. *Proposed model of regulation of viral replication in the combination therapy with oncolytic adenovirus and CDK4/6 inhibitors.*

The top panel (A, B) shows the current model of the activation of adenoviral gene transcription. When E2F is released upon phosphorylation of RB, active E2F proteins bind at E2F binding sites of adenoviral promoters and, transcription initiation occurs. In the bottom panel (C-D), we propose a new model based on our data which suggested that the E2F binding sites at E1A and E2 region might show competitive binding of RB/E2F complexes (C). Transcription is suppressed in the presence of the excess RB/E2F complexes. Upon disruption of these complexes by CDK4/6 inhibition, E2F proteins are either completely diminished or the amounts of free active E2F proteins is limited, which then drift the balance in favour of adenoviral transcription, thus leading to earlier activation of replication (D).

In conclusion, we propose a model of adenoviral replication which suggests that RB/E2F complex acts as negative regulators in early phases of viral gene expression by occupying the

adenoviral E1A enhancer and E2 promoter. Upon CDK4/6 inhibition, RB and E2F protein levels are decreased which might cause a shift towards low level of active E2F1, facilitating a quicker start of viral gene expression and replication. Consequently, E2F proteins are crucial in later time points for the successful completion of adenoviral lifecycle.

4.2. Targeting JAK-STAT pathway for therapy in Bladder cancer

In the second part of this thesis, JAK-STAT pathway components have been explored for their potential as therapeutic targets in bladder cancer. Several studies have demonstrated that STAT3 protein shows prognostic potential, and serves as a marker for invasion, which was contradicted by some other groups (Chan, Espinosa et al. 2009, Mitra, Pagliarulo et al. 2009, Ho, Lay et al. 2012, Degoricija, Situm et al. 2014, Gatta, Melocchi et al. 2019). In this study, we studied the specimen dataset from TCGA including 412 patient specimens of muscle invasive bladder cancer which revealed that JAK-STAT pathway components are frequently altered in bladder cancer, but they showed no prognostic significance. In a tissue micro array analysis, high levels of STAT3 were observed in MIBC patients but did not show any prognostic relevance either. From the data presented here, it could be concluded that STAT3 does not serve as a good prognostic marker for MIBC despite its frequent dysregulation.

Therapeutic targeting of JAK-STAT pathway was performed at two levels- targeting JAKs and targeting STATs. Targeting of JAK by a specific inhibitor Ruxolitinib revealed that it has no effect on the cell survival in bladder cancer cell lines in the concentrations used in this thesis. In a previous study, JAK inhibitor AG490 has shown success *in vitro* in bladder cancer, which is contradicting to the data presented here (Joung, Na et al. 2014). This could be explained by the target specificity of both the drugs. Ruxolitinib is a specific JAK1/2 inhibitor, whereas AG490 is nonspecific and also affects EGFR, HER2 or STAT5a/b besides JAK2. The observed effect on cell survival by AG490 could possibly be because of its additional effects rather than JAK inhibition (Baffert, Régnier et al. 2010, Quintás-Cardama, Vaddi et al. 2010). These data summarise that JAK proteins are not suitable targets for monotherapy in bladder cancer.

At STAT level, STAT3 was targeted as it was the most frequently dysregulated. We demonstrated in our group that STAT3 inhibitors Stattic, SH-4-54 and Nifuroxazide can inhibit cell growth in bladder cancer cell lines and in a 3D-xenograft model. These results are in-line with previously published data regarding STAT3 (Chen, Cen et al. 2008, Tsujita, Horiguchi et

al. 2017, Zhang, Ye et al. 2017). In this study, this observation was extended to a novel STAT3 inhibitor Napabucasin which is a cancer stemness inhibitor which acts via STAT3. It could be confirmed that Napabucasin effectively inhibits cell growth in bladder cancer cell lines, consistent with the results from other STAT3 inhibitors.

In the final step, we explored the possibility of combining JAK and STAT inhibitors with the oncolytic adenovirus XVir-N-31. It has been shown earlier that Ruxolitinib enhances replication of VSV oncolytic vesicular stomatitis virus therapy resulted in enhanced oncolysis and viral replication in non-small cell lung cancer (Patel, Dash et al. 2019). Adenovirus infection and replication are closely related to interferon signalling pathway, which is regulated by JAK-STAT pathway. Cytokines released upon infection, such as IFNs and IL-6, stimulate the expression of genes involved in anti-viral response via complex mechanisms. Interferon signalling has been shown to inhibit adenoviral DNA replication by inhibiting viral early gene expression in normal cells, but not in cancer cells (Zheng, Stamminger et al. 2016). It has been reported that adenoviruses can replicate much better in a STAT2 knockout Syrian hamster model which had disrupted interferon signalling (Toth, Lee et al. 2015). Priming the cells with Ruxolitinib enhanced the viral replication of oncolytic Herpes Simplex Virus (oHSV) in malignant peripheral nerve sheath tumours (Ghonime and Cassady 2018). Mice treated with Ruxolitinib showed reduced Interferon stimulated genes expression, thus rendering the tumours susceptible to oHSV infection.

Based on these data, we attempted to combine XVir-N-31 with Ruxolitinib, despite Ruxolitinib showing no effect on bladder cancer cells as monotherapy. We observed that Ruxolitinib could successfully enhance virus-induced cell death and also increase viral genome replication in bladder cancer cells, which came as a surprise. This suggests that JAK inhibitors may have an alternative functioning mechanism that regulate the adenoviral replication, and thus enhance their activity. STAT3 inhibitor Stattic also showed enhanced oncolysis, viral genome replication, and particle formation upon combination with XVir-N-31 in bladder cancer cells. As showed by our group previously, treatment with Stattic leads to G2 arrest (Hindupur, Schmid et al. 2020) and there are studies demonstrating enhanced adenoviral replication upon G2 arrest (Steinwaerder, Carlson et al. 2000). While it is exciting to see the enhanced oncolytic activity upon JAK and STAT inhibition, more studies are required to elucidate the mechanisms that drive this phenomenon.

5. Outlook

Based on the results in this study, the major conclusion is that E2F family of transcription factors are negative regulators of early adenoviral replication. While individually, they do not have any effect on adenoviral replication, when using the 'E2F trap' plasmids and viruses, an enhancement in viral replication is seen. This provides an encouraging aspect to investigate the exact roles of E2F proteins and their partners, RB proteins, in the context of combination therapy with CDK4/6 inhibitors.

To further understand the role of E2F-binding sites, pulldown assays, electrophoretic mobility shift assays (EMSA) and chromatin immunoprecipitation assays (ChIP) need to be performed to study the difference in the protein complexes binding at adenoviral E2-promoter and E1A enhancer regions. Performing these analyses in the presence of CDK4/6 inhibitors would give an insight into transcription factor complex changes that occur upon CDK4/6 inhibition. Proteomics analysis on the isolated complexes would give a complete overview of all the transcription factors and co-factors that interact with these regions.

Furthermore, transcriptomics and whole cell proteomics analysis would provide insights into the changes that occur in the molecular landscape upon combination therapy. Identifying the 'synergy-associated genes and proteins' which drive the synergy of XVir-N-31 and CDK4/6 inhibitors will help in better understanding the mechanism of action of the therapy strategy.

Findings from these above studies could be collectively used to produce new generation of oncolytic adenoviruses with improved efficacy at low concentrations. It would also give insights to develop novel combination therapy approaches to treat cancers with minimal side effects.

Publications

1. **Hindupur SV***, Schmid SC*, Koch JA, Youssef A, Baur E-M, Wang D, Horn T, Slotta-Huspenina J, Gschwend JE, Holm PS, Nawroth R. STAT3/5 Inhibitors Suppress Proliferation in Bladder Cancer and Enhance Oncolytic Adenovirus Therapy. International Journal of Molecular Sciences. 2020; 21(3):1106. https://doi.org/10.3390/ijms21031106. *-Equal contribution.

2. Mantwill K, Klein FG, Wang D, **Hindupur SV**, Ehrenfeld M, Holm PS, Nawroth R. Concepts in Oncolytic Adenovirus Therapy. International Journal of Molecular Sciences. 2021; 22(19):10522. https://doi.org/10.3390/ijms221910522

3. Koch, J*, Schober SJ.*, **Hindupur, SV.*** Caroline Schöning, Florian G. Klein, Klaus Mantwill, Maximilian Ehrenfeld, Ulrike Schillinger, Timmy Hohnecker, Pan Qi, Katja Steiger, Michaela Aichler, Jürgen E. Gschwend, Roman Nawroth*, Per Sonne Holm*. Targeting the RB/E2F repressive complex by CDK 4/6 inhibitors amplifies the oncolytic potency of XVir-N-31. Nature Communications, 2022. Manuscript under review. *-Equal contribution.

List of Figures

List of Tables

Acknowledgements

This thesis would not have been possible without the support of so many incredible people. Nearly half of the work for this thesis was performed during the pandemic, and I have a lot of people to thank for, who all made this a smooth and exciting journey despite the unforeseen and unpredictable interruptions.

First and foremost, I would like to thank Prof. Dr. Gschwend for offering me the great opportunity to work in the Molecular Uro-oncology department. I would also like to thank Prof. Dieter Saur for agreeing to be part of my thesis committee, and for all the valued insights during the yearly committee meetings.

I express my sincere gratitude to my thesis supervisor, PD.Dr.Roman Nawroth for giving me an opportunity to work in his group on this very exciting project. His immeasurable level of mentorship and guidance have helped me learn many aspects of research, such as scientific methodology, critical thinking, project management and scientific communication. I am certain that the scientific and management lessons that I've learned under his mentorship will help me immensely in my future scientific career. He ensured that his group felt safe and secure during the pandemic and made it possible that everyone's projects could be completed despite the interruptions. His kindness, empathy and compassion towards his group is something I would like to imbibe from him going forward in my career. Thank you Roman, for all the opportunities and excellent support you gave me over the years.

I extend my gratitude to Prof. Dr. Per Sonne Holm for his help and guidance with all things related to adenoviruses. He is an excellent scientist that I'm privileged to have worked with. His ability to remember the vast and extensive scientific literature has always amazed me. Thank you Per, for always answering my questions and helping me gain immense knowledge about adenoviral biology and virotherapy.

My sincere thanks to Klaus Mantwill for patiently answering all my virus-related questions and for his expert advice. Many thanks to Lena and Yuling for keeping the lab so organised always, and for all the help with my experiments. Special mention to Ana for her everyday support in the lab. My sincere thanks to Dongbiao, Jacqueline and Ting for proofreading this thesis. Your time and valuable feedback are highly appreciated. I would like to extend my gratitude to all the past and present members of AG Nawroth and AG Virotherapy. Thank you for sharing your knowledge, discussions, and all the fun times. The friendly atmosphere in the lab and the constant support from you all made this an excellent working experience. All the pequeño nights, in particular, have always made the late night working so much more fun.

I would like to thank Bettina Kratzer and Raphaela Blum for their support throughout the course of my PhD. Both of you have been incredibly accommodating with all the COVID-related delays and gave me enough support to complete this thesis in time.

Deepti, my time in Munich and at the Klinikum wouldn't have been the same without you. My heartfelt thanks to you for always answering all my program related questions, for expanding my scientific and social network, and for all the wonderful times outside of work. You and Milan have always been very welcoming and gracious, and for that, I am always grateful.

Ayush, I am thankful for all your encouragement and support during my final stages of PhD, and for proofreading my thesis. Your valuable feedback helped me a lot in polishing this

manuscript. I am also grateful to you for always being a generous host whenever I needed a getaway from Munich.

I am so lucky to have met wonderful people during my stay in Munich who have all been of incredible support. Yamini, I am fortunate to have you as my flatmate. My late-night working days in lab have never felt difficult all thanks to your support. You made my lockdown times infinitely better, and you continue to bring me comfort just by your presence. Pushpa, your strength, and endurance inspire me. I am so glad to have met you and to share hobbies with you. Thank you for always being there for me whenever I needed you. I look forward to more dinners, brunches, spontaneous trips together. Many thanks to all the wonderful friends I made at the graduate school. Hilansi, Raphela, Saumya, Steffi, you all have always been helpful with the lab supplies for my experiments due to unforeseen shortages, and I highly appreciate your timely help. I cherish all the times I've spent with you outside the lab. Young-hee, my movie and brunch buddy – I am glad to have met you. Thank you for all the insightful conversations, brunches, and fun times.

All my love and gratitude to my TC family. I cannot thank you all enough for all the group calls during the lockdowns. They played a massive role in keeping me sane during the isolation. It is extremely comforting to know that despite the distance, you all are just a call away. Some of my fondest memories from the last decade are with you guys, and I look forward to more adventures and crazy times with you all.

I would be remiss if I didn't thank my friends in Bangalore, especially Nanditha and Avinash. I will always cherish the memories made with you. You both gave me incredible support during my PhD applications, always listened to my rants, and made me believe that I could take on this journey. I have learnt a lot from both of you and I will always hold you dear.

I am forever indebted to Dr.Achyutha Prasad. I couldn't have started this PhD journey 4 years ago if not for his expert intervention. Your expertise, kindness and compassion have impacted me significantly. You gave me a new lease of life when I was in my absolute low phase, and I am eternally grateful to you.

Deepthi and Kruthi, you are the best sisters one could ask for. Deepthi, your intelligence, compassion, and strength have always inspired me. You have guided me in every step of my life right from our childhood. I am proud of the way you've built your life and career and I hope I can make you proud as well. Kruthi, words cannot express my gratitude to you. You have supported me so selflessly during this PhD dissertation. I am incredibly proud of what my little sister has become today, and I am so inspired by the strength and courage you have displayed in the past few years. I may not say this enough, but I love you both very much and I cannot go on a single day without you both.

Amma and Appa, I can never thank you enough for all that you have done for me. Thank you for your trust in my choices, and your support in everything I do. Your faith in me keeps me going even during the phases when I doubt myself. I couldn't have recovered physically and mentally after my setback, if not for the immense love and security I received from you. You both are my inspiration and I owe everything to you.

Bibliography

(1977). "Adenovirus strand nomenclature: a proposal." J Virol **22**(3): 830-831.

Alberts, P., A. Tilgase, A. Rasa, K. Bandere and D. Venskus (2018). "The advent of oncolytic virotherapy in oncology: The Rigvir(R) story." Eur J Pharmacol **837**: 117-126.

Ashwell, S. and S. Zabludoff (2008). "DNA damage detection and repair pathways--recent advances with inhibitors of checkpoint kinases in cancer therapy." Clin Cancer Res **14**(13): 4032-4037.

Babiss, L. E. (1989). "The cellular transcription factor E2f requires viral E1A and E4 gene products for increased DNA-binding activity and functions to stimulate adenovirus E2A gene expression." J Virol **63**(6): 2709-2717.

Babjuk, M., M. Burger, O. Capoun, D. Cohen, E. M. Comperat, J. L. Dominguez Escrig, P. Gontero, F. Liedberg, A. Masson-Lecomte, A. H. Mostafid, J. Palou, B. W. G. van Rhijn, M. Roupret, S. F. Shariat, T. Seisen, V. Soukup and R. J. Sylvester (2022). "European Association of Urology Guidelines on Non-muscle-invasive Bladder Cancer (Ta, T1, and Carcinoma in Situ)." Eur Urol **81**(1): 75-94.

Baffert, F., C. H. Régnier, A. De Pover, C. Pissot-Soldermann, G. A. Tavares, F. Blasco, J. Brueggen, P. Chène, P. Drueckes, D. Erdmann, P. Furet, M. Gerspacher, M. Lang, D. Ledieu, L. Nolan, S. Ruetz, J. Trappe, E. Vangrevelinghe, M. Wartmann, L. Wyder, F. Hofmann and T. Radimerski (2010). "Potent and selective inhibition of polycythemia by the quinoxaline JAK2 inhibitor NVP-BSK805." Mol Cancer Ther **9**(7): 1945-1955.

Bagheri, N., M. Shiina, D. A. Lauffenburger and W. M. Korn (2011). "A dynamical systems model for combinatorial cancer therapy enhances oncolytic adenovirus efficacy by MEK-inhibition." PLoS Comput Biol **7**(2): e1001085.

Bednova, O. and J. V. Leyton (2020). "Targeted Molecular Therapeutics for Bladder Cancer-A New Option beyond the Mixed Fortunes of Immune Checkpoint Inhibitors?" Int J Mol Sci **21**(19).

Ben-Israel, H. and T. Kleinberger (2002). "Adenovirus and cell cycle control." Front Biosci **7**: d1369-1395.

Berk, A. J. (1986). "Adenovirus promoters and E1A transactivation." Annu Rev Genet **20**: 45-79.

Bieler, A., K. Mantwill, T. Dravits, A. Bernshausen, G. Glockzin, N. Köhler-Vargas, H. Lage, B. Gansbacher and P. S. Holm (2006). "Novel three-pronged strategy to enhance cancer cell killing in glioblastoma cell lines: histone deacetylase inhibitor, chemotherapy, and oncolytic adenovirus dl520." Hum Gene Ther **17**(1): 55-70.

Bonelli, M., S. La Monica, C. Fumarola and R. Alfieri (2019). "Multiple effects of CDK4/6 inhibition in cancer: From cell cycle arrest to immunomodulation." Biochem Pharmacol **170**: 113676.

Braal, C. L., E. M. Jongbloed, S. M. Wilting, R. H. J. Mathijssen, S. L. W. Koolen and A. Jager (2021). "Inhibiting CDK4/6 in Breast Cancer with Palbociclib, Ribociclib, and Abemaciclib: Similarities and Differences." Drugs **81**(3): 317-331.

Braithwaite, A. W. and I. A. Russell (2001). "Induction of cell death by adenoviruses." Apoptosis **6**(5): 359-370.

Breitbach, C. J., B. D. Lichty and J. C. Bell (2016). "Oncolytic Viruses: Therapeutics With an Identity Crisis." EBioMedicine **9**: 31-36.

Bressy, C. and K. Benihoud (2014). "Association of oncolytic adenoviruses with chemotherapies: an overview and future directions." Biochem Pharmacol **90**(2): 97-106.

Chan, K. S., I. Espinosa, M. Chao, D. Wong, L. Ailles, M. Diehn, H. Gill, J. Presti, Jr., H. Y. Chang, M. van de Rijn, L. Shortliffe and I. L. Weissman (2009). "Identification, molecular characterization, clinical prognosis, and therapeutic targeting of human bladder tumor-initiating cells." Proc Natl Acad Sci U S A **106**(33): 14016-14021.

Chang, L. S. and T. Shenk (1990). "The adenovirus DNA-binding protein stimulates the rate of transcription directed by adenovirus and adeno-associated virus promoters." J Virol **64**(5): 2103-2109.

Chaurasiya, S., Y. Fong and S. G. Warner (2021). "Oncolytic Virotherapy for Cancer: Clinical Experience." Biomedicines **9**(4).

Chen, C. L., L. Cen, J. Kohout, B. Hutzen, C. Chan, F. C. Hsieh, A. Loy, V. Huang, G. Cheng and J. Lin (2008). "Signal transducer and activator of transcription 3 activation is associated with bladder cancer cell growth and survival." Mol Cancer **7**: 78.

Chong, J. L., P. L. Wenzel, M. T. Saenz-Robles, V. Nair, A. Ferrey, J. P. Hagan, Y. M. Gomez, N. Sharma, H. Z. Chen, M. Ouseph, S. H. Wang, P. Trikha, B. Culp, L. Mezache, D. J. Winton, O. J. Sansom, D. Chen, R. Bremner, P. G. Cantalupo, M. L. Robinson, J. M. Pipas and G. Leone (2009). "E2f1-3 switch from activators in progenitor cells to repressors in differentiating cells." Nature **462**(7275): 930-934.

Comins, C., G. R. Simpson, W. Rogers, K. Relph, K. Harrington, A. Melcher, V. Roulstone, J. Kyula and H. Pandha (2018). "Synergistic antitumour effects of rapamycin and oncolytic reovirus." Cancer Gene Ther **25**(5-6): 148-160.

Connell, C. M., A. Shibata, L. A. Tookman, K. M. Archibald, M. B. Flak, K. J. Pirlo, M. Lockley, S. P. Wheatley and I. A. McNeish (2011). "Genomic DNA damage and ATR-Chk1 signaling determine oncolytic adenoviral efficacy in human ovarian cancer cells." J Clin Invest **121**(4): 1283-1297.

Cress, W. D. and J. R. Nevins (1994). "Interacting domains of E2F1, DP1, and the adenovirus E4 protein." J Virol **68**(7): 4213-4219.

Cress, W. D. and J. R. Nevins (1996). "A role for a bent DNA structure in E2F-mediated transcription activation." Mol Cell Biol **16**(5): 2119-2127.

Crisostomo, L., A. M. Soriano, M. Mendez, D. Graves and P. Pelka (2019). "Temporal dynamics of adenovirus 5 gene expression in normal human cells." PLoS One **14**(1): e0211192.

Cunliffe, T. G., E. A. Bates and A. L. Parker (2020). "Hitting the Target but Missing the Point: Recent Progress towards Adenovirus-Based Precision Virotherapies." Cancers (Basel) **12**(11).

Dallaire, F., S. Schreiner, G. E. Blair, T. Dobner, P. E. Branton and P. Blanchette (2016). "The Human Adenovirus Type 5 E4orf6/E1B55K E3 Ubiquitin Ligase Complex Enhances E1A Functional Activity." mSphere **1**(1).

Degoricija, M., M. Situm, J. Korac, A. Miljkovic, K. Matic, M. Paradzik, I. Marinovic Terzic, A. Jeroncic, S. Tomic and J. Terzic (2014). "High NF-kappaB and STAT3 activity in human urothelial carcinoma: a pilot study." World J Urol **32**(6): 1469-1475.

Emens, L. A., P. A. Ascierto, P. K. Darcy, S. Demaria, A. M. M. Eggermont, W. L. Redmond, B. Seliger and F. M. Marincola (2017). "Cancer immunotherapy: Opportunities and challenges in the rapidly evolving clinical landscape." Eur J Cancer **81**: 116-129.

Farrera-Sal, M., L. Moya-Borrego, M. Bazan-Peregrino and R. Alemany (2021). "Evolving Status of Clinical Immunotherapy with Oncolytic Adenovirus." Clin Cancer Res **27**(11): 2979-2988.

Fattaey, A. R., E. Harlow and K. Helin (1993). "Independent regions of adenovirus E1A are required for binding to and dissociation of E2F-protein complexes." Mol Cell Biol **13**(12): 7267-7277.

Ferreon, J. C., M. A. Martinez-Yamout, H. J. Dyson and P. E. Wright (2009). "Structural basis for subversion of cellular control mechanisms by the adenoviral E1A oncoprotein." Proc Natl Acad Sci U S A **106**(32): 13260-13265.

Finn, R. S., A. Aleshin and D. J. Slamon (2016). "Targeting the cyclin-dependent kinases (CDK) 4/6 in estrogen receptor-positive breast cancers." Breast Cancer Res **18**(1): 17.

Flint, J. and T. Shenk (1989). "Adenovirus E1A protein paradigm viral transactivator." Annu Rev Genet **23**: 141-161.

Gatta, L. B., L. Melocchi, M. Bugatti, F. Missale, S. Lonardi, B. Zanetti, L. Cristinelli, S. Belotti, C. Simeone, R. Ronca, E. Grillo, S. Licini, D. Bresciani, R. Tardanico, S. R. Chan, E. Giurisato, S. Calza and W. Vermi (2019). "Hyper-Activation of STAT3 Sustains Progression of Non-Papillary Basal-Type Bladder Cancer via FOSL1 Regulome." Cancers (Basel) **11**(9).

Ghonime, M. G. and K. A. Cassady (2018). "Combination Therapy Using Ruxolitinib and Oncolytic HSV Renders Resistant MPNSTs Susceptible to Virotherapy." Cancer Immunol Res **6**(12): 1499-1510.

Ginsberg, D. (2002). "E2F1 pathways to apoptosis." FEBS Lett **529**(1): 122-125.

Goel, S., M. J. DeCristo, S. S. McAllister and J. J. Zhao (2018). "CDK4/6 Inhibition in Cancer: Beyond Cell Cycle Arrest." Trends Cell Biol **28**(11): 911-925.

Goodrum, F. D. and D. A. Ornelles (1997). "The early region 1B 55-kilodalton oncoprotein of adenovirus relieves growth restrictions imposed on viral replication by the cell cycle." J Virol **71**(1): 548-561.

Goradel, N. H., N. Mohajel, Z. V. Malekshahi, S. Jahangiri, M. Najafi, B. Farhood, K. Mortezaee, B. Negahdari and A. Arashkia (2019). "Oncolytic adenovirus: A tool for cancer therapy in combination with other therapeutic approaches." J Cell Physiol **234**(6): 8636-8646.

Guo, C., G. Yang, K. Khun, X. Kong, D. Levy, P. Lee and J. Melamed (2009). "Activation of Stat3 in renal tumors." Am J Transl Res **1**(3): 283-290.

Han, J., X. Gu, Y. Li and Q. Wu (2020). "Mechanisms of BCG in the treatment of bladder cancer-current understanding and the prospect." Biomed Pharmacother **129**: 110393.

Hanahan, D. and R. A. Weinberg (2011). "Hallmarks of cancer: the next generation." Cell **144**(5): 646-674.

Hannus, M., M. Beitzinger, J. C. Engelmann, M. T. Weickert, R. Spang, S. Hannus and G. Meister (2014). "siPools: highly complex but accurately defined siRNA pools eliminate off-target effects." Nucleic Acids Res **42**(12): 8049-8061.

Hardy, S., D. A. Engel and T. Shenk (1989). "An adenovirus early region 4 gene product is required for induction of the infection-specific form of cellular E2F activity." Genes Dev **3**(7): 1062-1074.

Havunen, R., J. M. Santos, S. Sorsa, T. Rantapero, D. Lumen, M. Siurala, A. J. Airaksinen, V. Cervera-Carrascon, S. Tahtinen, A. Kanerva and A. Hemminki (2018). "Abscopal Effect in Non-injected Tumors Achieved with Cytokine-Armed Oncolytic Adenovirus." Mol Ther Oncolytics **11**: 109-121.

He, S., B. L. Cook, B. E. Deverman, U. Weihe, F. Zhang, V. Prachand, J. Zheng and S. J. Weintraub (2000). "E2F is required to prevent inappropriate S-phase entry of mammalian cells." Mol Cell Biol **20**(1): 363-371.

Helin, K. and E. Harlow (1994). "Heterodimerization of the transcription factors E2F-1 and DP-1 is required for binding to the adenovirus E4 (ORF6/7) protein." J Virol **68**(8): 5027-5035.

Hindupur, S. V., S. C. Schmid, J. A. Koch, A. Youssef, E. M. Baur, D. Wang, T. Horn, J. Slotta-Huspenina, J. E. Gschwend, P. S. Holm and R. Nawroth (2020). "STAT3/5 Inhibitors Suppress Proliferation in Bladder Cancer and Enhance Oncolytic Adenovirus Therapy." Int J Mol Sci **21**(3).

Ho, P. L., E. J. Lay, W. Jian, D. Parra and K. S. Chan (2012). "Stat3 activation in urothelial stem cells leads to direct progression to invasive bladder cancer." Cancer Res **72**(13): 3135-3142.

Holm, P. S., S. Bergmann, K. Jurchott, H. Lage, K. Brand, A. Ladhoff, K. Mantwill, D. T. Curiel, M. Dobbelstein, M. Dietel, B. Gansbacher and H. D. Royer (2002). "YB-1 relocates to the nucleus in adenovirus-infected cells and facilitates viral replication by inducing E2 gene expression through the E2 late promoter." J Biol Chem **277**(12): 10427-10434.

Holm, P. S., H. Lage, S. Bergmann, K. Jürchott, G. Glockzin, A. Bernshausen, K. Mantwill, A. Ladhoff, A. Wichert, J. S. Mymryk, T. Ritter, M. Dietel, B. Gänsbacher and H. D. Royer (2004). "Multidrug-resistant cancer cells facilitate E1-independent adenoviral replication: impact for cancer gene therapy." Cancer Res **64**(1): 322-328.

Holzmuller, R., K. Mantwill, C. Haczek, E. Rognoni, M. Anton, A. Kasajima, W. Weichert, D. Treue, H. Lage, T. Schuster, J. Schlegel, B. Gansbacher and P. S. Holm (2011). "YB-1 dependent virotherapy in combination with temozolomide as a multimodal therapy approach to eradicate malignant glioma." Int J Cancer **129**(5): 1265-1276.

Homicsko, K., A. Lukashev and R. D. Iggo (2005). "RAD001 (everolimus) improves the efficacy of replicating adenoviruses that target colon cancer." Cancer Res **65**(15): 6882-6890.

Ingham, M. and G. K. Schwartz (2017). "Cell-Cycle Therapeutics Come of Age." J Clin Oncol **35**(25): 2949-2959.

Iwata, H. (2018). "Clinical development of CDK4/6 inhibitor for breast cancer." Breast Cancer **25**(4): 402-406.

Joung, Y. H., Y. M. Na, Y. B. Yoo, P. Darvin, N. Sp, D. Y. Kang, S. Y. Kim, H. S. Kim, Y. H. Choi, H. K. Lee, K. D. Park, B. W. Cho, H. S. Kim, J. H. Park and Y. M. Yang (2014). "Combination of AG490, a Jak2 inhibitor, and methylsulfonylmethane synergistically suppresses bladder tumor growth via the Jak2/STAT3 pathway." Int J Oncol **44**(3): 883-895.

Kamat, A. M., N. M. Hahn, J. A. Efstathiou, S. P. Lerner, P.-U. Malmström, W. Choi, C. C. Guo, Y. Lotan and W. Kassouf (2016). "Bladder cancer." The Lancet **388**(10061): 2796-2810.

Kennedy, M. A. and R. J. Parks (2009). "Adenovirus virion stability and the viral genome: size matters." Mol Ther **17**(10): 1664-1666.

Koch, J. A. (2021). Combining Oncolytic Virotherapy with Target Therapy in Bladder Cancer. Dr.rer.nat, Technical University of Munich.

Kong, L. J., J. T. Chang, A. H. Bild and J. R. Nevins (2007). "Compensation and specificity of function within the E2F family." Oncogene **26**(3): 321-327.

Kovesdi, I., R. Reichel and J. R. Nevins (1986). "Identification of a cellular transcription factor involved in E1A trans-activation." Cell **45**(2): 219-228.

Kovesdi, I., R. Reichel and J. R. Nevins (1987). "Role of an adenovirus E2 promoter binding factor in E1A-mediated coordinate gene control." Proc Natl Acad Sci U S A **84**(8): 2180-2184.

Kulanayake, S. and S. K. Tikoo (2021). "Adenovirus Core Proteins: Structure and Function." Viruses **13**(3).

Kuryk, L., A. W. Moller and M. Jaderberg (2019). "Abscopal effect when combining oncolytic adenovirus and checkpoint inhibitor in a humanized NOG mouse model of melanoma." J Med Virol **91**(9): 1702-1706.

Kuryk, L., A. W. Møller and M. Jaderberg (2019). "Combination of immunogenic oncolytic adenovirus ONCOS-102 with anti-PD-1 pembrolizumab exhibits synergistic antitumor effect in humanized A2058 melanoma huNOG mouse model." Oncoimmunology **8**(2): e1532763.

Leal, J., R. Luengo-Fernandez, R. Sullivan and J. A. Witjes (2016). "Economic Burden of Bladder Cancer Across the European Union." Eur Urol **69**(3): 438-447.

Lenis, A. T., P. M. Lec, K. Chamie and M. D. Mshs (2020). "Bladder Cancer: A Review." JAMA **324**(19): 1980-1991.

Li, R., J. Zhang, S. M. Gilbert, J. Conejo-Garcia and J. J. Mule (2021). "Using oncolytic viruses to ignite the tumour immune microenvironment in bladder cancer." Nat Rev Urol **18**(9): 543-555.

Libertini, S., A. Abagnale, C. Passaro, G. Botta, S. Barbato, P. Chieffi and G. Portella (2011). "AZD1152 negatively affects the growth of anaplastic thyroid carcinoma cells and enhances the effects of oncolytic virus dl922-947." Endocr Relat Cancer **18**(1): 129-141.

Lichtenegger, E., F. Koll, H. Haas, K. Mantwill, K. P. Janssen, M. Laschinger, J. Gschwend, K. Steiger, P. C. Black, I. Moskalev, R. Nawroth and P. S. Holm (2019). "The Oncolytic Adenovirus XVir-N-31 as a Novel Therapy in Muscle-Invasive Bladder Cancer." Hum Gene Ther **30**(1): 44-56.

Lindskrog, S. V., F. Prip, P. Lamy, A. Taber, C. S. Groeneveld, K. Birkenkamp-Demtroder, J. B. Jensen, T. Strandgaard, I. Nordentoft, E. Christensen, M. Sokac, N. J. Birkbak, L. Maretty, G. G. Hermann, A. C. Petersen, V. Weyerer, M. O. Grimm, M. Horstmann, G. Sjodahl, M. Hoglund, T. Steiniche, K. Mogensen, A. de Reynies, R. Nawroth, B. Jordan, X. Lin, D. Dragicevic, D. G. Ward, A. Goel, C. D. Hurst, J. D. Raman, J. I. Warrick, U. Segersten, D. Sikic, K. E. M. van Kessel, T. Maurer, J. J. Meeks, D. J. DeGraff, R. T. Bryan, M. A. Knowles, T. Simic, A. Hartmann, E. C. Zwarthoff, P. U. Malmstrom, N. Malats, F. X. Real and L. Dyrskjot (2021). "An integrated multi-omics analysis identifies prognostic molecular subtypes of non-muscle-invasive bladder cancer." Nat Commun **12**(1): 2301.

Liu, X. and R. Marmorstein (2007). "Structure of the retinoblastoma protein bound to adenovirus E1A reveals the molecular basis for viral oncoprotein inactivation of a tumor suppressor." Genes Dev **21**(21): 2711-2716.

Love, M. I., W. Huber and S. Anders (2014). "Moderated estimation of fold change and dispersion for RNA-seq data with DESeq2." Genome Biol **15**(12): 550.

Macedo, N., D. M. Miller, R. Haq and H. L. Kaufman (2020). "Clinical landscape of oncolytic virus research in 2020." J Immunother Cancer **8**(2).

Macosko, E. Z., A. Basu, R. Satija, J. Nemesh, K. Shekhar, M. Goldman, I. Tirosh, A. R. Bialas, N. Kamitaki, E. M. Martersteck, J. J. Trombetta, D. A. Weitz, J. R. Sanes, A. K. Shalek, A. Regev and S. A. McCarroll (2015). "Highly Parallel Genome-wide Expression Profiling of Individual Cells Using Nanoliter Droplets." Cell **161**(5): 1202-1214.

Manohar, C. F., J. Kratochvil and B. Thimmapaya (1990). "The adenovirus EII early promoter has multiple EIA-sensitive elements, two of which function cooperatively in basal and virus-induced transcription." J Virol **64**(6): 2457-2466.

Mantwill, K., F. G. Klein, D. Wang, S. V. Hindupur, M. Ehrenfeld, P. S. Holm and R. Nawroth (2021). "Concepts in Oncolytic Adenovirus Therapy." Int J Mol Sci **22**(19).

Matthews, H. K., C. Bertoli and R. A. M. de Bruin (2022). "Cell cycle control in cancer." Nat Rev Mol Cell Biol **23**(1): 74-88.

Minoli, M., M. Kiener, G. N. Thalmann, M. Kruithof-de Julio and R. Seiler (2020). "Evolution of Urothelial Bladder Cancer in the Context of Molecular Classifications." Int J Mol Sci **21**(16).

Mitra, A. P., V. Pagliarulo, D. Yang, F. M. Waldman, R. H. Datar, D. G. Skinner, S. Groshen and R. J. Cote (2009). "Generation of a concise gene panel for outcome prediction in urinary bladder cancer." J Clin Oncol **27**(24): 3929-3937.

Mondal, M., J. Guo, P. He and D. Zhou (2020). "Recent advances of oncolytic virus in cancer therapy." Hum Vaccin Immunother **16**(10): 2389-2402.

Nakajima, T., M. Masuda-Murata, E. Hara and K. Oda (1987). "Induction of cell cycle progression by adenovirus E1A gene 13S- and 12S-mRNA products in quiescent rat cells." Mol Cell Biol **7**(10): 3846-3852.

Neill, S. D., C. Hemstrom, A. Virtanen and J. R. Nevins (1990). "An adenovirus E4 gene product trans-activates E2 transcription and stimulates stable E2F binding through a direct association with E2F." Proc Natl Acad Sci U S A **87**(5): 2008-2012.

Nevins, J. R. (1992). "E2F: a link between the Rb tumor suppressor protein and viral oncoproteins." Science **258**(5081): 424-429.

O'Connor, R. J. and P. Hearing (1994). "Mutually exclusive interaction of the adenovirus E4-6/7 protein and the retinoblastoma gene product with internal domains of E2F-1 and DP-1." J Virol **68**(11): 6848-6862.

O'Connor, R. J. and P. Hearing (2000). "The E4-6/7 protein functionally compensates for the loss of E1A expression in adenovirus infection." J Virol **74**(13): 5819-5824.

Obert, S., R. J. O'Connor, S. Schmid and P. Hearing (1994). "The adenovirus E4-6/7 protein transactivates the E2 promoter by inducing dimerization of a heteromeric E2F complex." Mol Cell Biol **14**(2): 1333-1346.

Ojha, R., S. K. Singh and S. Bhattacharyya (2016). "JAK-mediated autophagy regulates stemness and cell survival in cisplatin resistant bladder cancer cells." Biochim Biophys Acta **1860**(11 Pt A): 2484-2497.

Owen, K. L., N. K. Brockwell and B. S. Parker (2019). "JAK-STAT Signaling: A Double-Edged Sword of Immune Regulation and Cancer Progression." Cancers (Basel) **11**(12).

Pan, Q., A. Sathe, P. C. Black, P. J. Goebell, A. M. Kamat, B. Schmitz-Draeger and R. Nawroth (2017). "CDK4/6 Inhibitors in Cancer Therapy: A Novel Treatement Strategy for Bladder Cancer." Bladder Cancer **3**(2): 79-88.

Parekh, S., C. Ziegenhain, B. Vieth, W. Enard and I. Hellmann (2016). "The impact of amplification on differential expression analyses by RNA-seq." Sci Rep **6**: 25533.

Patel, M. R., A. Dash, B. A. Jacobson, Y. Ji, D. Baumann, K. Ismail and R. A. Kratzke (2019). "JAK/STAT inhibition with ruxolitinib enhances oncolytic virotherapy in non-small cell lung cancer models." Cancer Gene Ther **26**(11-12): 411-418.

Patel, V. G., W. K. Oh and M. D. Galsky (2020). "Treatment of muscle-invasive and advanced bladder cancer in 2020." CA Cancer J Clin **70**(5): 404-423.

Pelka, P., J. N. Ablack, J. Torchia, A. S. Turnell, R. J. Grand and J. S. Mymryk (2009). "Transcriptional control by adenovirus E1A conserved region 3 via p300/CBP." Nucleic Acids Res **37**(4): 1095-1106.

Pelka, P., M. S. Miller, M. Cecchini, A. F. Yousef, D. M. Bowdish, F. Dick, P. Whyte and J. S. Mymryk (2011). "Adenovirus E1A directly targets the E2F/DP-1 complex." J Virol **85**(17): 8841-8851.

Peter, M. and F. Kuhnel (2020). "Oncolytic Adenovirus in Cancer Immunotherapy." Cancers (Basel) **12**(11).

Quintás-Cardama, A., K. Vaddi, P. Liu, T. Manshouri, J. Li, P. A. Scherle, E. Caulder, X. Wen, Y. Li, P. Waeltz, M. Rupar, T. Burn, Y. Lo, J. Kelley, M. Covington, S. Shepard, J. D. Rodgers, P. Haley, H. Kantarjian, J. S. Fridman and S. Verstovsek (2010). "Preclinical characterization of the selective JAK1/2 inhibitor INCB018424: therapeutic implications for the treatment of myeloproliferative neoplasms." Blood **115**(15): 3109-3117.

Rajan, P., V. Dhamankar, K. Rundell and B. Thimmapaya (1991). "Simian virus 40 small-t does not transactivate RNA polymerase II promoters in virus infections." J Virol **65**(12): 6553-6561.

Ramesh, N., Y. Ge, D. L. Ennist, M. Zhu, M. Mina, S. Ganesh, P. S. Reddy and D. C. Yu (2006). "CG0070, a conditionally replicating granulocyte macrophage colony-stimulating factor--armed oncolytic adenovirus for the treatment of bladder cancer." Clin Cancer Res **12**(1): 305-313.

Raychaudhuri, P., S. Bagchi, S. D. Neill and J. R. Nevins (1990). "Activation of the E2F transcription factor in adenovirus-infected cells involves E1A-dependent stimulation of DNA-binding activity and induction of cooperative binding mediated by an E4 gene product." J Virol **64**(6): 2702-2710.

Reichel, R., S. D. Neill, I. Kovesdi, M. C. Simon, P. Raychaudhuri and J. R. Nevins (1989). "The adenovirus E4 gene, in addition to the E1A gene, is important for trans-activation of E2 transcription and for E2F activation." J Virol **63**(9): 3643-3650.

Ressler, J. M., M. Karasek, L. Koch, R. Silmbrod, J. Mangana, S. Latifyan, V. Aedo-Lopez, H. Kehrer, F. Weihsengruber, P. Koelblinger, C. Posch, J. Kofler, O. Michielin, E. Richtig, C. Hafner and C. Hoeller (2021). "Real-life use of talimogene laherparepvec (T-VEC) in melanoma patients in centers in Austria, Switzerland and Germany." J Immunother Cancer **9**(2).

Richters, A., K. K. H. Aben and L. Kiemeney (2020). "The global burden of urinary bladder cancer: an update." World J Urol **38**(8): 1895-1904.

Russell, W. (2009). "Adenoviruses: update on structure and function." Journal of General Virology **90**(1): 1-20.

Sathe, A., N. Koshy, S. C. Schmid, M. Thalgott, S. M. Schwarzenbock, B. J. Krause, P. S. Holm, J. E. Gschwend, M. Retz and R. Nawroth (2016). "CDK4/6 Inhibition Controls Proliferation of Bladder Cancer and Transcription of RB1." J Urol **195**(3): 771-779.

Schaley, J. E., M. Polonskaia and P. Hearing (2005). "The adenovirus E4-6/7 protein directs nuclear localization of E2F-4 via an arginine-rich motif." J Virol **79**(4): 2301-2308.

Seifried, L. A., S. Talluri, M. Cecchini, L. M. Julian, J. S. Mymryk and F. A. Dick (2008). "pRB-E2F1 complexes are resistant to adenovirus E1A-mediated disruption." J Virol **82**(9): 4511-4520.

Shen, H. B., Z. Q. Gu, K. Jian and J. Qi (2013). "CXCR4-mediated Stat3 activation is essential for CXCL12-induced cell invasion in bladder cancer." Tumour Biol **34**(3): 1839-1845.

Skehan, P., R. Storeng, D. Scudiero, A. Monks, J. McMahon, D. Vistica, J. T. Warren, H. Bokesch, S. Kenney and M. R. Boyd (1990). "New colorimetric cytotoxicity assay for anticancer-drug screening." J Natl Cancer Inst **82**(13): 1107-1112.

Steinwaerder, D. S., C. A. Carlson and A. Lieber (2000). "DNA replication of first-generation adenovirus vectors in tumor cells." Hum Gene Ther **11**(13): 1933-1948.

Sung, H., J. Ferlay, R. L. Siegel, M. Laversanne, I. Soerjomataram, A. Jemal and F. Bray (2021). "Global Cancer Statistics 2020: GLOBOCAN Estimates of Incidence and Mortality Worldwide for 36 Cancers in 185 Countries." CA Cancer J Clin **71**(3): 209-249.

Swaminathan, S. and B. Thimmapaya (1996). "Transactivation of adenovirus E2-early promoter by E1A and E4 6/7 in the context of viral chromosome." J Mol Biol **258**(5): 736-746.

Taguchi, S., H. Fukuhara, Y. Homma and T. Todo (2017). "Current status of clinical trials assessing oncolytic virus therapy for urological cancers." Int J Urol **24**(5): 342-351.

Taipale, K., S. Tähtinen, R. Havunen, A. Koski, I. Liikanen, P. Pakarinen, R. Koivisto-Korander, M. Kankainen, T. Joensuu, A. Kanerva and A. Hemminki (2018). "Interleukin 8 activity influences the efficacy of adenoviral oncolytic immunotherapy in cancer patients." Oncotarget **9**(5): 6320-6335.

Takemoto, S., K. Ushijima, K. Kawano, T. Yamaguchi, A. Terada, N. Fujiyoshi, S. Nishio, N. Tsuda, M. Ijichi, T. Kakuma, M. Kage, D. Hori and T. Kamura (2009). "Expression of activated signal transducer and activator of transcription-3 predicts poor prognosis in cervical squamous-cell carcinoma." Br J Cancer **101**(6): 967-972.

Täuber, B. and T. Dobner (2001). "Molecular regulation and biological function of adenovirus early genes: the E4 ORFs." Gene **278**(1-2): 1-23.

Teijeira Crespo, A., S. Burnell, L. Capitani, R. Bayliss, E. Moses, G. H. Mason, J. A. Davies, A. J. Godkin, A. M. Gallimore and A. L. Parker (2021). "Pouring petrol on the flames: Using oncolytic virotherapies to enhance tumour immunogenicity." Immunology **163**(4): 389-398.

Tong, M., J. Wang, N. Jiang, H. Pan and D. Li (2017). "Correlation between p-STAT3 overexpression and prognosis in lung cancer: A systematic review and meta-analysis." PLoS One **12**(8): e0182282.

Tong, Z., A. Sathe, B. Ebner, P. Qi, C. Veltkamp, J. E. Gschwend, P. S. Holm and R. Nawroth (2019). "Functional genomics identifies predictive markers and clinically actionable resistance mechanisms to CDK4/6 inhibition in bladder cancer." J Exp Clin Cancer Res **38**(1): 322.

Toth, K., S. R. Lee, B. Ying, J. F. Spencer, A. E. Tollefson, J. E. Sagartz, I. K. Kong, Z. Wang and W. S. Wold (2015). "STAT2 Knockout Syrian Hamsters Support Enhanced Replication and Pathogenicity of Human Adenovirus, Revealing an Important Role of Type I Interferon Response in Viral Control." PLoS Pathog **11**(8): e1005084.

Tran, L., J. F. Xiao, N. Agarwal, J. E. Duex and D. Theodorescu (2021). "Advances in bladder cancer biology and therapy." Nat Rev Cancer **21**(2): 104-121.

Tribouley, C., P. Lutz, A. Staub and C. Kedinger (1994). "The product of the adenovirus intermediate gene IVa2 is a transcriptional activator of the major late promoter." J Virol **68**(7): 4450-4457.

Trikha, P., N. Sharma, R. Opavsky, A. Reyes, C. Pena, M. C. Ostrowski, M. F. Roussel and G. Leone (2011). "E2f1-3 are critical for myeloid development." J Biol Chem **286**(6): 4783-4795.

Tsimberidou, A. M., E. Fountzilas, M. Nikanjam and R. Kurzrock (2020). "Review of precision cancer medicine: Evolution of the treatment paradigm." Cancer Treat Rev **86**: 102019.

Tsujita, Y., A. Horiguchi, S. Tasaki, M. Isono, T. Asano, K. Ito, T. Asano, Y. Mayumi and T. Kushibiki (2017). "STAT3 inhibition by WP1066 suppresses the growth and invasiveness of bladder cancer cells." Oncol Rep **38**(4): 2197-2204.

Witjes, J. A., H. M. Bruins, R. Cathomas, E. M. Comperat, N. C. Cowan, G. Gakis, V. Hernandez, E. Linares Espinos, A. Lorch, Y. Neuzillet, M. Rouanne, G. N. Thalmann, E. Veskimae, M. J. Ribal and A. G. van der Heijden (2021). "European Association of Urology Guidelines on Muscle-invasive and Metastatic Bladder Cancer: Summary of the 2020 Guidelines." Eur Urol **79**(1): 82-104.

Woller, N., E. Gurlevik, B. Fleischmann-Mundt, A. Schumacher, S. Knocke, A. M. Kloos, M. Saborowski, R. Geffers, M. P. Manns, T. C. Wirth, S. Kubicka and F. Kuhnel (2015). "Viral Infection of Tumors Overcomes Resistance to PD-1-immunotherapy by Broadening Neoantigenome-directed T-cell Responses." Mol Ther **23**(10): 1630-1640.

Xin, P., X. Xu, C. Deng, S. Liu, Y. Wang, X. Zhou, H. Ma, D. Wei and S. Sun (2020). "The role of JAK/STAT signaling pathway and its inhibitors in diseases." Int Immunopharmacol **80**: 106210.

Xiu, W., J. Ma, T. Lei, M. Zhang and S. Zhou (2016). "Immunosuppressive effect of bladder cancer on function of dendritic cells involving of Jak2/STAT3 pathway." Oncotarget **7**(39): 63204-63214.

Yang, G., W. Shen, Y. Zhang, M. Liu, L. Zhang, Q. Liu, H. H. Lu and J. Bo (2017). "Accumulation of myeloid-derived suppressor cells (MDSCs) induced by low levels of IL-6 correlates with poor prognosis in bladder cancer." Oncotarget **8**(24): 38378-38388.

Yang, L., X. Gu, J. Yu, S. Ge and X. Fan (2021). "Oncolytic Virotherapy: From Bench to Bedside." Frontiers in Cell and Developmental Biology **9**.

Yang, Z., L. He, K. Lin, Y. Zhang, A. Deng, Y. Liang, C. Li and T. Wen (2017). "The KMT1A-GATA3-STAT3 Circuit Is a Novel Self-Renewal Signaling of Human Bladder Cancer Stem Cells." Clin Cancer Res **23**(21): 6673-6685.

Zajchowski, D. A., H. Boeuf and C. Kédinger (1987). "E1a inducibility of the adenoviral early E2a promoter is determined by specific combinations of sequence elements." Gene **58**(2-3): 243-256.

Zhang, H., Y. L. Ye, M. X. Li, S. B. Ye, W. R. Huang, T. T. Cai, J. He, J. Y. Peng, T. H. Duan, J. Cui, X. S. Zhang, F. J. Zhou, R. F. Wang and J. Li (2017). "CXCL2/MIF-CXCR2 signaling promotes the recruitment of myeloid-derived suppressor cells and is correlated with prognosis in bladder cancer." Oncogene **36**(15): 2095-2104.

Zhang, W. and M. J. Imperiale (2003). "Requirement of the adenovirus IVa2 protein for virus assembly." J Virol **77**(6): 3586-3594.

Zhang, Y. and Z. Zhang (2020). "The history and advances in cancer immunotherapy: understanding the characteristics of tumor-infiltrating immune cells and their therapeutic implications." Cell Mol Immunol **17**(8): 807-821.

Zhao, H., M. Chen and U. Pettersson (2014). "A new look at adenovirus splicing." Virology **456-457**: 329-341.

Zheng, Y., T. Stamminger and P. Hearing (2016). "E2F/Rb Family Proteins Mediate Interferon Induced Repression of Adenovirus Immediate Early Transcription to Promote Persistent Viral Infection." PLoS Pathog **12**(1): e1005415.

Zhu, A., J. G. Ibrahim and M. I. Love (2019). "Heavy-tailed prior distributions for sequence count data: removing the noise and preserving large differences." Bioinformatics **35**(12): 2084-2092.